Manufacturing of Biocomposite Shell Mimetic via the Powder Compaction Method.

by

Taslima Akter, B.Sc. (Eng.)

A thesis submitted in fulfillment of the requirement for the degree of

Masters in Engineering

Supervisors:

Dr. Joseph Stokes and Professor M.S.J.Hashmi

Dublin City University
School of Mechanical and Manufacturing Engineering

March 2006

DECLARATION

I hereby certify that this material, which I now submit for assessment on the programme of study leading to the award of Masters in Engineering (M. Eng.), is entirely my own work and has not been taken from the work of others save and to the extent that such work has been cited and acknowledge with the text of my work.

Signed: Taslima Akter **ID No: 53145259**

Taslima Akter

ACKNOWLEDGEMENTS

I would like to express my highest gratitude to my supervisor Dr. Joseph Stokes, School of Mechanical and Manufacturing Engineering (MME) and Materials Processing Research Center (MPRC), DCU for his guidance, limitless energy, encouragement and equanimity. I will be thankful to him forever for his guidelines, penitence and kind co-operative mind over the last two years.

I would like to give special thanks to my academic supervisor Professor M. S. J Hashmi, School of MME, DCU, for my entrance to the field of powder metallurgy and providing me resources and funding throughout this work and also for special guidance in my practical life.

I am grateful to Dr. Malika Ardhaoui, School of MME, DCU, for helping me in experimental designs and statistical analysis. I would also like to thank her for her valuable and innovative suggestion in my research.

Many thanks specially to Mr. Christopher Crouch, the technical staff, School of MME, who devoted much time in assisting in the use of the powder processing and compaction machine and also to Mr Michael May for materials characterisation and Mr. Liam Domican for providing me with all I requested.

I should acknowledge Dr Tim Prescott and Dr. Aran Rafferty , School of MME, DCU, for helping me with powder characterization and their valuable suggestions.

I am very thankful to my family members, specially my mother Mrs. Nasima Akter, without her support and encouragement it was impossible to come this far. Special thanks to my elder brothers and sister who wised me success in my research.

Finally, I would like to give special thanks and regards to my beloved husband, Md. Mahfujur Rahman, for helping me during material characterisations and continuous moral support, patience and good humor in every part of my life.

ABSTRACT

Manufacturing of Synthetic Shell Media for Industrial Waste Air Treatment Process.

Taslima Akter, B.Sc. (Eng.)

Natural sea shells are used in the treatment of waste air-streams in biofitration process, however this industry requires new methods of fabricating synthetic shell media to perform in the way natural shell performs. This present study investigates the manufacturing of seashells-like bioceramic/biocomposites as a filter bed with optimum porosity and compressive load capacity using uniaxial die compaction method.

According to the structure of natural sea shell, calcium carbonate bioceramics/biocomposites were designed and manufactured in three steps. In the first step, optimisation of the process parameters and their effects on the porosity (P_r) and compressive load (C_s) of bio-ceramic 1 have been studied. Statistical analyses of the data indicates that only the weight fraction of the pore former and the compaction load influenced significantly the porosity and the compressive load. The compaction speed has no significant influence on the properties of the artificial bioceramic. Higher weight fraction of pore former and lower compaction load leads to high porosity and low compressive load. In the second step, the effect of the particle size of the pore former on porosity and compressive load of calcium carbonate bioceramic 2 was investigated and optimised. The particle size of the pore former has a significant effect on compressive load. No substantial effect of the particle size of the pore former has been found to vary the porosity of the bioceamic 2. In the third step, the effect of the addition of biopolymers on compressive load of calcium carbonate biocomposite has been analysed. The mixing of individual or both biopolymers together increased the compressive load of the calcium carbonate biocomposites significantly.

This new synthetic bioceramic/composites were also examined using X-ray diffraction (XRD), Scanning Electron Microscopy (SEM) and their behaviour under compression test was also determined. Porosity and compressive load of the natural seashells were compared with artificial calcium carbonate bioceramic/biocomposites. The biocomposite performed well mechanically under dry conditions however more research is required to identify the problems that occurred under wet conditions.

DEDICATION

This thesis is dedicated to my father who always wished my success in life.

Table of Contents

List of Figures

List of Tables

NOMENCLATURE

Y	response
β_0	constant coefficient
X_i	variables
X_j	variables
β_i	linear coefficient
β_{ij}	interaction coefficients
P_f	percentage of pore former
P_c	compaction pressure
V_c	compaction speed.
P_r	percentage of porosity
C_s	compressive load
h	height
D	diameter
m	mass
σ	resulting strength of the material
B'	material dependent constant
σ_0	the wrought (initial) strength
P	applied pressure
ε	fractional porosity
K	proportionality constant
ε_a	apparent porosity at the before compaction
R^2	determination of coefficient

CHAPTER 1 INTRODUCTION

Biomimetics is a newly emerging field in materials science, engineering and biology, that studies how nature designs and fabricates high performance mineral-polymer composites, in order to develop methods of processing and micro-structural design for innovative materials. Biological organisms produce complex composites that are hierarchically organised in terms of composition and microstructure, containing both inorganic and organic components in complicated mixtures. This insight inspires new research and fabrication routes for new materials design. The synthesis of biological composite via modern technology can offer attractive mechanical properties with controlled structure for different applications.

Many natural biological materials such as seashells are well known for their mechanical properties- superior to many man made ceramics and composites. They are mainly composed of calcium carbonate ($CaCO_3$) in two forms; calcite and aragonite or a mixture of them with some organic compounds. It represents the highly regular arrangement of organic (protein/biopolymer) and inorganic ($CaCO_3$) layers and "macro defect free" lamellar structure, which play a key role in enhancing the mechanical properties of the seashell. The study of biological materials is generating a lot of interest within a number of applications such as bioengineering, bioscaffold, bone cement and the biological treatment of airstreams.

These natural seashells are used as filter beds for micro-organism growth in the biological treatment of airstreams with high odour concentration (H_2S and other organic sulphide compounds). Shell filter media contain a high level of $CaCO_3$ which neutralises acid as it is produced by the action of bacteria. Though this media shows high cleaning efficiency, it also has some disadvantages. Harvesting enough seashells is difficult as it depends on the seasonal changes. Moreover, they can decompose and compact upon themselves which can break up the uniformity of the air-flow flowing through the filter bed.

This project investigates an artificial alternative for producing seashells as a support matrix for the biological treatment of acid gases. There are number of ways the synthetic shell media could be manufactured from naturally found materials containing high percentages of calcium carbonate. Considering economic advantages, the uniaxial die compaction technique was utilized in this present study to produce seashell-like bioceramics/biocomposites using calcium carbonate powder. This bioceramic/biocomposite should fulfil the desired porosity and compressive strength as a filter material as compared with that of natural seashell.

Chapter two of this study describes different types of composites especially the biological composite; natural seashell. Structure, growth mechanism, protein/biopolymer combination, mechanical properties and mineralogical composition of seashells are thoroughly investigated. The process of mimicking natural seashell and their properties of along with other man-made mineral-biopolymer composites are also discussed. Along with this, common filter beds currently been using in biofiltration processes are investigated with their difficulties, cost and efficiencies. Finally different steps used in powder metallurgical processes and die compaction techniques are analysed regarding the production of porous calcium carbonate bioceramic/biocomposites.

Chapter three describes the experimental procedure used to produce the artificial seashell like bioceramic or biocomposites. Three experimental designs have been developed to produce calcium carbonate bioceramic 1, bioceramic 2 and biocomposites on the basis of prior experimental results. Material selection and processing through die compaction technique is described in detailed. The material processing equipment are also presented and described in this section. The MODDE 7.0 software used to develop experimental designs and statistical analysis aided optimisation of the process parameters and mixture composition for calcium carbonate bioceramic/biocomposite to determine the optimum porosity and compressive strength for the synthetic seashell. A detail description of analysis characterisation techniques and the equipment used to analysis the porous calcium carbonate bioceramic/biocomposite is described in this Chapter.

Chapter four presents the results and discussion for the experimental work carried out for the porous calcium carbonate bioceramic1, bioceramic 2 and biocomposite. The microstructure and load-displacement behaviour during compression tests of porous bioceramic 1, bioceramic 2 and biocomposite are all determined and shown. Experimental design 1 investigates the effect of process parameters on porosity and compressive strength for calcium bioceramic 1 and the optimum conditions are determined by MODDE 7.0 software. The effect of the particle size of the pore former on the compressive strength of bioceramic 2 is investigated using experimental design 2 and compared with bioceramic 1. Experimental design 3 analyses the effect of the biopolymers (chitin and chitosan) on compressive strength of the calcium carbonate biocomposite. The optimum mixture combination of biopolymer and calcium carbonate powder is determined by MODDE 7.0 software. The composition and structure of calcium carbonate powder, and porosity and compressive strength of bioceramic 1, bioceramic 2 and biocomposite are compared with that of natural seashells. The behaviour of the calcium carbonate biocomposite with steam or water is also discussed.

Chapter five draw out the conclusions of the results of this investigation and suggests recommendations for future work in this topic.

The aim of this research is the manufacture of bioceramic/biocomposite shell mimetics using the powder compaction method and the characterisation of these materials in terms of porosity and compressive strength.

CHAPTER 2 LITERATURE SURVEY

2.1 Introduction

Seashells have been used as money, pharmaceuticals, ornaments, the primary ingredients for dyes and objects of art and jewelry. In biofiltration technology, seashells play a new and important role in cleaning up the environment. Natural seashells used as a filter bed in biofiltration processes, have proven to be a good support carrier media for micro-organism to grow and live.

The biological composite, comprising seashells, is composed of a calcium carbonate ceramic phase combined with a minor amount of organic or biopolymer constitutes. Mimicking of this seashell is now one of the major attractions for many researchers due to their excellent mechanical properties. Combinations of calcium based ceramic with organic biopolymer biocomposites like natural seashell have been manufactured by different researchers for biomedical applications followed by chemical methods.

As this research attempts to manufacture the seashell like biocomposite filter media for biofiltration processes via powder metallurgical method, this chapter thoroughly discusses the structure, property and composition of natural seashells. To understand the seashell like a biocomposite, classifications of composite materials are also discussed. Different filter media used in biofiltration processes are described and analysed from different view points. As porosity and mechanical strength are prime requirements of a filter media, the powder metallurgy processes also described in respect of different porous calcium base bioceramic or biocomposites.

2.2 Composites

A composite material is a heterogeneous solid consisting of two or more components that are mechanically or metallurgically bonded together [1]. Each of the various components retains its identity in the composite and has its characteristic structure and properties. On the basis of the structural constituents, composites can be classified into five general groups as described in Table 2.1.

Table 2.1 Classification of different composites [1-3]

TYPE	DEFINITION	EXAMPLES AND USES
Laminar Composite	Composed of layer or laminar constituents	1. Plywood- Household building and construction 2. Electrolytic tinplates- Tin cans 3.Electro galvanized Steel- Roofing
Particulate Composite	Consist of discrete particles of one material surrounded by a matrix of another material.	1. Silicon carbide (SiC) with glass or polymer- Grinding or cutting wheel 2. Sand with other binder- Foundry mould.
Fibre Reinforced Composite	Composed of continuous or discontinuous thin fibre of one material embedded in a matrix of another.	1. Polyester and wool- textile 2. Straw and mud- bricks 3. Nylon, rayon and rubber fibre-automobile tires
Flake Composite	Composed of flat flakes with or without a matrix	1. Flake aluminium- Automobile paint 2. AlB_2- US space shuttle
Filled or Skeletal	Composed of a continuous skeletal matrix (honeycomb structure; sponge like network of open pores) filled by a second material.	1. Tungsten skeletal filled with copper or silver- Rocket Nozzles 2. Sponge like copper based alloy impregnated with Babbitt metal-automotive bearing.

However, by combining the components, resultant characteristics are imparted that become the properties of the composite. Composites are not only used for their structural properties but also for electrical, thermal, tribological and environmental applications. Modern composite materials are usually optimised to achieve a particular balance of properties for a given range of applications.

Composites can also classified with respect to the matrix which constitute them.
The major composite classes are:
1. Polymer-Matrix composite (PMC)
2. Carbon-Carbon composite (CCC)
3. Metal-Matrix composite (MMC)
4. Ceramic-Matrix composite (CMC)

A comparative schematic representation of the developmental and applications history of each group is shown in Figure 2.1

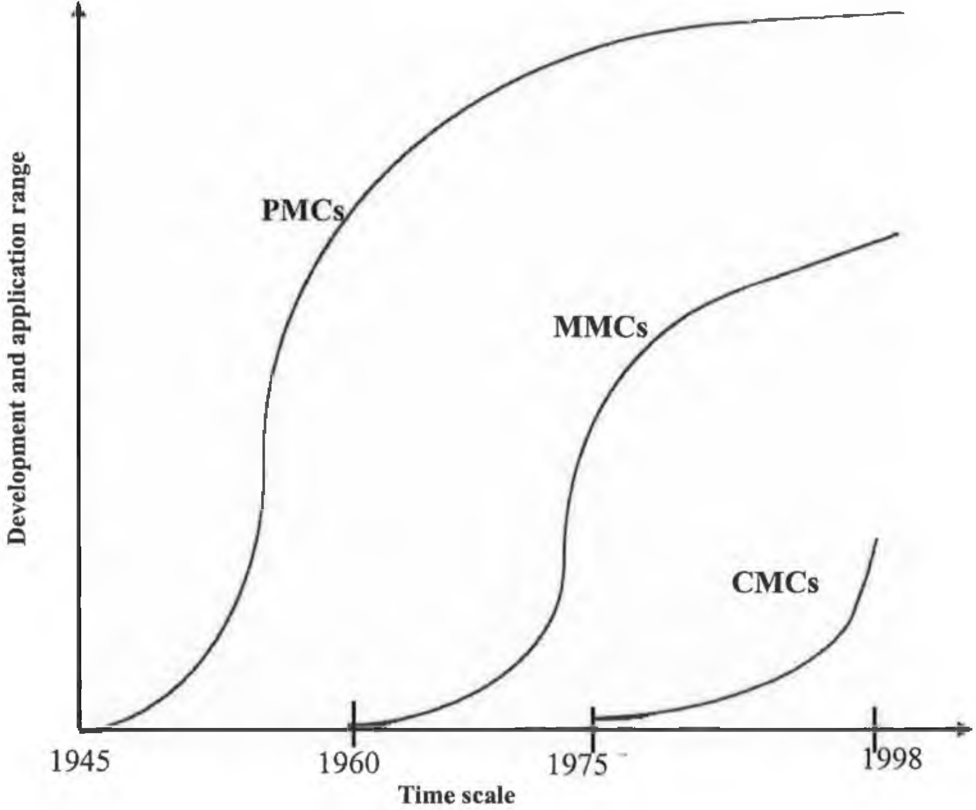

Figure 2.1. Development and application of different composite groups with time [3].

2.2.1 Polymer Matrix Composite (PMCs)

Polymers reinforced with continuous carbon fibre offer the highest thermal conductivity of all commercial PMCs [4]. Common polymer matrix materials are polyester, vinyl ester resins, epoxy resins and so on and are reinforced with different fibre materials such as aluminium oxide, carbon, boron, E-glass and so on. Hand lay up is the most common process for PMCs processing specially for polyester matrix composite [5]. Other fabrication methods; vacuum bag, pressure bag, autoclave moulding, die compaction in a matched die are used for other polymer matrix materials [1, 5]. A selection of suitable reinforcement, resin and manufacturing techniques can produce a product of the required performance, at minimum cost. PMCs are used in different applications such as sports goods, chemical plant, marine and transport applications. The combination of boron fibre and resin matrix is principally used in aerospace application where their high cost is not such a disadvantage [5].

2.2.2 Carbon Carbon Composite (CCCs)

Carbon matrix composites have number of advantages including stable mechanical properties when subjected to temperatures greater than 2205 ^{0}C (4000 ^{0}F), high strength to weight ratio, high thermal conductivity, thermal shock, abrasion, and corrosion resistance, [1] often due to graphite fibre in a carbon matrix [2]. Though oxidation at low temperature and high cost of carbon-carbon composites restricted such composite applications, they have been successfully utilised in commercial aircraft brakes, where their superior performance outweighs their increased costs [4].

2.2.3 Metal Matrix Composite (MMCs)

Metal matrix composites (MMCs) can be defined as materials consisting of a metal or metallic alloy (matrix material) reinforced with a non-metallic or different metallic phase. MMCs are used in structural applications requiring wear resistance, thermal management and weight savings. The most common commercial MMCs are based on aluminium, magnesium and titanium alloys reinforced with silicon carbide (SiC), alumina (Al_2O_3), carbon or graphite. The incorporation of the reinforcement increases the stiffness and strength of the matrix. Different fabrication processes have been used in the processing of MMCs such as casting, hot isostatic pressing, infiltration and so on. The material property tailoring is normally achieved by varying parameters such as volume fraction of reinforcement, the reinforcement size or the reinforcement form [3]. MMCs are now widely used in different applications. The ground transportation industry (automotive and rail) accounts for 62% of the total MMC world market [4]. Some renowned MMC; such as Kovar (Fe-Ni-Co alloy) or DRA (discontinuously reinforced Aluminium) provide better performance in thermal, electrical packaging and aerospace applications [4].Although MMCs are almost always more expensive on a per-euro basis relative to the material displaced, however an overall cost reduction is often a result of several considerations such as simplified processing or life cycle considerations (reduced repair frequency, higher reliability, longer life) which enhance the cost comparison.

2.2.4 Ceramic Matrix Composite (CMCs)

The term ceramic covers a wide variety of inorganic materials, which are generally non-metallic and are frequently processed at high temperatures. Ceramic matrix composite development has continued to focus on achieving useful structural and environmental properties [4]. The reasons for reinforcing ceramics are fundamentally different from those for polymers and metals as these are reinforced to increase strength and modulus, while ceramics are reinforced for toughening and damage tolerance [1].

Ceramic matrix materials can be categorized into four groups; glass ceramics such as lithium aluminosilicate (LAS), oxides such as alumina and mullite, nitrides such as silicon nitride, and carbides such as silicon carbide and all are reinforced with different fibres and particulates [1].

Many fabrications have been investigated for CMC processing [5, 1]. The property of the composite is not only dependent on the properties and fractions of the constituent phases, but also on the processing technique. Porosity has a marked effect on fracture strength, hardness and elastic modulus. However, pore size distribution determines the scatter of the strength of the component [6]. Other microstructural parameter such as matrix grain size and morphology, reinforcement particle size, phase continuity and properties of grain boundaries and interface have a significant effect on the property of CMCs. The most conventional techniques are cold and hot pressing followed by sintering [7]. Cutting tool inserts, nozzles and exhaust ducts, brake rotors for automobiles, jet engines, and energy related applications such as heat-exchangers tubes are the prime applications of CMC's [7].

2.3 Biological Composites

In the natural world, living organisms produce more than 60 minerals and they have very different functions [8]. Many examples of rigid biological structures and materials such as sea shells, bone, and teeth are composed of complex composite structures that are hierarchically organised in terms of composition and microstructure containing inorganic materials and organic polymers in a complicated mixture [9]. Table 2.2 shows the list of important groups of animals that have composite skeletal materials.

Table 2.2. List of the animal groups that have composite skeletal materials [5]

SPECIES	**COMPOSITE SKELETAL MATERIALS**
Sponges	$CaCO_3$ and SiO_2 spicules in compliant matrix. SiO_2 spicules occasionally form coherent skeleton *(Euplectella)*
Coelenterates	(Sea anemones, jellyfish, Corals) $CaCO_3$ spicules in compliant matrix. Massive $CaCO_3$ skeletons with tenuous organic matrix (TOM)
Platyhelminathes	(Flatworms) Occasionally $CaCO_3$ spicules in compliant matrix.
Annelids	(Segmented worms, earthworms, leeches, fanworms) Tubes made of $CaCO_3$ in TOM, or sandgrains with TOM.
Arthropods	(Ubsects, Crustaceans, Spiders and many others) Cuticle of chitin fibrils in protein matrix. Crustaceans and millipedes add $CaCO_3$. $CaCO_3$ with TOM (Barnacles)
Molluscs	(Clams, snails, squids) $CaCO_3$ still with TOM. $CaCO_3$ spicules chitons' body wall, higes of clams). Teeth, organic fibres in an organic matrix
Brachipods	(Lamp shells; no real common name) $CaCO_3$ with TOM . Feeding arms often have high volume fraction $CaCO_3$ spicules in compliant matrix. Calcium phosphate rich and poor layers alternate *(Lingula)*
Bryozoa	(Tiny, colonial animals) $CaCO_3$ shell with TOM. Spicules in fairly rigid matrix.
Chordates	Enamel, bone (and varieties such as dentine), Keratins.

The main purpose of the rigid natural composites are to provide protection, shape, and support and to serve as weapons, for example [10]. Biological hard tissues are structured from the nanometre scale to microscale and the macroscale and these control the structures highly functional properties. Such unique structures have been widely studied and inspired the creativity of materials scientists to develop new synthetic materials exhibiting high performing properties [11-13]. However, neither the sophistication of biomineral assembly mechanisms nor the complex composite microarchitectures can be duplicated by non-biological methods [14]. Substantial progress has been made in understanding the biomineralisation process and applied in the relavant industrial applications, namely in the design of appropriate biomimetic routes [14]. It is a new field of materials science or bioengineering in which lessons must be learned from biology, in order to develop methods of processing and micro structural design for new materials [15]. However, successful mimicking requires looking at the effects of other influences such as water which have a effect on strength, toughness, ductility and stiffness [16].

(a) Composite materials

The raw materials used in development of biological structures can be divided into four groups [5], although their detailed structures are usually adjusted to the organism's needs.

1. Ceramics

Calcium carbonate is the most widely used in pharmaceutical and paper coatings. The most widely crystalline form found in nature is calcite (trigonal crystal structure) and aragonite (orthorhombic crystal structure) and occasionally it is amorphous. Calcium phosphate, or some variant such as hydroxyapatite is used by vertebrates. Silica is the other common material particularly used in sponges.

2. Polysaccharide

Simple sugar molecules, such as glucose, can combine to form very long chain polymers [5]. Particularly important among these are cellulose (polycellobiose) and chitin (poly-N-acetyl-D-Glucosamine) [5] and often form side links to neighbouring polysaccharide molecules.

3. Proteins

Proteins are long chain polymers made of many amino acids bound by peptide bonds [5]. The general formula for an α-amino acid, the type found in proteins is: R-NH_2-CH-CHOOH [5]. The carboxylic acid group and amino group are both attached to the α-carbon. 'R' is one of about twenty side groups which range in complexity from the single hydrogen in glycine to the aromatic-ring containing tryptophan [5]. These side groups may be polar or non- polar, acidic, basic or neutral. Proteins in biological composites tend to be fibrous, in which case the primary structure of the protein tends to be simple, and the amino acid are often small, allowing close packing [5].

4. Other organic materials

Organisms make use of compounds of proteins with polysaccharides as in the mucopolysaccarides [5]. Lignin is an amorphous material, made of long chain polymers of phenyl propane derivatives. Lignin is very widely used as a matrix material in wood.

Water is very common in biological composites and it has a profound effect on the mechanical properties of the materials.

(b) Mineralised Composites

The composites found in organisms can be classified in many ways; according to the organisms they are found in; according to their function; to their composition; to their mechanical properties; and so on. Weiner and Addadi [17] differentiated three types of biological materials based on the organisation of their mineral constituents. The first one is composed of multicrystalline arrays, in which individual crystals are generally all aligned at least in one direction and often in all three directions such as bone, or shells. The second type is a single crystal or a limited array of relatively large crystals which constitute the entire structure and the third type contains an amorphous mineral.

Biological composites can also be defined into two groups;

1. Ceramic-ceramic composite

Some biological composites form in combination with minerals without any organic matrix such as sea Urchins teeth. Sea urchins teeth core regions are made of calcite fibre in a matrix of amorphous calcium carbonate. The fibres have a high volume fraction (about 55%), and can be shown, by etching with dilute acid, to have rather uniform crystallographic orientation. The mechanical properties of this core region are not as well known [5]. However, the modulus of elasticity of the central part of the tooth has been found to be 60 GPa [5].

2. Ceramic- organic groups

There are a considerable range of materials, volume fractions of fibres and matrix in biological ceramic-organic composites. The most common examples are mollusk shell and bone. A detailed discussion of natural sea shell is outlined in the following section .

2.3.1 Natural Sea Shell

(a) Structure and Growth Mechanism

Great attention has been paid to seashells due to their outstanding mechanical properties and interesting structure [18-21]. Figure 2.2 shows the growth structure of the sea shell.

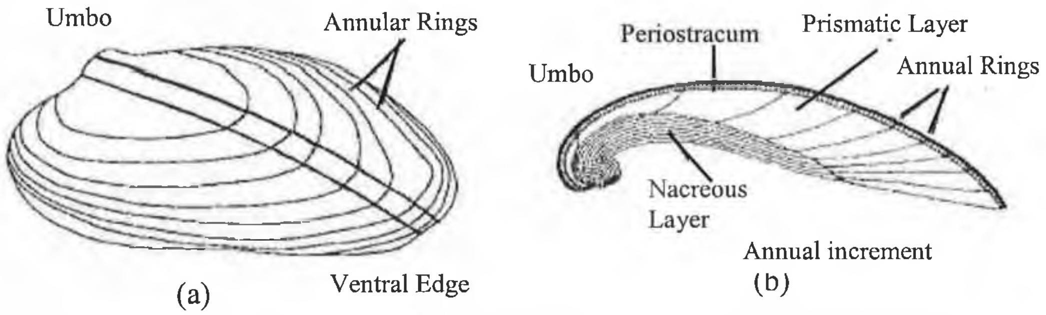

Figure 2.2. (a) Shell section cut from freshwater bivalve shell, (b) Schematic of the cross section of a shell[22].

Sea shells are natural nanocomposite materials and contain layers of nanoscale inorganic calcium carbonate ($CaCO_3$) crystals sandwiched between biopolymer/ organic matrices (1-5%) [8,19,21]. Two polymorphs of $CaCO_3$ have been observed in seashells; calcite and aragonite or sometimes mixtures of them [8,20,23]. The organic matrix is complex in

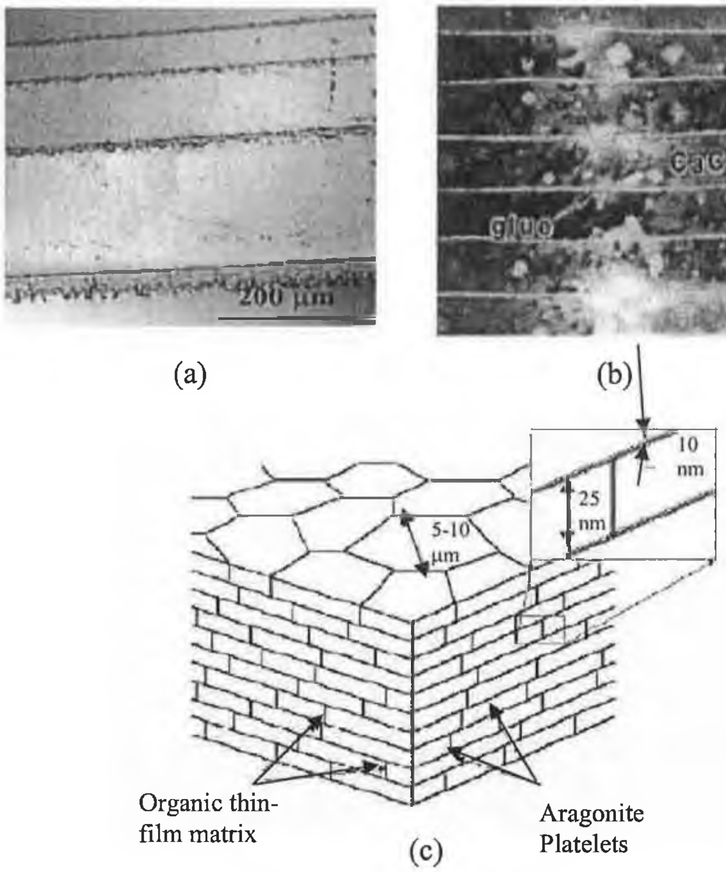

(a) (b) (c)

Figure 2.3. (a) Optical micrograph, (b) TEM micrograph of cross-section of abalone shell showing layered structure, (c) Brick and mortar diagram of seashell nacre structure [16, 25].

nature but it can be classified into three groups; asparitic acid rich (glycol) proteins, glutamic acid rich glycoproteins and the third group being rich in polysaccharides [24]. The platelets/tablets of calcium carbonate (thickness ~ 200-900nm) are stacked with organic protein layers (thickness ~ 10-50nm) in brick mortar fashion [19] as shown in Figure 2.3.

Calcium carbonate crystal nucleation occurs on an organic sheet (β chitin or other organic matter of unknown composition) coated with hydrophilic; acidic macromolecules where growth occurs within an organic envelope containing silk fibroin as shown in Figure 2.4 [17, 26].

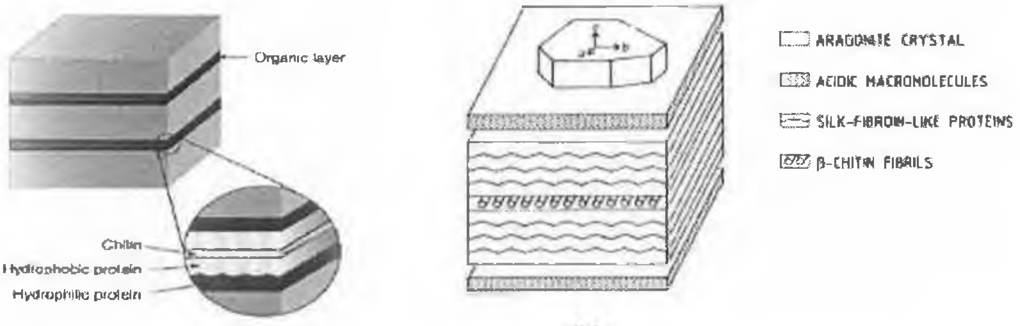

(a) (b)

Figure 2.4. (a) Schematic illustration of layered organic matrix. (b) Schematic block diagram showing the spatial relation between the crystallographic axes of an aragonitic nacreous polygon and the underlying organic matrix. [26, 17]

The mineralisation of seashell is affected by the hydrophobic macromolecules in the nacre layer. Therefore, crystal growth is modulated by specific proteins and there can be competition between crystal and the protein growth. Checa and Rodriguez-Navarro [27] explained that during crystal growth, protein/fibres become progressively oriented with their three crystallographic axes aligned which results from geometrical constraints and space limitation and finally determine the crystal arrangements. Arias and Fernandez [28] divided the mechanism of biomineralisation of a shell into four steps describing the arrangements of sequentially deposited macromolecules. The first step is the fabrication of an inert laminar substrate consisting of well-ordered hydrophobic organic material that is usually composed of β chitin or other characterized biopolymers. In the second step a particular polyanionic macromolecule is deposited on to the previously formed inert scaffolding, where nucleation of calcium crystals takes place. These macromolecules are aspartate or glutamate- acid rich proteins. In the third step the gel structure of silk fibroin like proteins not only controls polymorphism but also the diffusion controlled growth, face growing rates and the habits of the crystals formed. The fourth step is the inhibiting of crystal formation and is related to the fabrication of new inert scaffolding or the deposition of particular inhibitory hydrophobic proteins. Figure 2.5 shows the hypothetical growth of calcium carbonate crystals and proteins.

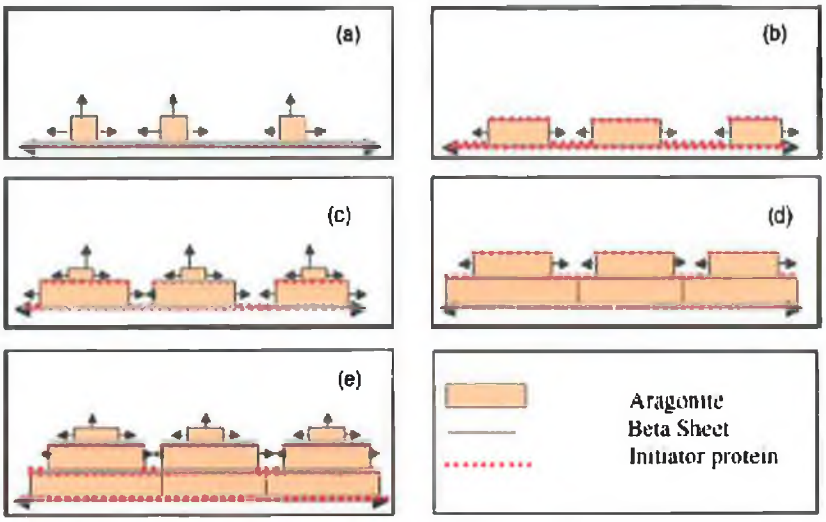

Figure 2.5. Hypothetical growth mechanism of calcium carbonate crystals (aragonite) and proteins (a) nucleation of aragonite perpendicular to protein layer, (b–e) growth with periodic protein regulation [29].

(b) Protein Combination

Extensive research has been carried out on the investigation of shell protein structures [18, 26, 30-38]. However, it is still not fully understood as a variety of microstructures are produced by different shells which complicate the problem. In Table 2.3 a summary of the composition of biopolymer/protein structures in different seashells is shown. Among them chitin, chitosan and silk fibroin have been found to be the most common organic materials in shells.

Table 2.3 List of the proteins for different seashells [22, 26, 30-39]

LATIN NAME FOR THE SHELL	LOCAL NAME FOR THE SHELL	ORGANIC POLYMER/PROTEIN
Haliotis rufescens (a marine gastropod mollusc)	Abalone	Lustrin A (amino acid sequence, cDNA coding, unique modular structure) glutamic rich protein; glycine, lysine and valine
Haliotis Laevigata	Abalone	Perlucin, Perlusitrin **Chitin**, Lustrin A
	Mollusk	**Silk-fibroin** like protein, glycoprotein rich aspartic acid, **β-chitin**, **chitosan**
Atrina serrata	Mollusk (Bivalve)	**β-Chitin** , **Silk-fibroin**, Glycoproteins rich in asparitic acid.
Pinna nobilis	Fan Mussel (Bivalvia)	Serine and proline rich protein, mucin (mucoperlin), Caspartin, Calprismin
Pinctada fucata	Pearl oyster	Aspein, MSI31, N16, MSI60, Nacrein, EF-1α,
Mytilus edulies	Edible mussel	**Silk-fibroin** like hydrophobic protein

(c) Mechanical Properties

The composite structure as discussed above is most common in the nacre (nacreous layer; Figure 2.2b) position of the sea shell and it is believed that such a hard inorganic and soft organic layer, plays a key role in enhancing the toughness , strength and hardness of a seashell by restricting crack growth and delocalising the deformation fields [21,40,41]. It has been found that this nacre is about 3000 times more fracture resistant than a single crystal of pure mineral [18,41,42]. Okumura and de Gennes [43] developed a three dimensional finite element model of the nacre and proved that the organic matrix of the sea shell nacreous layer reduces the stress concentration. It was also suggested that the viscoplastic deformation of the organic layer increased the toughness of the shell, a theory supported by Menig et al. [44]. Moreover Menig et al. [44] described that $CaCO_3$ platelets led to the delocalisation of the failure, by which single sharp cracks become replaced by a large number of smaller cracks within a broader region and this effects the toughness mechanism.

There are many uncertainties when performing mechanical tests with seashells. The important fact is the lamellar micro architecture which varies across the shell thickness. Thus, different layers of a shell play specific roles in the mechanical response to externally applied loads. In terms of microstructural variation of shells, five main types exist as shown in Figure 2.6.

Nacre

Crossed lamellar

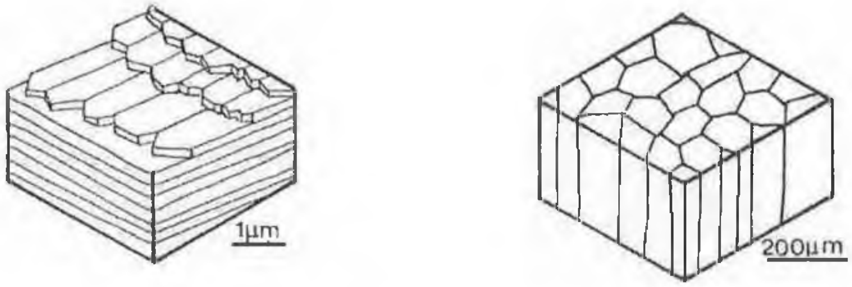

Foliated

Prismatic

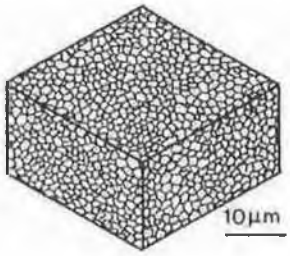

Homogeneous

Figure 2.6. Block diagram of the different layers of molluscan shell [5]

Prismatic structure have been shown to have higher residual compressive stress compared to crossed lamellar structures which gives rise to delamination of the structure upon mechanical deformation [45]. The mechanical properties of different layered structures are given in Table 2.4

Table 2.4 Mechanical properties of natural seashells [5, 16]

Structure	Tensile strength (MPa)	Compressive strength (MPa)	Bending strength (MPa)	Young's modulus (GPa)	Stiffness (GPa)	Vicker's hardness (Kg/mm)
Nacre	83	365	196	46	60	168
Crossed Lamellar	40	271	85	52	60	250
Prismatic	61	252	139	26	30	162
Foliated	40	104	102	32	40	110
Homogen -eous	30	248	60	60	60	---

Instead of examining the mechanical properties of only the lamellar structure of a seashell (where the sample was prepared in a cubic shape) some researcher have determined the strength of a seashell by reporting the force required to break a fresh bivalve sea shell [18,46,47]. These researchers observed that the load required to fracture such shells was 30-200 N for weak shells and 1200 N for stronger shells as the individual bivalve shells were quite variable in surface texture, shape, thickness and loading conditions. It has been reported that the shell strength was found to be higher in wet seashells than in dry (heated ~ 115 ^{0}C) or calcinated (heated ~ 600 ^{0}C) seashells (heating is used in order to understand the effect of the organic matrix of natural seashells) which reduced the tendency of blunting around the crack tip [18 ,43]. In addition fibrils of the organic matrix can be stretched by one hundred percent before they detach from the $CaCO_3$ [48]. During a thermogravimetry analysis, it was shown that between 250-450 ^{0}C a loss of organic matrix occurred and above 600^{0}C the calcium carbonate started to decompose to carbon dioxide (Figure 2.7).

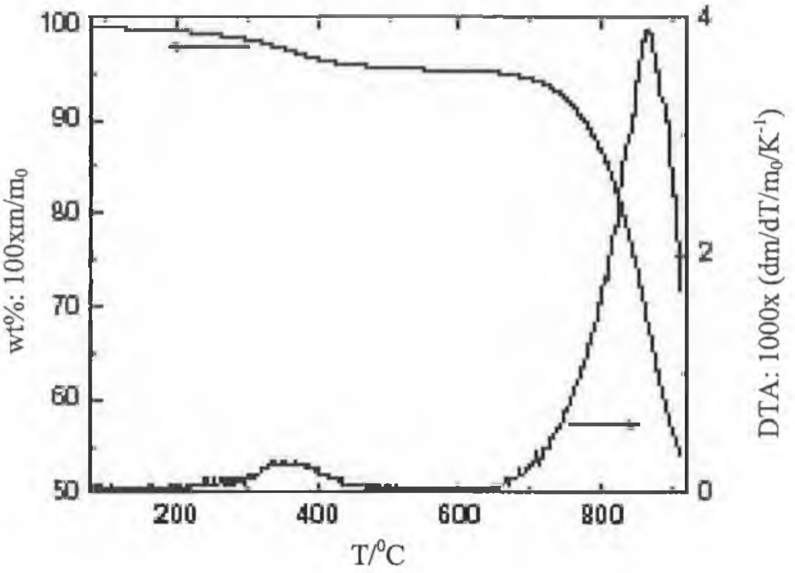

Figure 2.7. Thermogravimetric analysis (TGA) and differential thermal analysis (DTA) data of shells held in nitrogen. The content of the organic phase was calculated from the loss of mass taking place between 150 and 550 ^{0}C [48]

Therefore it can be assumed that the drying can minimise the mechanical properties of the shell. Porosity in seashells has not been widely investigated in literature, though 2-4% in wet shells and 45-49% in calcinated shells has been reported by Cheng et al. [49] but no effect was described in relation to the shells properties.

(d) Mineralogical Composition

Seashells are mainly made up of 95-98% $CaCO_3$. Besides this, other minerals are also found but in very small percentages. Loss on ignition (LOI) is a common and widely used method to estimate the organic and carbonate content of sediments. At first, organic matter is oxidised at 500–550 °C to carbon dioxide and ash. Secondly, carbon dioxide is evolved from carbonate at 900–1000 °C. The weight loss during the reactions is easily measured by weighing the samples before and after heating and is closely correlated to the organic matter and carbonate The chemical compositions of different types of shells are presented in Table 2.5.

Table 2.5 Chemical compositions of different seashells after LOI [23, 50]

Chemicals	Mussel Shell Wt%	Clam Shell Wt%	Oyster Shell Wt%
CaO	53.65	54.60	53.36
SiO_2	-----	------	0.85
Al_2O_3	0.05	0.05	0.137
MgO	0.10	-----	0.37
MnO	-----	0.02	-----
P_2O_5	-----	0.03	-----
Fe_2O_3	0.10	0.05	0.079
Na_2O	0.20	0.15	------
SO_3	-----	------	0.643
LOI (Loss on Ignition; carbon dioxide+ ashes)	46	45.10	43.89
Total	100	100	99.293

(e) Mimicking Shell Structures

Biocomposites like seashells are unusual engineering composites because they contain high percentages of ceramic phase combined with small amounts of polymeric/protein phase and their excellent combination of stiffness and fracture strength compares to that of polymer-matrix composites which have high levels of ceramic filler but no regular architecture [16]. Ceramic laminated with organic material has been found to be more fracture resistant then non-laminated ceramics [41].

Despite the wide investigation of seashell layer structures only a few researchers have attempted to mimic the seashell biocomposite. This may be due to the lack of an appropriate process. However, this nanoscale layer structure of seashells has been used to noticeably improve the mechanical and thermal properties of composite materials. Tang, et al [19] proposed the synthesis of a seashell nacre structure by alternating sequential deposition of negatively charged, nano-metre thick clay platelets onto positively charged polymers. It resulted in an organic-inorganic hybrid (brick and mortar arrangement) of films and they obtained similar mechanical properties to that of seashells. Almqvist [48] developed a number of physical processes to mimic the nacre structure of abalone shells by the combination of talc (inorganic) and polymer (organic) materials and characterised its mechanical properties. The strength of this new biocomposite was found not to be similar to nacre, therefore they suggested the use of fibrils like organic material (which was found in abalone nacre) instead of other organic polymers to achieve high strength. Hosod and Kato [51] proposed the thin film formation of $CaCO_3$ crystal on the insoluble chitin/chitosan/cellulose (organic polymer) solid matrix, to produce novel environmentally friendly materials exhibiting high mechanical strength and unique optical properties.

2.3.2 Chitin and Chitosan and their Composites

Chitin, basically extracted from shellfish sources, is a unique biopolymer consisting of N-acetyl-glucosamine monomer. It is a natural polysaccharide and the second most abundant biopolymer, which is particularly found in crab shells. Three polymorphic crystal structures of chitin have been investigated such as α , β, and γ chitin [52]. α-, β-, γ- chitin differ with regards to the arrangement of the chains within the crystalline regions. α-chitin is a tightly compacted mostly crystalline orthorhombic form where the chains are arranged in anti-parallel fashion with strong intermolecular hydrogen bonding and have low solubility, rigid and brittle nature [52]. β-chitin has a monoclinic structure where the chains are parallel and γ chitin is the mixture of α- and β-chitin [52]. Among them α-chitin is the most extensive and stable form as it is produced in huge amounts in nature [52-53]. α- and β-chitin can be obtained from crab and the Pen of loligo respectively [52]. In many applications cellouse is more preferable than chitin because of its insolubility in many organic solvents. However, α-chitin is insoluble in water and also in most organic solvents. It is mainly soluble in hexafluoroisopropanol, hexafluoroacetone, chloroalcohols in conjugation with aqueous solutions mineral acids and dimethylacetamide containing 5% lithium chloride [54].

Chitosan is the N-deacetylated derivative of chitin (although N-deacetylation is almost never complete). The degree of N-acetylation means the ratio of 2-actamido-2deoxy-D-glucopyranose to 2-amino-2-deoxy-D-glucopyranose structural units [54]. When the number of N-acetyl-glucosamine units is higher than 50%, the biopolymer is termed chitin.

Conversely, when the number of N-glucosamine is higher than 50%, the term chitosan is used [55]. This ratio has an effect on chitin solubility and solution properties. Chitosan has been researched more extensively because of its solubility in dilute acids such as acetic acid, formic acid; rendering chitosan more accessible for utilisation in chemical reactions [55].

The alkali treatment used to obtain chitin from shells mainly involves the removal of proteins and the dissolution of calcium carbonate which is present in crab shells in high concentrations. The resulting chitin is deacetylated in 40% sodium hydroxide at 120 ^{0}C [54]. This treatment produces 70% deacetylated chitosan. The nitrogen content of chitin varies from 5 to 8% depending on the extent of deacetylation whereas the nitrogen in chitosan is mostly in the form of primary atomic groups [54]. Chitin and chitosan contain high percentage of nitrogen (6.89%) compared to synthetically substituted cellulose (1.25%), which makes chitin useful as a chemical agent [55]. The average molecular weight (MW) of chitin is $1.03X10^6$ but N-deacetylation reaction reduces this to $1X10^5$ to $5X10^5$ [54]. Besides chitosan other derivatives have been obtained from chitin and their potential use have been reported by Mozzarelli [56]. Figure 2.8 shows the structure of chitin, chitosan and cellulose.

(a) Thermal Analysis

Thermogravimetric analyse of chitin and chitosan have also been carried out [58-60]. Chitin's decomposition temperature was reported to be between 350 to 380^{0}C depending on the heating rate [57]. Its decomposition temperature was related to the degree of biopolymer polymerisation and for chitin DP (degree of polymerization) was 2000-5000 [57]. Wanjun [59] also studied the thermal decomposition and reported that the weight loss started at 300^{0}C for chitin and 225^{0}C for chitosan. The weight loss of chitosan was shifted to lower temperature as a consequence of decreased acetyl content. Kittur et al.[58] described the thermal transition of chitin and chitosan and their derivatives by differential scanning calorimetry (DSC). This research observed an exothermic peak in chitin and chitosan occurring in the range of 390-430^{0}C which was shifted to lower temperatures with the increased content of N-deacetylation (25-89%). N-deacetylation of chitin under alkaline conditions caused substantial depolymerization due to glycosidic bond cleavage as a result of 'peeling' reaction. So it was reasonable to assume that a decrease in degree of polymerization could also lead to a decrease in thermal stability and this was also confirmed by analysing chitosan with the same acetyl content (but with different molecular weight 95000-8000) as the DSC curves shifted to lower temperature as the decreased molecular weight. Recent studiess [52, 60] investigated the comparison of X-ray powder diffractograms of chitin (α-form) and chitosan with different degrees of deacetylation (DD). It was found that the maximum peak intensity decreased with an increase of DD.

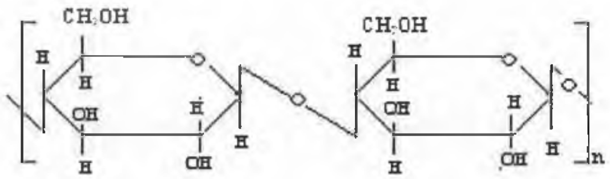

Cellulose

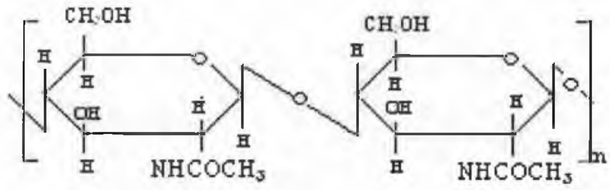

Chitin

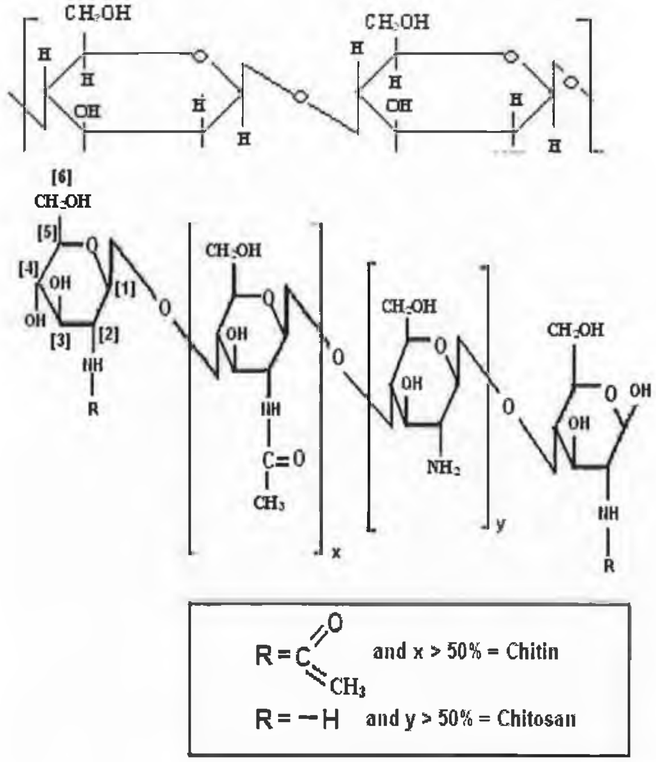

Figure 2.8. Structure of Chitosan , Chitin and Cellulose[54 , 55]

(b) Mechanical Properties

Now-a-days polymers are synthetic materials and their biocompatibility and biodegradability are much more limited than those of natural polymers such as cellulose, chitin, chitosan and their derivatives, despite the limitation in their reactivity and processability. In this respect chitin and chitosan are recommended as suitable functional materials because these natural polymers provide properties such as biocompatibility, biodegrability, non-toxicity and absorption properties [54, 61]. Chitin and chitosan obtained from crab shells also have high mechanical strength [62]. Tensile strength of chitin and chitosan were found to be around 45.3 and 67.9 MPa, respectively [62]. However, when they were annealed at 120^0C, the tensile strength was about three times larger (235 MPa) corresponding to the formation of intermolecular hydrogen bonds [62]. The tensile strength of chitosan that was prepared from chitin was found to be lower than those found naturally from crab shells but increased when grafted with 2-hydroxyethylmethacrylate (HEMA) upto 14-15 % , using a gamma-irradiation technique [63].

The formation of polymer matrix-calcium based composite materials in nature has allowed biomaterial's to use them as hard tissue substitutes in biomedical applications [65]. The combination of these polymer with hydroxyapatite (HA) has proven effective as a bone substitute material as mixture with polymers enhanced the osteo-conductive behaviour of HA allowing bone ingress into the receiving implant [65,66].

Wan et al. [67, 68] prepared a chitin-apatite composite using the freeze drying method to produce a highly porous structure bone substitute. The tensile properties of HA incorporated in a chitin composite showed that there was a decrease in the maximum tensile stress (72-28MPa) with an increase in percentage mass (0-50%) of HA in the composite, with as elongation at yield from 14.7 to 18.3%. HA-chitin composite suitable as a bone substitute material have also been developed by many authors [64,69].

One advantageous property of chitosan is that it can be molded into various forms and used to build up a porous structure [70, 71]. Porous scaffolds have been generated by freezing and lyophilizing chitosan solution or by processes such as an internal bubbling process (where $CaCO_3$ was added to a chitosan (CS) solution to generate CS-$CaCO_3$ gels. The pore size and orientation influenced the mechanical properties of these scaffolds and the tensile strength was reported in the range of 30-60 kPa [70, 71].

Several studies have concentred on the chitosan incorporated composite material in the development of bone substitute [66, 72-76]. Chitosan and β-tricalcium phosphate combination has also been investigated [61] and both the compressive modulus and yield strength of this composite were greatly improved with the ratio of 30/70 (weight % of chitosan/β-TCP). Other combinations of chitosan include; alginate [77], gelatine [78], starch [79], montmorillonite (hydrated sodium calcium Aluminium magnesium) [80], glycerol [81] and polycaprolactone [82] to improve mechanical, biological and the thermal properties of the composite compared to using pure chitosan [70]

Chitosan has also been used as a tableting excipient by direct compression [83, 84]. Directly compressed tablets of combined powders of lactose with chitin and chitosan with potato starch were also investigated by Sawayanagi et al. [85]. The properties of these tablets made from these powders , were compared with those of combined powders of lactose with microcrystalline cellulose (MCC) and potato starch with MCC. The reported hardness of the tablets followed the following order, the chitosan tablets yielded the highest hardness followed by MCC, followed then by potato starch and MCC, which were all harder that compressed chitin on its own.

2.4 Bioceramic/Biocomposite Applications

2.4.1 Biomedical Applications

Recently, bone bioceramic / biocomposite substitutes are mainly associated with therapeutic agents like proteins (growth hormone, bone morphogenetic protein) and antibiotics. As therapeutic agents are temperature sensitive, non-fired calcium carbonate materials have been also successfully developed [86,87]. Since the compressive strength of these non-sintered materials is weaker than in the case of conventional ceramics, the influences of process parameters, and their possible interactions, on the total porosity and compressive strength of non-sintered aragonite materials compacted at high pressure has also been investigated [88].

Calcium carbonate is widely used in the pharmaceutical powder industry and the pharmaceutical tablets are typically manufactured using the die compaction process. It has been reported that the mixture of calcium carbonate with other binders such as polyethylene glycols or lubricants such as microcrystalline cellulose, increased the overall strength of the compact [89,90]. It has also been reported that, the mixing of chitin and chitosan with other pharmaceutical powders can decrease the friction properties in direct compression processes [85].

The formation of polymer matrix-calcium based biocomposite materials in nature has allowed biomaterial's to use them as hard tissue substitutes or wound dressing in biomedical applications [65]. The combination of these polymers with hydroxyapatite (HA) has proven effective as a bone substitute material as this mixture has enhanced the osteo-conductive behaviour of HA allowing bone ingress into the receiving implant [65,66].

Several studies investigated chitosan incorporated into calcium based composite materials in the development of bone substitute [66, 72-76]. Chitosan and β-tricalcium phosphate combination has also been investigated [61] and both the compressive modulus and yield strength of this composite were greatly improved with the ratio of 30/70 (weight % of chitosan/β-TCP).

2.4.2 Biofiltration

Biofiltration is a promising air pollution control (APC) technology in which off-gases containing biodegradable volatile compounds (VOC) or inorganic air toxins are removed through a damp, porous medium on which an active culture of micro- organisms resides. The contaminants are transferred from the air phase to the water and are then biodegraded. Microbes have a simple life cycle; they are born, eat, grow, reproduce and die, where their diet is based primarily on carbon-based compounds, water, oxygen (for aerobic reactions) and macronutrients [91]. In biofiltration, microbes are used to remove pollutants from emissions by consuming the pollutants. Nature has provided bacteria and fungi that are capable of using almost any organic material as a food source and the end product of this degradation is generally carbon dioxide and water vapour. The concept is simple, but the execution can be quite complicated. Micro biological studies have offered a great help in understanding the operating mode of the microbes in biofiltration processes. In the US and Europe, biofiltration has developed since the early 1960s and is now successfully used in a variety of VOC control applications [92,93]. There are two common biological treatment systems ; biofilter and biotrickling filters (Figure 2.9). In biofilters, the porous bed of a biofilter is kept moist by controlling the humidity of incoming air and occasional water sprinkled, but for biotickling filters, water flows through the medium aided by continuous collection and recirculation. Successful operation of a biofiltration system requires knowledge and understanding of the physical and biological parameter involved, including air and contaminant load, medium characteristics, bed permeability, water content and biological activity [94].

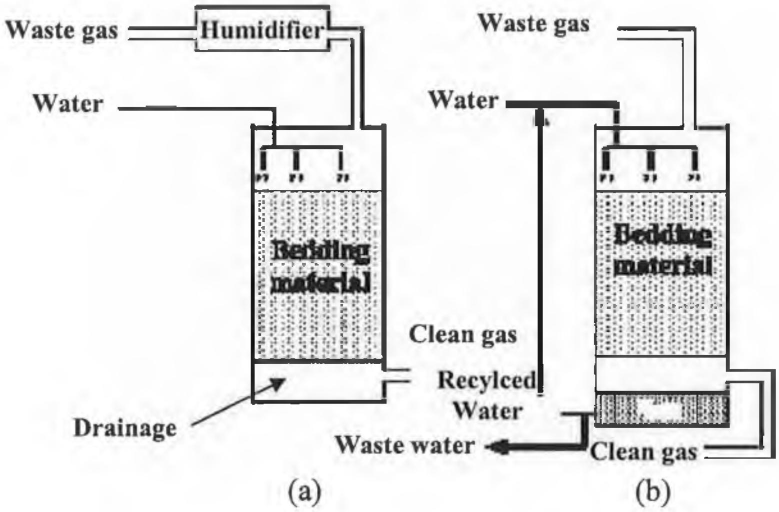

Figure 2.9. The two different constructions of biofilters treating gas: (a) Biofilters treating humidified gas. In these systems a small amount of water is sprayed upon the bedding material to maintain optimal water content. (b) Trickling biofilters - in these biofilters the gas is not humidified. The water trickles freely through the bedding material and is recycled to a certain extent [95].

(a) Filter Material

Biofilter performance is highly dependent on the nature of the carrier material or its filter bed. The filter beds are typically 1 meter in height [94]. To operate the biofilter efficiently, the filter material must meet certain characteristics. Firstly, it must provide optimum environmental conditions for the growth of the microbial population to accomplish high degradation rates. Secondly, the filter particle size distribution and pore structure should provide a large reactive surface and low pressure drop. Thirdly, the compaction should be kept to a minimum, reducing the need for maintenance and replacement of filter material and preferably low cost [94].

Huge investigations have been carried out on different types of packing material for the biofiltration process. Among them, compost has been reported to be the most common support media because of its low cost and high cleaning efficiency [96-98]. Other filter bed materials include peat, coal, wood chips, and some other organic materials which have shown better performance in removing H_2S or other volatile compounds [99-102]. The particle size of the filter material which is usually ground to a uniform size has been found to range from 20.34 μm to 25 mm [97,99,100, 103]. Hirai, et al. [104] described four inorganic packing materials and reported that the best performance was found when a porous ceramic was used. Lim, et al. [105] evaluated porous ceramics (used as microbial carrier in biofilters) fabricated by diatomite powder and fly ash using a foaming method. This research reported that a mixture of 95% fly ash and 5% diatomite yielded compressive strength of approximately 75.54 kg cm^{-2} (7 MPa) whereas pure fly ash or diatomite ceramic yielded 16.29 kg cm^{-2} (1.59 MPa) and 9.33 kg cm^{-2} (0.9 MPa) respectively. They also suggested that 14.26 μm was a reasonable pore size to allow micro-organism attachment. Leenen, et al. [106] characterised the natural polymer alginate and carrageenan and synthetic polymers such as polyvinyl alcohol, polycarbamoyl sulphonate and polyethylene glycol. The synthetic polymers showed better mechanical properties (tensile and compressive strength) than those found from natural polymers but diffusivity was higher in the natural polymer which aided cells growing in the interior of the supports. Moreover the procedure of preparing polymer beads was more hostile for synthetic polymer than natural polymers, and a high H_2S cleaning efficiency, greater than 95-98%, was found with natural polymer beads [95,106].

Phillips and Mullins [107] invented a new filter material; natural sea shell, especially half mussel shells in the treatment of H_2S or VOC and showed 99% cleaning efficiency. Under microbial action the H_2S converted to H_2SO_4 which caused the pH in the system to decrease and when it fell below pH 4.0 it prevented biological growth of the microrganism. Reaction between $CaCO_3$ and H_2SO_4, produce CaSO4, H_2O and CO_2 and this ensures acid neutralisation produced during filtration. It has been noted that the presence of carbon in a filter material increases the filters buffer capacity and it can reduce the required filter volume significantly [94].

Different types of micro-organisms have been used in the biofiltration process and the pH range of the filter material strongly affects their activity [95]. Sulphur oxidizing bacteria can live in a wide pH range 1-8 depending on the species [108]. For sea shell filter medium *Thiosphaera pantotropha, Thiobacillus, Nitrosomonas and Nitrobacter* micro-organisms have been used [107]. Micro-organisms have a dipolar character which means they can act as a cation or anion depending on the pH solution. It has been described that an increase in pH from 3 to 7.5 causes an increase in the cell charge from -10 to -30 mV while a decrease in pH causes a drop in the cell charge. Moreover low pH value conducts low negative cell charge which leads to a reduction in the electrostatic repulsion between the micro organisms and negatively charge bedding material and greater microbial attachment [95].

Gradual compaction of a filter material causes the air pressure to drop. The pressure drop depends on the way the filter materials are packed. So the degree of porosity is an important requirement for filter material not only for low pressure drop but also for micro-organism absorption. When the pore size is five times larger than the bacteria size, it has been found that maximum biomass occurred [95]. Yang and Allen [103] showed the effect of particle size on particle size of packing material as shown in Figure 2.10, for air flow rates.

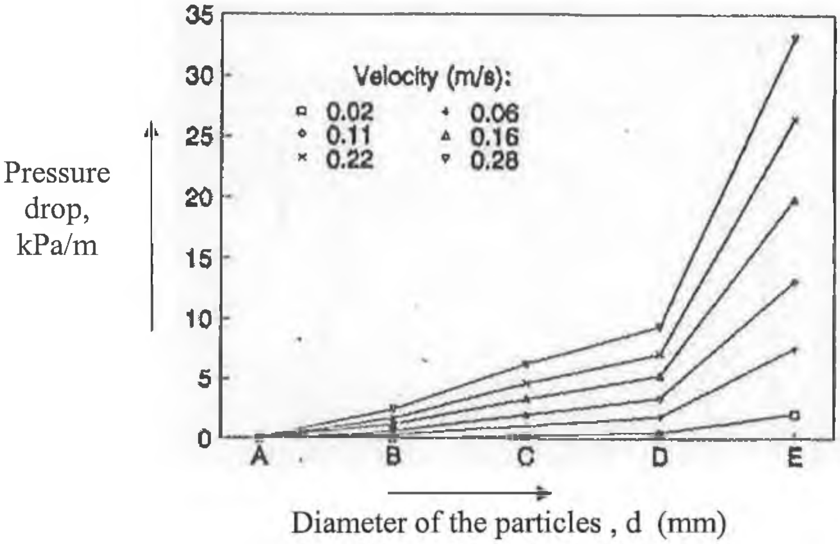

(b) Economic Comparison

Biofiltration is a cost effective technology and produces very small hazardous by-products [108]. Applications of this technology are currently increasing through a wider range of industries and expanding the list of airborne organics. Presently other APC (Air Pollution Control) technologies such as thermal and catalytic oxidation (incineration) absorption by activated carbon or condensation by refrigeration, compete with biofiltration process for removing H_2S or VOC from off-gases. These APC technologies suffer some technological disadvantages if applied to other types of off gases. The energy cost for biofiltration is typically one-forth to one-tenth the energy costs of thermal oxidation technologies [109]. Additionally, the capital cost for a biofilter system is typically two-thirds to three-fourths that of competing technologies [109].

Gero and Arthur [94] concluded the cost of the biofiltration system for Europe and US, which includes total operating and maintainace cost, to be approximately \$0.60 (0.5 euro) - \$1.50 (1.2 euro) per 100,000 cubic feet of off gas produced depending on the size of the filter. The cost for filters with multiple beds are twice as high. The appropriate choice of microorganism and environmental condition can reduce the filter bed size and make it more competitive with APC technology [94]. It has been suggested that an improvement of the physical properties and longevity of filter material are required because it will reduce cost for energy and also maintenance.

Hence this report sets out to produce a filter material made of $CaCO_3$ mixed with polymers such as chitin and chitosan, to be used in VOC air filtration systems. The method of producing this filter media is referred to as the compaction method.

2.5 Powder Metallurgical Process

The manufacturing of various products, parts and machine components through powder technologies has become a common process. Many specific properties can be obtained through these technologies that are inexpensive to produce compared to other methods. The powder metallurgy (PM) route generally compete with other technologies such as casting, forging and so on but has proven to have economic advantages because of the unit cost reduced with the increasing number of produced parts as shown in Figure 2.11.

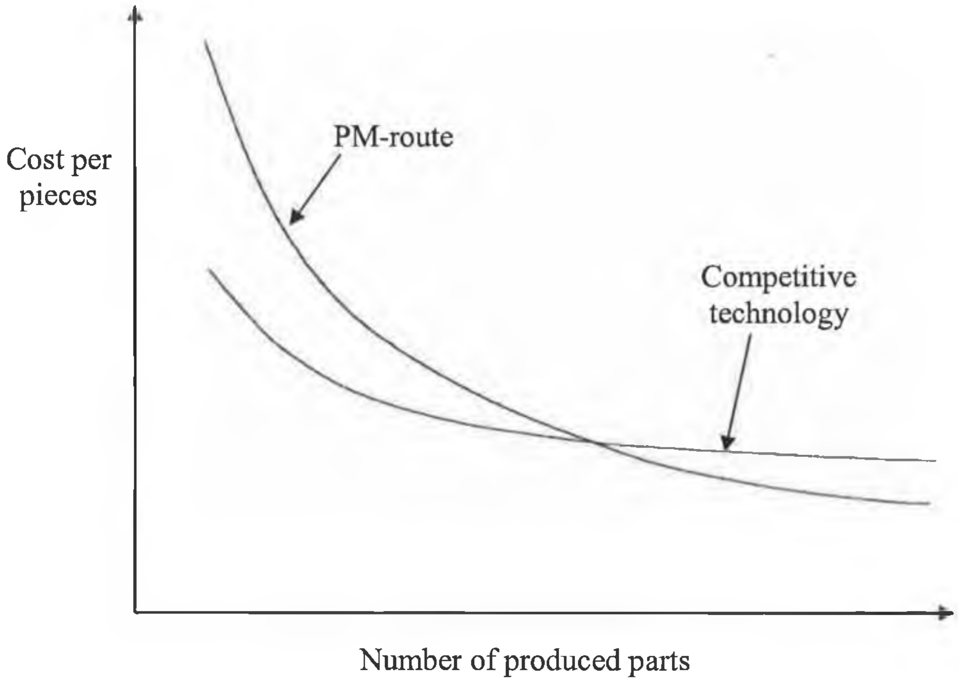

Figure 2.11. Schematic of the costs per piece against number of produced parts for the powder metallurgy route and for competitive technologies [110].

Different types of composites are most commonly manufactured using the powder metallurgy process. In ceramic metal composites the matrix may change from metallic to ceramic in nature, depending on concentration and processing route [110, 111]. Current research has reported an enhancement in mechanical properties of the ceramic composite through the powder processing route and has increased their applications. Some bio-ceramics such as Al_2O_3 ceramic, hydroxyl apatite, $CaCO_3$ ceramics [87,110, 112,113] are used as medical implants and have been produced having good mechanical properties.

PM processing of composite materials involves the mixing of metal or ceramic powder with suitable binder or lubricants to exhibit a uniform powder distribution throughout the matrix. Mixed powder is pressed by placing the powder into a die of desire shape and applying pressure to achieve the powder compact refered to as green compact. The pressed parts gain enough strength and toughness to allow them to be handled and machined. Increasing the pressure provides better packing and leads to decreasing porosity [113]. Sometimes the resulting properties of the green compact are unattractive. Therefore, sintering involves binding together the packed powder by heating the component to temperatures in excess of approximately half the absolute melting temperature, reducing the porosity due to shrinkage of the pore structure [113].

However, a porous compact with controlled pore characteristics fabricated by the PM process has a possible application in filters, flow reactors and air distribution surface processes. Important properties of the porous materials uses for filtration are, pore size, pore size distribution, porosity, permeability and surface area. Powder metallurgy filters are most effective in low viscosity fluids like gases [113]. However, Choi et al. [114] successfully manufactured a porous material filter via the PM route that resulted in higher permeability when coarse particles (420-840 μm) were used.

The following sections describe the different stages involved in the bioceramic/biocomposite processing route.

2.5.1 Mixing

Powder mixing is a fundamental, important and often the first processing step for many industrial processes. The widespread use of powder is attributable to both economic and technical factors; powder mixtures often are less expensive, have better compacting properties and sometimes permit shorter sintering times [115].

The mixing process can be performed in different rotating containers, such as a V-blender. This process is complex and depends on different factors [113,115]. The final mixing efficiency depends on particle size, powder volume, speed of the mixer and also mixing time. In some research cylindrical shape mixer has been used for calcium carbonate powders [89,90]. Though calcium carbonate powders have been used for different purposes especially pharmaceutical tablets via the PM manufacturing route, no literature has been found related to the effect of mixing process parameters on the properties of calcium carbonate powder.

2.5.2 Lubrication/Binder

Due to the friction between powder particles and the die wall at high pressure, ejection of the powder mass from the die becomes more difficult. Therefore lubricants are used to minimise die wear and for easy ejection from the die body. Materials that provide temporary bonds between the ceramic particles are referred to as a binder. Organic binders such as wax, or gums can act as lubricants during pressing and still give the pressed parts enough strength and toughness [116]. The organic binder can then be removed by thermal decomposition but if a reaction occurs between the binder and the base powder, the final part could become contaminated. Polymeric binders such as microcrystalline cellulose or polyethylene glycols can increase the strength of calcium carbonate compacts [89]. Soft binders have a tendency to produce flash between the die and the component thus causing sticking or reducing production rates. In general, the amount of the binder required is quite low, typically ranging from 0.5-5% [116]. Other binders such as starches or lignins can be classified as hard binders and they are not self lubricating and thus require small additions of lubricant prior to pressing.

Generally lubricants are premixed directly with the powders or brushed on the die wall pre-pressing. The compact ejection force is drastically reduced by the presence of lubricant and improves powder flow into the die. Therefore, lubricant mixed with the powder can reduce the green strength of the compact [113,115]. Thus it has been suggested that, lubricate the die wall be lubricated instead of mixing them with the powder [113]. In addition, the die wall lubrication offers the possibility of achieving the required density in a single pressing of a parts compared with conventional double pressing and double sintering route or by warm compaction techniques [117]. Dry lubricants such as zinc stearate powder have been commonly used as a die lubricant for ceramic manufacturing [118,119]. Graphite powder has shown the better lubricant ability when applied to dies [120,121]. Magnesium stearate powder has also been used as a die lubricant for calcium carbonate compaction in pharmaceutical applications [89].

2.5.3 Compaction

Compacting is one of the most controlling steps in the PM process. Loose powder is compressed and densified into a shape known as a green compact. During compacting, the powder particles move in the direction of the applied force. The powder does not flow like liquid, but develops an equal opposite force by means of friction between the particles themselves and the die surfaces. When the pressure is applied by only one punch, the maximum density occurs below the plunger and decreases as one moves down. On the other hand, a double punch press enables more uniform density to be obtained or thicker products to be compacted [3].

Isostatic pressing (IP) offers better mechanical properties than uniaxial pressing for calcium carbonate powders as reported by Lucus [88]. Tadic and Epple [122] proposed that cold isostatic pressing (CIP) of synthetic calcium base powders can be processed into objects of the desired shape with considerable mechanical strength, like a biomimetic structure, and also permit further mechanical shaping; by drilling or cutting. Isostatic pressing involves the application of pressure equally to the powder from all sides. In CIP, the powder is enclosed in a liquid tight rubber mold and immersed in the fluid (glycerine, hydraulic oil, water , or any other non-compressible fluid) in a pressure vessel. The fluid is pressurised, transmitting the pressure uniformly to all surfaces of the mold.

Uniaxial die compaction is widely used for making porous calcium based bioceramics [123,124]. Porous bioceramic were prepared using different pore formers and compact under the pressures in the range of 44-220 MPa and then drying them at low temperature to obtain the desired porosity. Sintering at higher temperature increases the mechanical strength of the bioceramics [88].

Calcium carbonate is also well known in the pharmaceutical powder industry and as pharmaceutical tablets are typically manufactured by the die compaction process. It has been reported that the mixture of calcium carbonate with other binders such as polyethylene glycols or lubricants such as microcrystalline cellulose, increased the overall strength of the compact [89,90]. For most powdered pharmaceuticals, the compaction of smaller particles results in stronger tablets because the smaller particles provide a larger total area for bonding than larger particles [125]. According to the Sawayangi, et al. [85], the mixing of chitin and chitosan with other pharmaceutical powders can decrease the friction properties in direct compression processes.

During the die compaction process, different mechanisms are involved to form the powder compact [115]. In the first stage, powder particles are restacked or rearranged. So that bridging, which always occurs in a randomly arranged stack of loose powder particles, is partially eliminated. Elastic and plastic deformation of the particles occurs in the second stage. The amount of the plastic deformation depends on the ductility of the powder material. Deformation is more extensive in the compaction of a ductile powder (metal) than in that of a brittle powder (ceramic). Lower compressibility results when powder particles are strain hardened during disintegration. In the third stage, the powder particles which are inherently brittle, as in ceramic powders, fracture under the applied load and form smaller fragments.

The green strength refers to the mechanical strength of the cold pressed powder compact. Powder characteristics such as particle size and shape can influence the green strength. Fine particles are difficult to press as large pores collapse under lower pressures than fine pores and hinder compaction and because of lower pressed density, fine particle size results in a decreased green strength unless the compaction pressure is increased [113]. Though the rate of densification is higher for large particle size and pack efficiency at low pressure [113, 125], the tensile strength increases with decreasing particle size [125,126]. The fragmentation of larger crystals under pressure reduces the effects of differences in initial particle size [125]. The particle shape has a similar effect. Irregular shapes give a lower apparent density and hinder achieving a high pressed density but can produce higher green strengths because of mechanical interlocking. Spherical powders exhibit high initial packing densities but cannot provide acceptable green strengths. Calcium phosphate powders used for bone materials were found to have morphological influences on their compaction properties, where fibrous graded compacts produced higher strength compared to more regularly shaped counterparts, due to differences in their surface areas [127]. The

particle size effect becomes more important as the particle shape becomes less regular [113].
Green strength is directly dependant on compaction pressure. Though green strength increases linearly with increasing pressure but it may be lower than expected at high compacting pressure or speed, due to air entrapment during compaction [115]. In general, green strength increases with the increasing intrinsic softness, or plasticity of the powder. If the compaction pressure exceeds the work-hardening capacity of a powder, particle fracture may occur and may cause green strength irregularities. Galen and Zavaliangos [128] observed that ductile powders have greater strengths than brittle powder in the transverse direction due to an increased crack deflection that results from greater particle overlap.

However increasing compaction pressure decreased the amount of porosity inside the compact [129-132]. Increasing porosity reduced the mechanical strength of the compact, as reported by many researchers [133-135]. It has been observed that compaction speed has less effect on the mechanical properties of brittle inorganic powder [136-138]. Nevertheless, pore morphology, stress concentration, pore size and distribution has an effect on the strength of the green compact [139-142].

For calcium base ceramics, the dynamic compaction technique has been used to avoid external high temperature heating [127,143]. This compaction is achieved by a shock wave produced by a piston impact or explosives placed around the powder. This wave deforms powder particles so quickly that inter particle melting and welding can occur, leading to the formation of grain boundaries. This allows powders to be consolidated without exposure to high temperatures and produces bulk material from powders at room temperature.

2.5.4 Sintering

Sintering is a series of complex processes, of which densification is only one phase. During the processing of powder metallurgy component, the sintering step subjects the fragile green compact to heating in a protective atmosphere to establish the desired mechanical properties. Green parts are heated to the sintering temperature, gases can be absorbed (hydrogen or oxygen) or evolved (nitrogen, hydrogen, or carbon monoxide). Grain growth also occurs as pores shrink and virtually disappear. On a microstuctural scale, cohesion takes place as necks grow at the point of particle contact. Thus properties of the powder compact in the green state are altered by sintering. Besides neck growth, the compact can densify, shrink, lose surface area, become stronger, increase in conductivity and become harder [113]. Increasing the sintering temperature decreases the amount of time required to achieve full density and over sintering.

The sintering process increases the mechanical strength of the ceramics which have been reported by different researchers [144,145]. Recent research focused on the properties of the calcium based bioceramics and they were improved by sintering at high temperature [146-148]. However, the mechanical property of the ceramics is dependent significantly on sintering temperature where higher temperature exhibited better results than the lower temperature [147]. Lin et al.[150] prepared porous calcium silicate ceramics and concluded that the mechanical strength and pore characteristics of the ceramic were affected by the sintering process. The result showed that the porosity decreased from 60 to 52 % and compressive strength increased from 6 to 20 MPa with increasing temperature of 900 to 1200^0 C.

High temperature sintering can cause defects in ceramics and deleteriously affect the material property. In ceramic technology, sintering is defined in terms of dimensional changes of shrinkages [113]. Shrinkage is the most common problem in the sintering process as it can result in crack and shape deformation which increases reject rate and cost per part [116]. Lower porosity can reduce this shrinkage effect during sintering. Rapid removal of the binder can also cause cracking of the part. Proper binder removal is normally accomplished by slowly raising the temperature to a level at which the binder can volatilise and holding at this temperature until the binder is gone. Ceramics are frequently prepared using a different starting composition to that desired as a final composition. However ceramic powders can decompose at high temperature and react with other constituents to form the desired composition. Thus carbonates, sulphates, nitrates or other salts are often used rather than the oxides, even though the final product is an oxide [116].

After reviewing the powder metallurgical processes, the uniaxial die compaction method has been selected for manufacturing artificial seashell like bioceramic/biocomposite in this present research due to low cost and high production rate. Chapeter 3 will describe the materials selections, processing equipment, processing steps and experimental designs to produce seashell like bioceramic/biocomposite. Characterization techniques of this new bioceramic/biocomposite are also discussed in chapter 3.

CHAPTER 3 EXPERIMENTAL EQUIPMENT AND PROCEDURES

3.1. Introduction

This chapter focuses on the biopolymer for the production of porous calcium carbonate bioceramics and biocomposites and the experimental equipment and procedures carried out to optimise the process parameters. The natural sea shell composition was followed during the material selection. Three sequential experimental designs were then conducted, each of which concentrated on different variables. The MODDE 7.0 software was used to develop those experimental designs and for all experimental designs, disk shape samples were prepared and analysed. Section 3.1 describes all of the experimental designs 1 to 3, indicating each of the variables and responses. Each experimental design was based on the results of the previous experimental design resulting in sequentially improving the final porous calcium carbonate compact. Furthermore, the fundamental steps in material processing for each experimental design will also be described.

3.2. Material Selection

A series of powder materials were selected based on the composition of natural sea shells.

3.2.1. Matrix Powders

Calcium carbonate (calcite) powder was selected as a synthetic shell material in this present work according to natural sea shell composition as described in the literature (given in Table 2.5). The theoretical density 2.7 gm/cc of the powder (was supplied by MINELCO SPECIALITIES Limited, England). The chemical composition of the powder is given below (supplied by MINELCO SPECIALITIES Limited, England).

Table 3.1 Chemical composition of the calcium carbonate powder.

Chemicals	**Percentage (%)**
Silicon as SiO_2	2-4
Aluminium as Al_2O_3	0.3-0.6
Iron as Fe_2O_3	0.05-0.25
Calcium as CaO	52-55
Magnesium as MgO	0.3-0.6
Potassium as K_2O	0.04-0.12
Loss on ignition (LOI)	41.5-42.5
Acid insoluble matter	4-5.5

3.3.2. Porogen agent or pore former

Naphthalene powder was used as the porogen agent to produce the required macro porous structure, and due to its low sublimation temperature. This porogen agent has also been used by other researchers [87,146].

3.3.3. Biopolymer

Chitin and Chitosan biopolymers were selected in this present work after thoroughly investigating natural sea shell organic layer compositions in literature.

3.3.4. Lubricant

To reduce the die wall friction between the calcium carbonate powder (plus porogen biopolymer mix) and to provide easy ejection of the compact from the die, a graphite powder was used as a lubricant in this work. Instead of mixing the lubricant with calcium carbonate powder, graphite powder was brushed onto the die wall. The graphite powder was selected as a lubricant on the basis of its lubricating ability on tungsten carbide dies [120].

3.3. Processing Equipments and Procedures

3.3.1. Powder Mixing

A V-shaped stainless steel mixer tool (Figure 3.1) was used to mix the powders used in experimental designs 1 and 2 (will be described in next section). Calcium carbonate and naphthalene powder were placed in the mixer and then sealed. The mixer was set up on a rotating chuck of a lathe machine and rotated at a speed of 50 r.p.m of 45 minutes [3]. The total (calcium carbonate + naphthalene) 100g powder mixture was prepared for each combination of naphthalene 5 % or 20% in experimental design 1 and 2. For 5% naphthalene, 95 g calcium carbonate and 5 g naphthalene were mixed. Consequently, for 20% naphthalene, 80 g of calcium carbonate and 20 g naphthalene powder were blended together.

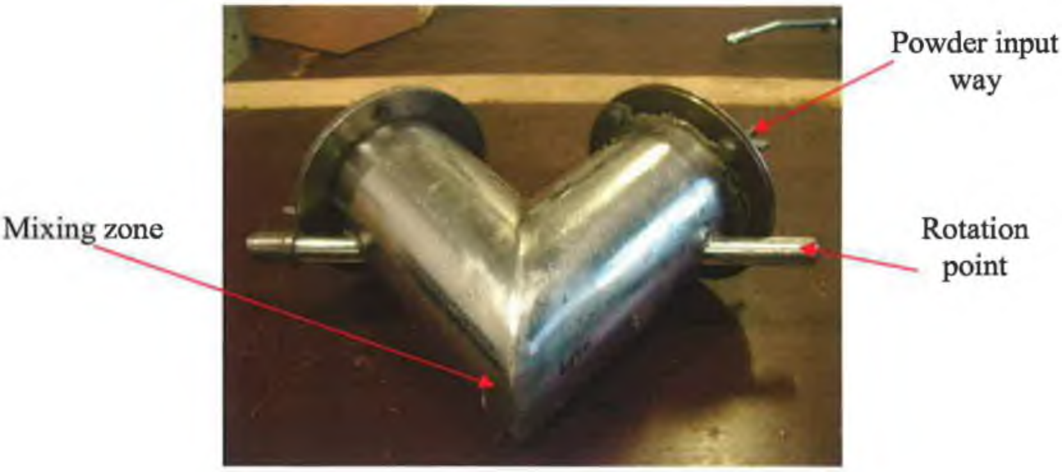

Figure 3.1. V-shaped mixture tool used for mixing powder in experimental designs 1 and 2.

As some agglomerates was observed during the experimental design 1 and 2 mixing process, a small plastic container was used to mix the powders used in experimental design 3 [3]. Figure 3.2 shows the mixing plastic container. In these tests a constant amount (20%)

of naphthalene powder was mixed with the predetermined quantities of calcium carbonate, chitin and chitosan powders. Individual powder was weighted in digital balance and put into the plastic container and shaken for 4 minutes. For each test a 20 g mixture of each combination was prepared.

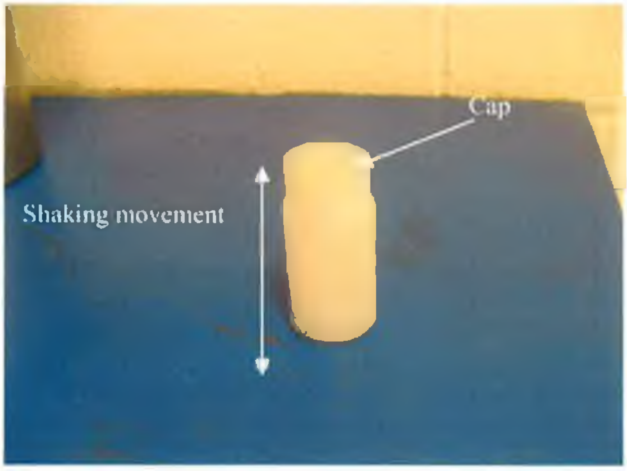

Figure 3.2: Small plastic container used for the mixing process in experimental design 3.

3.3.2. Powder Compaction

The compaction of powder mixture for all experimental designs was carried out using a 40 mm height floating die set as shown in Figure 3.3(a). The die set was designed to produce a compact of 17 mm diameter with different heights. The die body was made of cylindrical mild steel die body into which a hollow (internal 17mm diameter die cavity) cylindrical tungsten carbide insert was pressed. This prevented the die wall from galling and green compact surface damage from occurring [3]. Three pin holes in the die body (set at 120^0 from each other) were used to the align the compaction unit along guide pins (Figure 3.3(b)). The upper and bottom punches used to produce the compact height are also shown in Figure 3.3(a).

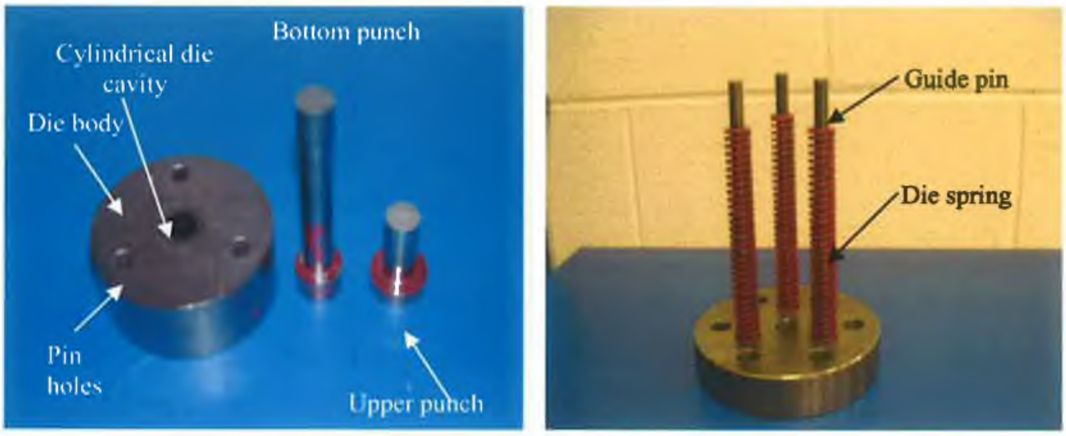

(a) (b)

Figure 3.3. Die set (a), Compaction unit (b).

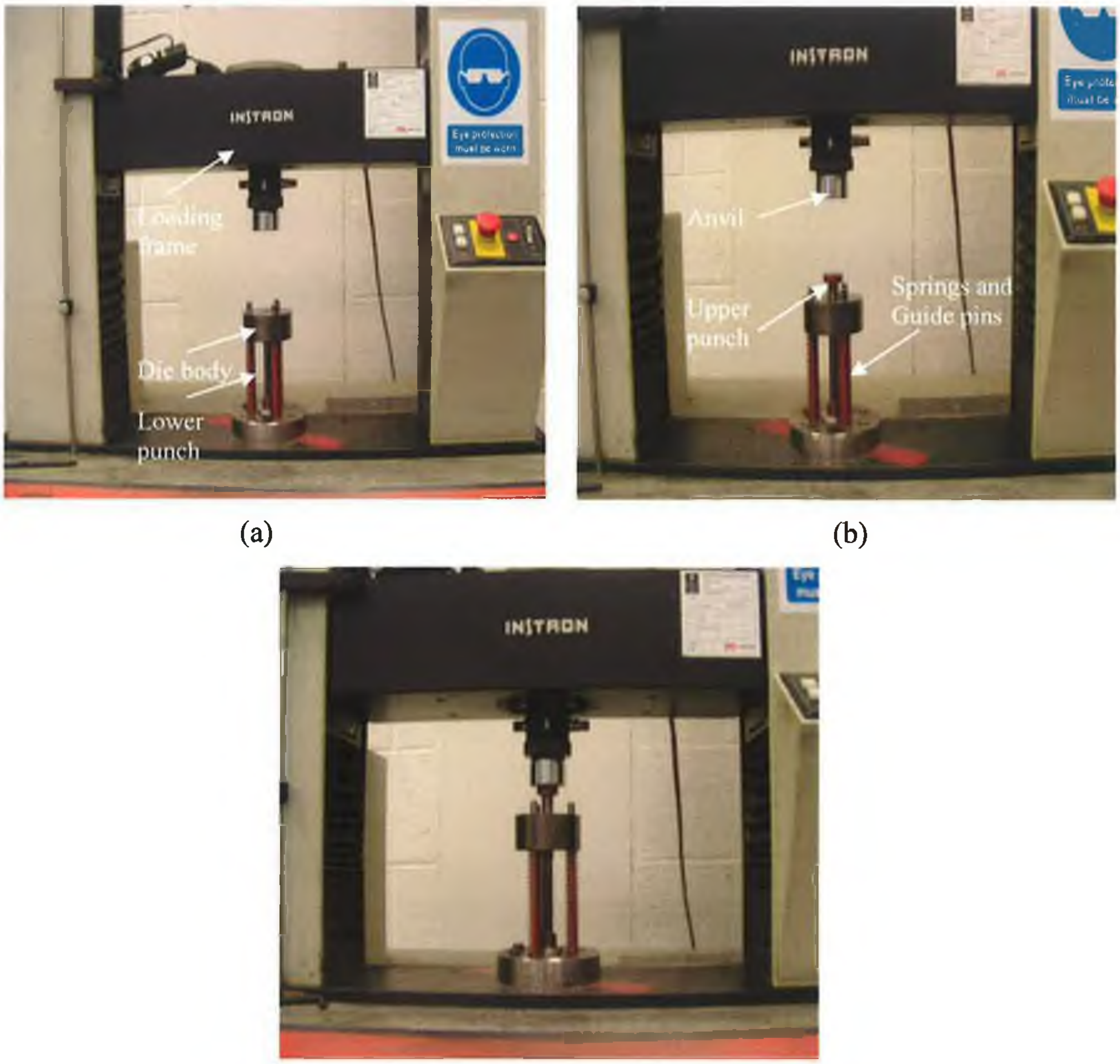

(a) (b)

(c)

Figure 3.4. Compaction set up steps; (a) compaction with bottom punch in position, (b) die cavity filled with powder and upper punch in position, (c) applying the load.

The die spring and guide pins located in the centre of each spring of the compaction unit allowed the vertical movement or floating action of the die body during the compaction process. The full compaction unit was set up with universal testing machine (INSTRON model 4204) as shown in Figure 3.4. The machine consisted of a loading frame and separate control unit. The maximum capacity (50 kN load cell) was used for powder compaction which resulted in a maximum pressure of 220 MPa applied over the 17 mm diameter die cavity. The machine allowed the user to change the limits of compaction pressure and compaction speed.

The die body was allowed rest on the die spring and the bottom punch was set up in position between 1 to 2 mm inside the die cavity.

Two grams of powder was weighted using digital balance (with an accuracy of ±0.01 g) and poured into the die cavity. The upper punch was inserted into the die cavity and the loading frame was moved down to make the contact between upper punch and the anvil as shown in Figure 3.4(c). The compaction parameters (compaction pressure and compaction speed) were set up according to the experimental designs 1 to 3. It should be noted that, for experimental designs 2 and 3, the compaction pressure (220 MPa) and compaction speed (20 mm/min) were kept constant as determined from experimental design 1.

The load/pressure was applied and increased gradually until it reached its maximum load/pressure. The load/pressure was held for 2-5 seconds and then removed. The upper punch was removed and two small blocks were placed on the die body to eject the compact as shown in Figure 3.5(a). The anvil was moved down manually and slowly ejected the compact as shown in Figure 3.5(b).

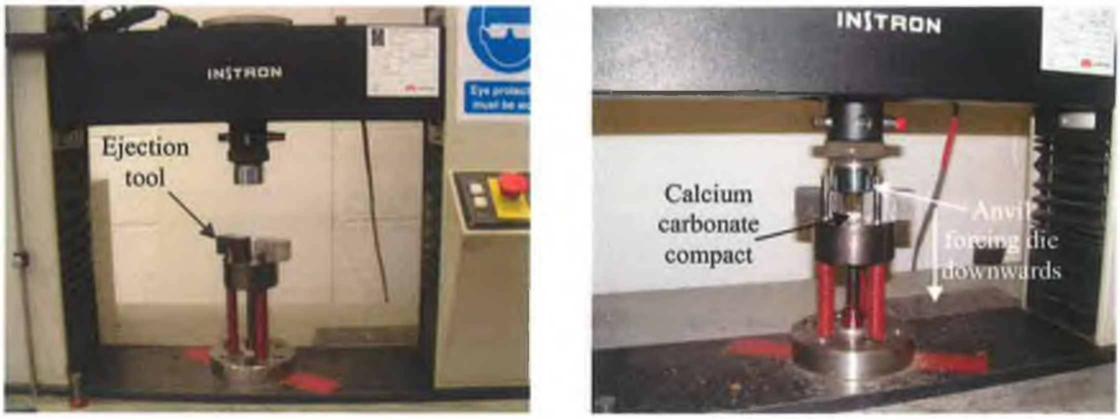

(a) (b)

Figure 3.5. Ejection set up steps; (a) positions of the two ejection tool on top of the die body, (b) load applied to eject the compact.

It should be noticed that, die cavity and punches were cleaned and lubricated after making every two samples to prevent sticking the sample inside the die. An example of two disk shape samples are shown in Figure 3.6.

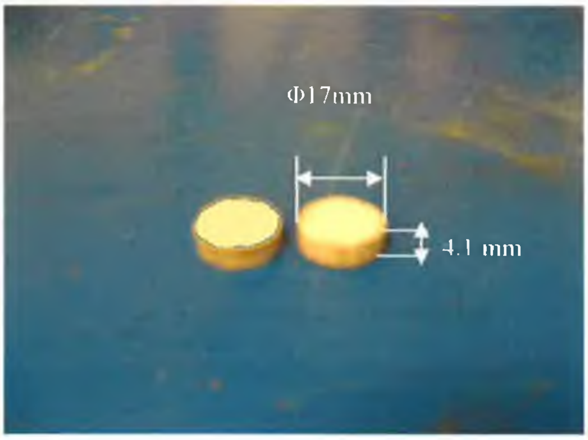

Figure 3.6 Disk shape samples

3.3.3. Post Heat Treatment

A drying step (post heat treatment) was carried out to burn off the pore former (naphthalene) in each of the experimental designs. All of the compacts prepared according to the experimental designs, were dried in a small furnace. The samples were heated to temperature 368 K for 2 hours (started at 298 K (room temperature) and increased by 278 K every minute and held then finally at 368 K). It has been already reported that naphthalene starts to change in to a gas at 323 K and burns out completely below 423 K [151]. The samples were then cooled slowly at room temperature inside the furnace. The drying temperature and time were chosen on the basis of the sublimation temperature of naphthalene used in previous research [87]. Low temperature drying was carried out in this research rather than high temperature (1273-1473 K) sintering due to the low temperature decomposition of calcium carbonate powder (953-1148 K) [152].

3.4. Experimental Designs

Statistical experimental design provides a powerful tool for analysing the effects of processing parameters for any manufacturing process. However it is important to select suitable limits for the process factors to ensure that the trends are identified satisfactorily. Each of the experimental designs were approached as follows:

(a) Experimental Design 1

The optimisation of the process parameters were investigated in experimental design 1, due to the lack of information about calcium carbonate powder in literature.

A full factorial experimental design (2^k, k=3) with interaction effects was built within the MODDE 7.0 software (Umetrics). Three factors were investigated: pore former (P_f, %), compaction pressure (P_c, MPa) and compaction speed (V_c, mm/min). The design involved eight experiments (Table 3.2) and the compact bioceramic properties were evaluated by analysing two responses: porosity (P_r, %) and compressive load (C_s, N). A second order polynomial model was used to describe the relationship between the response and tested factors:

$$\mathrm{Y} = \beta_0 + \sum_{i=1}^{3} \beta_i X_i + \sum_{i=1}^{2} \sum_{j=i+1}^{3} \beta_{ij} X_i X_j \text{ ....Equation (3.1)}$$

Where Y is the response, β_0 the constant coefficient, X_i and X_j the variables, β_i the linear coefficient and β_{ij} the interaction coefficients. The two responses (P_r and C_s) were then applied to this polynomial model

Table 3.2. Experimental design 1 used to optimise the process parameter responses for calcium carbonate bioceramic 1.

Expt No.	Variables				Responses		
	P_f (%)	P_c (kN)	P_c (MPa)	V_c (mm/min)	P_r (%)	C_s (N)	C_s (MPa)
1	5	30	132	20			
2	5	50	220	20			
3	5	30	132	30			
4	5	50	220	30			
5	20	30	132	20			
6	20	50	220	20			
7	20	30	132	30			
8	20	50	220	30			

The MODDE software was used to correlate between the factors and responses using the Multiple Linear Regression (MLR) method. Figure 3.7 shows the steps that were followed in material processing of porous calcium carbonate bioceramic 1 during the experimental design 1, plus their variables.

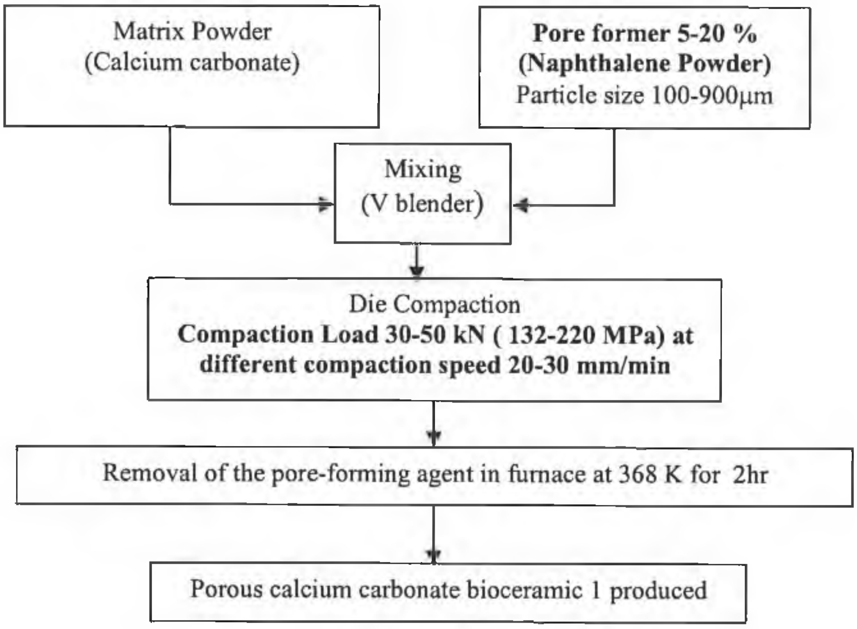

Figure 3.7. Fabrication chart of the processing of porous calcium carbonate bioceramic1

The porosity and compressive load of the porous bioceramic 1 were evaluated and entered into the MODDE7 software for statistical analysis. Characterisation (microstructural, phase analysis) of the porous calcium carbonate bioceramic 1 was also carried out.

(b)Experimental Design 2

Based on the results found from experimental design 1 the optimized parameters were used in experimental design 2. Due to the conflict information in literature, experimental design 2 was aimed to investigate the effect of the particle size of the pore former (naphthalene) on the properties (porosity and compressive strength) of porous calcium carbonate bioceramics. Four experiments were carried out in combination of with two particle size ranges and percentage of the pore former as shown in Table 3.3. The optimised process parameters; compaction pressure and speed were held constant.

Figure 3.8 shows the flow chart used in the processing of porous calcium carbonate bioceramic 2, where the porosity, compressive load and characterisation of porous bioceramic 2 were carried out.

Table 3.3 Experimental design 2 to optimise particle size of the pore former for porous bioceramic 2.

Expt No	**Naphthalene Size (μm)**	**Naphthalene (%)**	**Porosity (%)**	**Compressive strength**	
				(N)	**(MPa)**
1	250-350	5			
2	250-350	20			
3	400-600	5			
4	400-600	20			

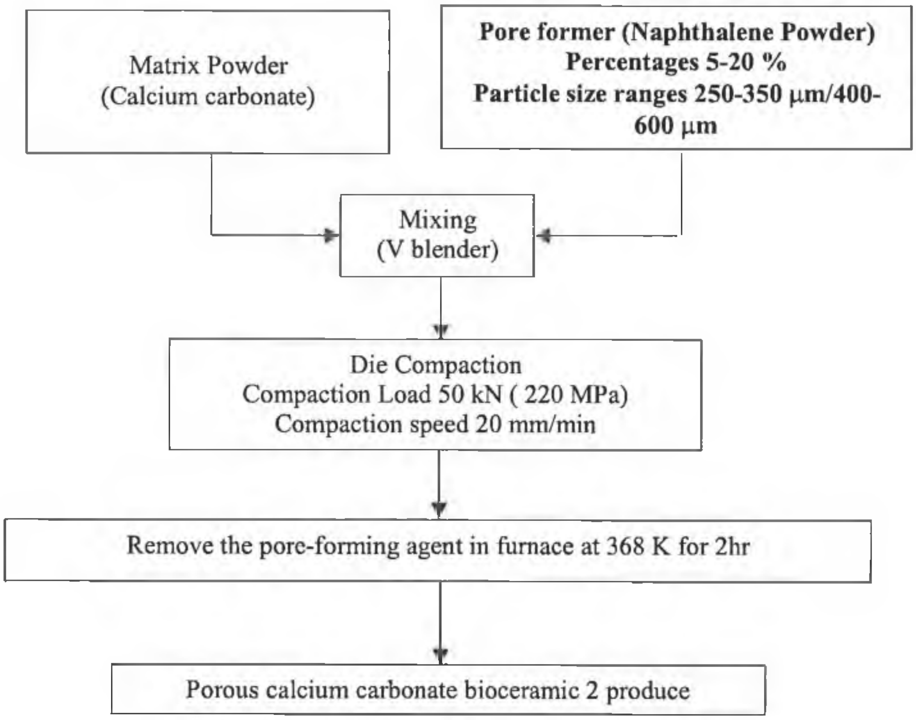

Figure 3.8. Fabrication chart of the processing of porous calcium carbonate bioceramic 2

Porosity , compressive load and microstructure analysis were carried out and compared with bioceramic 1.

(c) Experimental Design 3

The modified simplex centroid mixture experimental design 3 was developed using the MODDE 7.0 software to study the effect of the biopolymers on the compressive strength of porous calcium carbonate biocomposite. This mixture experiment was a special type of response surface experiment in which the factors were components of a mixture and the response was a function of the proportions of each ingredient. The mixture components could not range in an independent way as their sum had to be equal to 100% and specific experimental matrices and mathematic models have to be used [153, 154]. This approach is suitable for blending problems allowing investigation, with the least number of experiments, of the effects of changes in mixture composition and selection of the optimal composition for achieving the prefixed target [154]. In mixture experiments, the measured response is assumed to depend only on the relative proportions of the ingredient or components in the mixture and not on the amount of the mixture. The main distinction between mixture experiments and independent variable experiments, is that with the former, the input variables or components are non-negative proportionate amounts of the mixture, and if expressed as fractions of the mixture, they must sum to one. In the present case, where the powder mixture composition had to be optimised, the experimental range lay between 0 and 100% (wt%). Moreover, for economic considerations and to mimic the sea shell composition, constraints were applied to the proportions of the mixture constituents. Table 3.4 shows the restrictions imposed on the mixture component proportions.

Table 3.4. Restrictions of component proportions

Components (abbreviation)	Proportion restriction (%)
$CaCO_3$ (Ca)	0-100%
Chitin (Cht)	0-30%
Chitosan (Chs)	0-30%

The canonical form of the first-order mixture model used to describe the relationship between the response and tested factors is as follow:

$$E(Y) = \sum_{i=1}^{q} \beta_i x_i + \sum_{i=1}^{q} \sum_{i<j}^{q} \beta_i x_i x_j \quad \text{..............................Equation (3.2)}$$

Where Y is the response, X_i and X_j the variables (x_1= $CaCO_3$, x_2= chitosan, x_3 = chitin), β_i the linear coefficient and β_{ij} the interaction coefficients. The one response compressive load (Cs) was then applied to this model. Correlation between the factors and response were developed using the Multiple Linear Regression (MLR) method. This experimental design involved 12 experiments (Table 3.5) where the 11th and 12th experiments were the repetition of the 10th experiment as it was required for statistical analysis. Figure 3.9 shows the steps followed in materials processing for experimental design 3.

Table 3.5. Mixture experimental design 3 to optimise the biopolymers additions for porous biocomposite.

Expt No.	Variables			Response	
	Ca (wt %)	Chs (wt %)	Cht (wt %)	C_s (N)	(MPa)
1	1	0	0		
2	0.7	0.3	0		
3	0.7	0	0.3		
4	0.85	0.15	0		
5	0.85	0	0.15		
6	0.7	0.15	0.15		
7	0.9	0.05	0.05		
8	0.75	0.2	0.05		
9	0.75	0.05	0.2		
10	0.8	0.1	0.1		
11	0.8	0.1	0.1		
12	0.8	0.1	0.1		

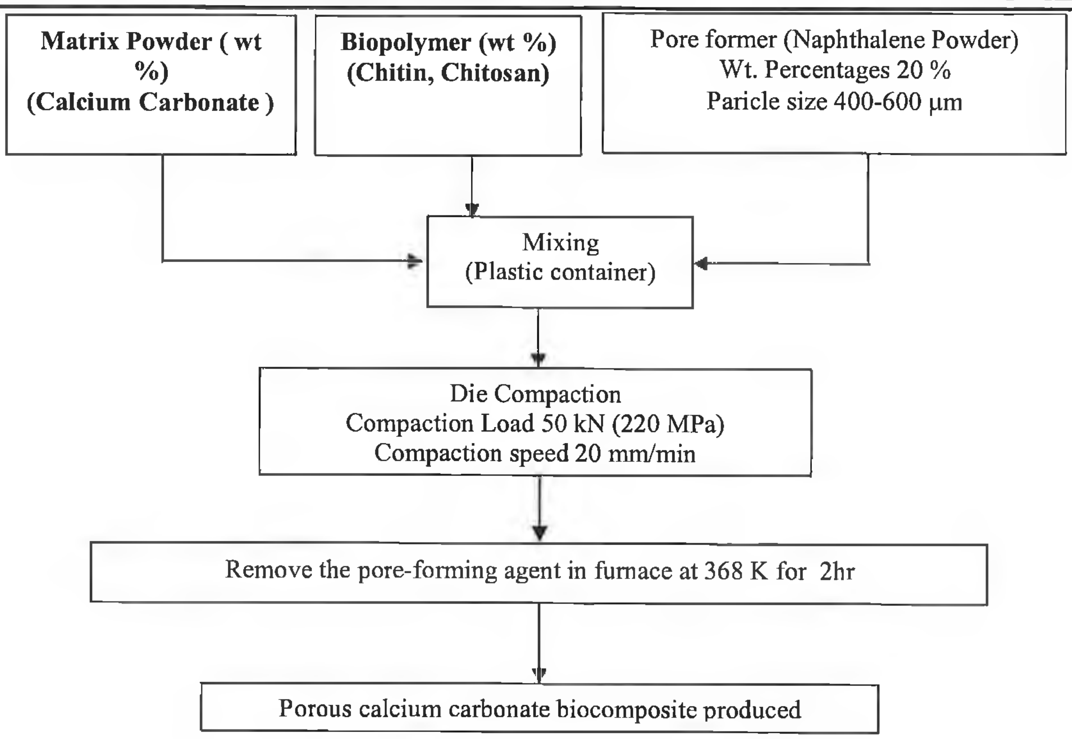

Figure 3.9 Fabrication chart of the processing of porous calcium carbonate biocomposite.

3.5. Analysis Equipment and Procedure

A series of equipments were used to characterise the powders and porous compacts so that the calcium carbonate porous bioceramics could fulfil their structural properties as a filter bed in air cleaning process.

3.5.1. Powder size and shape

Particle size analysis of the calcium carbonate powder was carried out using Malvern Mastersizer Particle Size Analyser followed by laser diffraction method. Naphthalene, chitin and chitosan does not dissolve in water, hence due to this limitation, their particle size and shape were examined using the Leica (Leo) Stereoscan 440 scanning electron microscope (SEM) instead of the laser diffraction method. For SEM observation, the powder samples were mounted on an aluminium stab covered with silver glue. All of the samples were coated with gold before observation, (due to low conductivity of the powders), to reveal the features of the individuals particle contained within the samples.

For experimental design 2, the two particle size ranges of the naphthalene were separated using sieve analysis. Firstly, the smaller particles (<250 μm) were removed by passing the powder through a sieve size of 212 μm. Sieve sizes of 355 μm and 600 μm were then used to prepare the 250-350 μm and 400-600 μm particle size ranges of the naphthalene respectively.

3.5.2. XRD analysis

X-Ray diffraction analysis were carried out to determine the structural phase change after post heat treatment process of porous bioceramic 1 using Bruker D8 X-Ray diffractometer with CuK$_\alpha$ radiation. On the basis of the results in experimental design 1, structural analysis of the porous calcium carbonate compact was not investigated in experimental designs 2 and 3.

3.5.3. Microstructural analysis

The SEM (scanning electron microscope) was used to investigate the microstructural analysis of the cross section of each porous calcium carbonate bioceramic 1. bioceramic 2, and biocomposite .

3.5.4. Porosity

Porosity tests were carried out for experimental design 1 and 2. Two samples were considered for each experiment. After drying the disk shaped sample, the density was calculated by [88]:

$$d_{\text{sample geometric density}} = 4m/\pi D^2h \text{......................Equation (3.3)}$$

Where h, D and m are the sample height, diameter and mass respectively. As diameter (17 mm) of every sample was constant, the height of the samples were measured by vernier scale to an accuracy ±0.01 mm. Then the total porosity of the bioceramic 1 and 2 was evaluated using [88]:

$$P=1-(d_{\text{sample geometric density}}/d_{\text{calcium carbonate powder}}) \text{......Equation (3.4)}$$

Where $d_{\text{calcium carbonate powder}}$ was 2.7 gm/cm^3 (MINELCO SPECIALITES Limited).

3.5.5. Compressive Load

As filter bed compaction upon themselves is one of the problems in the biofiltration process, the compressive load/strength of the porous bioceramic/biocomposite has been measured similar to the work carried out by other researchers [118]. The compressive load test was carried out in all experimental designs and on natural seashell. The compressive strength was measured using the INSTRON 4204 testing machine, with a 500 N load cell used for the natural seashell, porous bioceramics 1, 2 and 50 kN load cell for the porous biocomposite. All samples were compressed vertically at a cross head speed of 4 mm/min [47]. In the case of seashells, the load was applied to the dome shaped single part of the shells. The samples yield point was taken from the graphical observation of load and extension recorded by the machine. In each experiment two samples were tested and the load-displacement behaviour of each experiment during compressive strength testing was analysed. Compressive strength (MPa) of the bioceramics/biocomposties were also calculated. It should be noted that due to the complex shape of the shells, it is very difficult to measure the area at the load point. Therefore, the results analysed in the next sections are presented as compressive load instead of compressive strength to enable direct comparison between natural seashell and porous calcium carbonate compact.

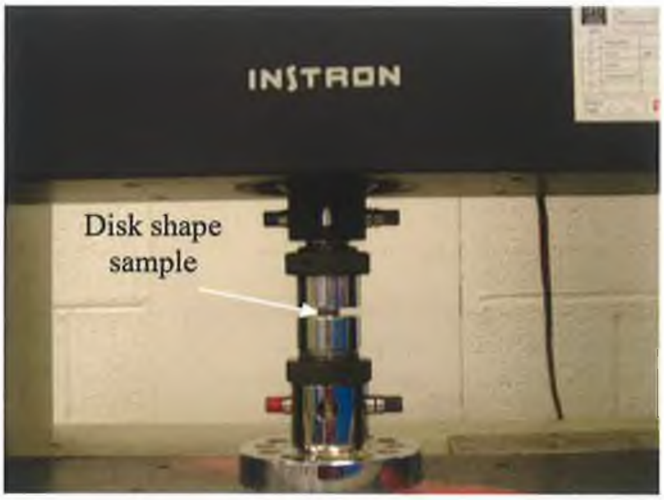

Figure 3.10: Compressive strength test setup

CHAPTER 4 RESULTS AND DISCUSSION

4.1. Introduction

This chapter investigates calcium carbonate powder used to produce a filter biocomposite/bioceramic with controlled porosity and compressive load using the uniaxial die compaction technique. This chapter describes the results and discussion of the experimental work carried out according to the experimental procedure described in Chapter 3.

This investigation was carried out in three steps. First, analyzing the influence of pore former, compaction pressure and speed on calcium carbonate bioceramic porosity and compressive load using a full factorial experimental design (2^3) with interaction (8 experiments). In the second step, the effect of pore former particle size on the bioceramic properties was investigated by testing two particle size ranges. In the third step, to improve the bioceramic strength, powder combinations ($CaCO_3$/chitin/chitosan) were tested and the effect of polymer addition percentages on the compressive load and porosity were studied using a modified simplex centroid mixture experimental design (12 experiments).

Statistical analyses were carried out for experimental design 1 and 3 by using the software MODDE 7. Characterisations of porous calcium carbonate compact were carried out for every experimental design 1 to 3. The properties of the natural seashell were investigated and compared with porous calcium carbonate compact. It should be noted that due to equipment limitation, porosity tests of the natural sea shell were not measured in house. All of the information about the porosity of natural seashells was collected from literature. The behaviour of the porous calcium carbonate biocomposite was also tested in the presence of water and steam.

4.2. Powder size and shape analysis

Pre-pressing, both laser diffraction analysis (Figure 4.1) and the microstructure (Figure 4.2(a)) of 3 samples of the calcium carbonate powder showed their particle size range to be between 0.2-10 µm in irregular shape. SEM micrograph of naphthalene powder was also examined and wide range of particles size ranging from 100-900 µm of irregular and nodular shape naphthalene was observed in the micrographs, see Figure 4.2(b). Figure 4.3 shows the SEM micrographs of chitin and chitosan. Elongated flake shape chitosan was observed with a size range of 1000-4000 µm. Figure 4.3(b) shows the mixture of flat round and fiber shape flakes of chitin with a size range of 1000 – 2500 µm.

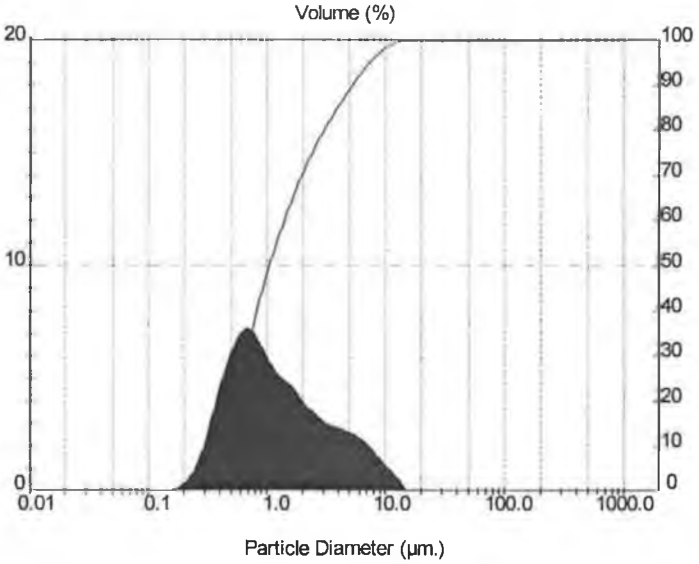

Figure 4.1 Particle size distribution of as received $CaCO_3$ powder.

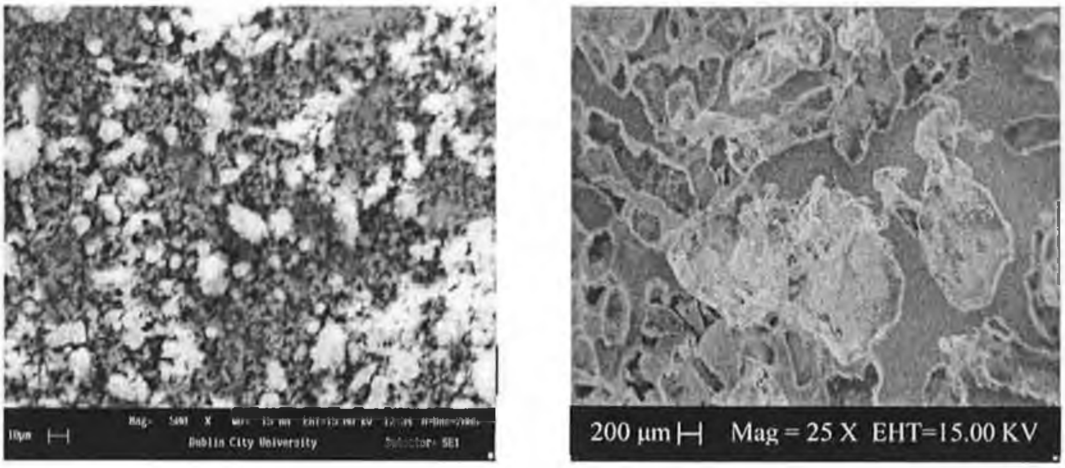

(a) (b)

Figure 4.2: Scanning electron micrographs of (a) Calcium carbonate, (b) Naphthalene powder.

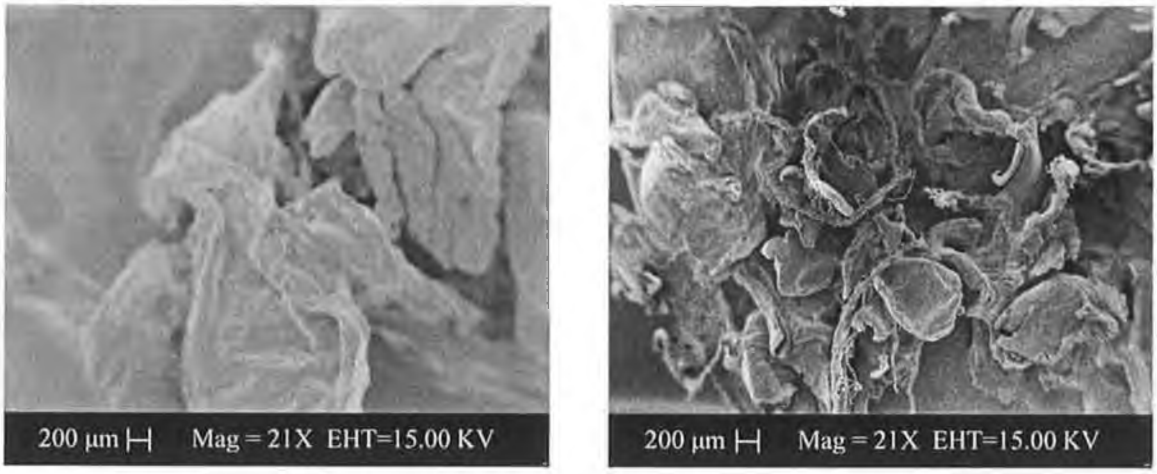

(a) (b)

Figure 4.3. Scanning electron micrographs of (a) Chitosan, (b) Chitin powder.

The summary of the observed powder size and shape is represented in Table 4.1.

Table 4.1. Powder size and shape analysis

Powder	**Particle size**	**Particle shape**
Calcium Carbonate	1-10 µm	Irregular
Naphthalene	100-900 µm	Nodular and Irregular
Chitosan	1000-4000 µm	Flat and elongated shaped flakes
Chitin	1000-2500 µm	Mixture of flat, round and fiber shaped flakes

4.3. Effect of the porogenic agent, compaction load and speed on the porosity and compressive load of the porous bioceramic 1

4.3.1. Full factorial experimental design

To study the influence of the naphthalene used, compaction load and speed, on the porosity and compressive load of the calcium carbonate bioceramic 1, a full factorial experimental design with interaction was built. The design involved eight experiments (Table 4.2) and the compact bioceramic properties were evaluated by analysing two responses: porosity ($P_{r,}$ %) and compressive load (Cs, N). The results were analyzed and are discussed in the following sections.

Table 4.2. Porosity (P_r) and compressive load (C_s) of bioceramic 1 for various conditions; pore former fraction weight (P_f), Compaction force (P_c) and speed (V_c)

Expt No.	Variables				Responses		
	P_f	P_c		V_c	P_r	C_s	
	(%)	(kN)	(MPa)	(mm/min)	(%)	(N)	(MPa)
1	5	30	132	20	33.60	52.161	0.229
2	5	50	220	20	31.32	53.033	0.234
3	5	30	132	30	32.23	52.805	0.232
4	5	50	220	30	30.09	54.678	0.241
5	20	30	132	20	51.40	50.212	0.220
6	20	50	220	20	50.33	50.309	0.222
7	20	30	132	30	51.34	49.409	0.218
8	20	50	220	30	50.00	50.267	0.221

4.3.2. Data analysis

Statistical analysis of the obtained data was performed using the MODDE 7.0 software. The analysis of the regression coefficients of the polynomial models describing the relationship between porosity (P_r) and compressive load (C_s, N) and the three factors (P_f, P_c, V_c) are presented in Table 4.3. It indicates that the two responses (P_r, C_s) were best described by the polynomial models from the coefficient of determination (R^2).

Table 4.3: R^2 of the polynomial models and P-values of both linear and interaction effects of P_f, P_c and V_c for the porosity (P_r) and the compressive load (C_s ,N) of the produced bioceramic 1.

	R^2	Constant	P_c	V_c	P_f	P_c*V_c	P_c*P_f	V_c*P_f
P_r (%)	1.000	0.000780	0.0646923	0.0941225	0.00506146	0.380172	0.124442	0.29198
C_s (N)	1.000	0.000370	0.0412377	0.104856	0.0122415	0.086105	0.0486588	0.048658

In terms of porosity (P_r), the statistical analysis of the data showed that P_f and P_c were the most significant factors ($P_{value} < 0.05$). For both Pr and Cs neither V_c nor the interaction effects (P_c*V_c, P_c*P_f , V_c*P_f) were significant. Only P_f, P_c and P_f*V_c had a significant effects on the compressive load.

The non significant effect of the compaction speed can be attributed to the fact that the calcium carbonate powder is a brittle inorganic material. In fact, under compression, brittle materials consolidate predominantly by fragmentation whereas plastic materials deform by plastic flow [136]. Therefore, compaction of brittle materials is less speed dependent because fragmentation is rapidly achieved, and prolonged exposure to the force has a more limited effect on bio-ceramic properties [136]. The compaction of brittle powders has been reported by others to be unaffected by the compaction speed [137, 138].

After the elimination of the non significant coefficients ($P\text{-}_{value} > 0.05$) the reduced models for porosity (P_r) and compressive load (C_s) may be expressed as follows:

$$P_r = 41.1644-0.729375 (P_c) + 9.35438 (P_f) \text{.....................................Equation (4.1)}$$

$$C_s = 51.6092 + 0.4625(P_c) -1.56(P_f) + 0.180497\ Vc - 0.391747(V_c*P_f) \text{....Equation (4.2)}$$

These two models show that the higher the amount of pore former (P_f) used, the higher the ceramic porosity and the lower the compressive load achieved. The decrease of ceramic strength is obviously due to the low strength porous structure left behind after post heat treatment. The compact pressure (P_c) also had a significant effect, but more on the porosity than the compressive load. In fact, increasing P_c led to an increase of compressive load but a decrease in porosity. The relationships between the factors and responses could be best understood by examining the isoresponse surfaces. The isoresponse representations are generated by plotting contours of the response versus both factors (Figure 4.4).

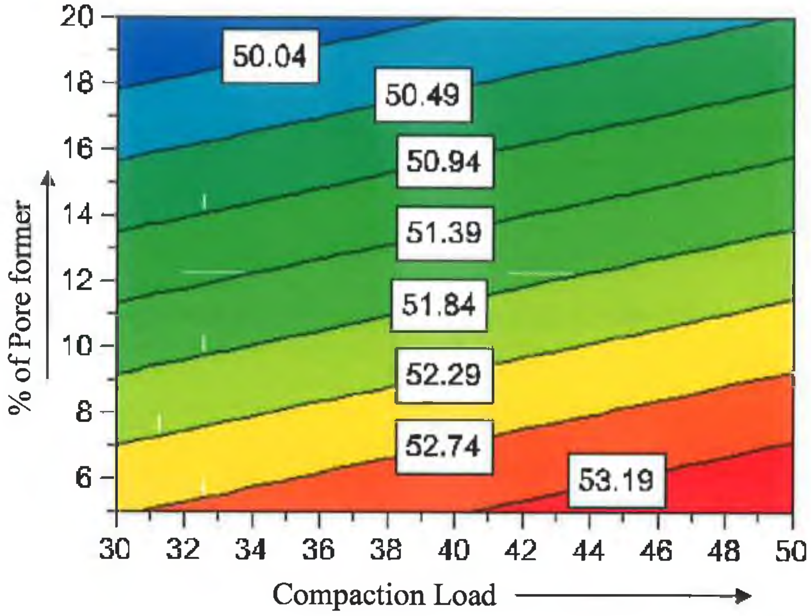

(a) Compressive Load

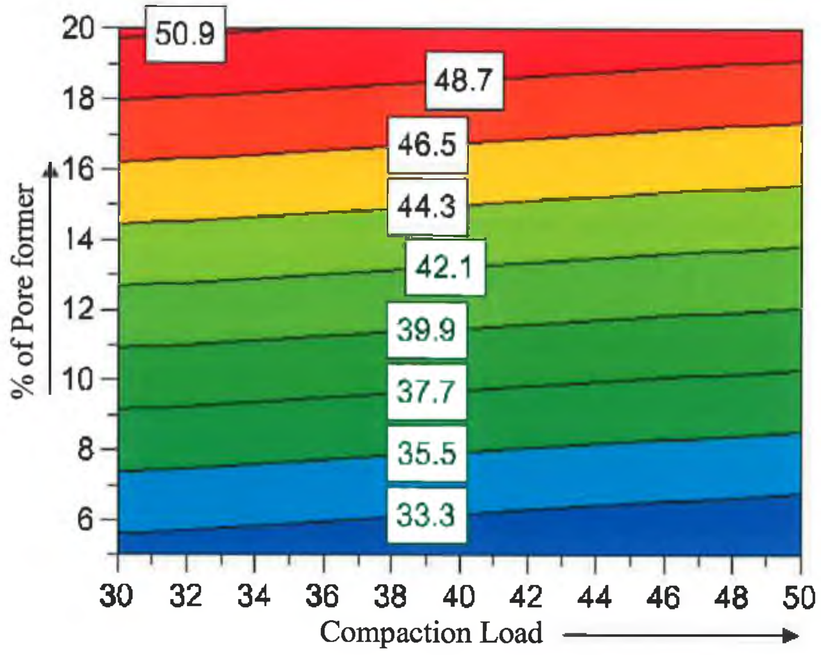

(b) Porosity

Figure 4.4. Isoresponse contour plots showing the effect of pore former amount and compaction load (kN) on (a) the compressive load, Cs (N), and (b) porosity, Pr (%).

Figure 4.4 (a) shows that the best compressive loads are obtained when a low pore former amount is used and high compaction force is applied. As an illustration, a compressive load of more than 53.19 N (0.234 MPa) is reached when only 6% of pore former was added to the calcium carbonate and a compaction force of about 44 kN (193.95 MPa) is applied. This is in agreement with the results published by Lucas-Girot et al. [88] who demonstrated that the compressive load was higher when their material was compacted at 750 MPa compared to 450 MPa. The strength-pressure relationship can be also defined by the following model of green strength dependence on compaction pressure [113]:

$$\sigma = B'\sigma_0 \mathrm{P} \quad \text{..........} \text{Equation (4.3)}$$

Where σ is the resulting strength of the material, B' is a material dependent constant, σ_0 is the wrought (initial) strength and P is the applied pressure. This model suggests that as pressure is increased, the strength increased.

As illustrated in Figure 4.4(b), the higher porosity is obtained when a higher amount of naphthalene is used. Indeed, porosity increased from 30.69 to 51.40 % when the percentage of pore former was increased from 5 to 20%. These results are in accordance with those reported by Lin et al. [129] and Soares et al. [130]. In addition the compaction force has a negative influence on the porosity. This behaviour is due to the fact that the increasing pressure provides better packing density and leads to decreasing porosity which can be explained by the following expression [113]:

$$\frac{d\varepsilon}{d\mathrm{P}} = -\mathrm{K}\,\varepsilon \quad \text{..........} \text{Equation (4.4)}$$

where P is the applied pressure , ε is the fractional porosity, and K is a proportionality constant. Rearranging and integrating Equation (4.4) gives the following expression:

$\ln \left(\frac{\varepsilon}{\varepsilon_a}\right) = - KP$ ....Equation (4.5)

where ε_a is the apparent porosity at the before compaction.

4.3.3. Data optimisation and Validation of the models

To determine the optimal operating conditions to produce a bioceramic with a high compressive load and an acceptable porosity mimicking the sea shell properties, the optimiser function of MODDE 7.0 was used (Table 4.4).

Table 4.4. Optimal pore former amount and compaction load obtained by MODDE 7.0 optimiser.

Compaction load/pressure		Speed (mm/min)	Pore former (wt%)	Compressive Strength		Porosity (%)
(kN)	(MPa)			(N)	(MPa)	
49.9999	220.39	29.6968	6.129	53.8791	0.237	31.8995
49.1724	185.89	20.0001	19.9794	50.3642	0.222	50.6837
48.5213	213.88	29.9997	5.6461	53.9674	0.238	31.3574
47.3511	208.72	20.0001	20	50.6005	0.223	50.3313
49.9999	220.39	29.9997	14.1342	51.827	0.229	42.0067
49.7974	219.50	30	5.6652	54.0215	0.238	31.2884

The adequacy of the models describing the porosity (Pr, %) and compressive load (Cs, N) was examined by an additional independent experiment using 20 % of naphthalene and applying a compaction load of 50 kN (220 MPa). The comparison of predicted (Pr= 50.6837 %, Cs= 50.3642 N and experimental (Pr= 50.33 %, Cs= 50.309 N) bioceramic 1 properties indicates good agreement between these data, indicating that the empirical model could be used to describe the relationship between the factors and the porosity and compressive load for the manufacturing of $CaCO_3$ based porous bioceramic using the uniaxial die compaction process. Thus, the parameters followed in experiment 6 (Table 4.2) were shown to be the optimum combination and these were used for next experimental design 2.

4.3.4. Relationship between porosity and compressive Load

As demonstrated by the two models, the compact pressure (P_c) has a positive significant effect on the compressive load but a negative influence on the porosity. In fact, increasing P_c leads to an increase of compressive load but a decrease in porosity. Similar results were already reported [88, 131, 132] for calcium based materials. For each of the porosity and compressive strength tests, 3 samples were used in each experiment and the mean values are presented in Figure 4.5.

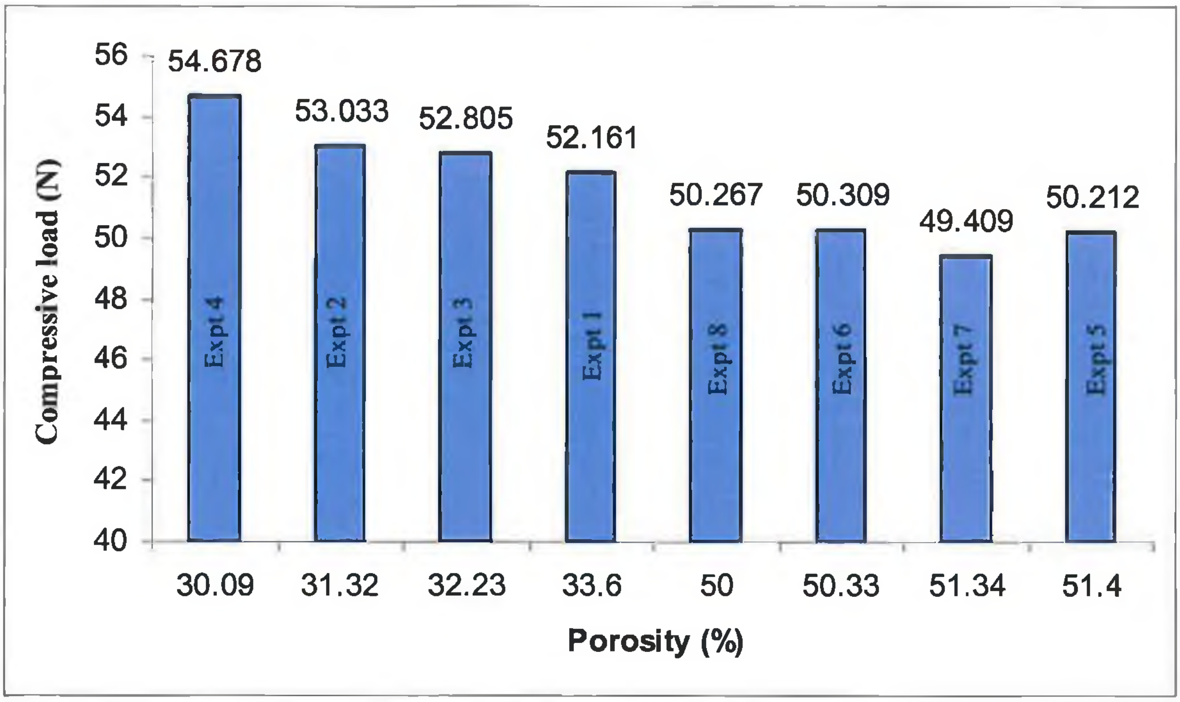

Figure 4.5. Effect of porosity (%) on compressive load (N)

These observations demonstrate that there is a direct relationship between the porosity and compressive load. In fact, an increase of bioceramic porosity provokes a decrease of its compressive load. This is in accordance with data reported by many researchers [133 -135]. In this experimental design the pore former particle size used was between 100 µm-900 µm. In these results a major change in compressive load (49.409-54.678 N) with increasing porosity, was not observed (Figure 4.5). This may due to the use of a wide particle size range and non uniform porous structure. In fact, the compressive load depends not only on the porosity percentage but also on the pore morphology, stress concentration, size and distribution [139, 140], which was not taken into account in this work.

4.4. Characterization of porous bioceramic 1

To understand the effect of porous structure on the compressive load of the porous calcium carbonate bioceramic 1, microstructural analysis were performed at different magnification as described in Section 4.4.1. The behaviour (brittle or ductile) of porous bioceramic 1 during compressive load tests were explained by load-displacement curve (Section 4.4.2). In Section 4.4.3. the determination of the complete burn out of naphthalene powder is described.

4.4.1. Microstructure Analysis

Figures 4.6 (a-c) shows the microstructure of a cross section of porous bioceramic 1 at different magnifications. Different size and shape of the macropores of approximately 100-900μm have been observed in Figure 4.4(a). It is obvious that the wide range of naphthalene particle sizes used created different macropore sizes and consequently a non-uniform porous structure in bioceramic 1.

Microstructure observed at higher magnification (Figure 4.6(b)) shows micro pores with a size of ~1μm and interparticle porosity (Figure 4.6(c)). A similar type of microporosity has been observed by other authors for calcium based material [87, 123]. These micrographs confirme that not only the percentage of porosity influences the strength of the porous bioceramic but also that different sizes and shapes of the porous structure have a significant effect on reducing the compressive load. In addition, the microporosity may have assisted the crack propagation during compression and contributed to its low strength. Porous structures are desirable as a filter bed media in biofiltration processes as they provide a large reactive surface, producing low pressure drops during air flow treatment [94].

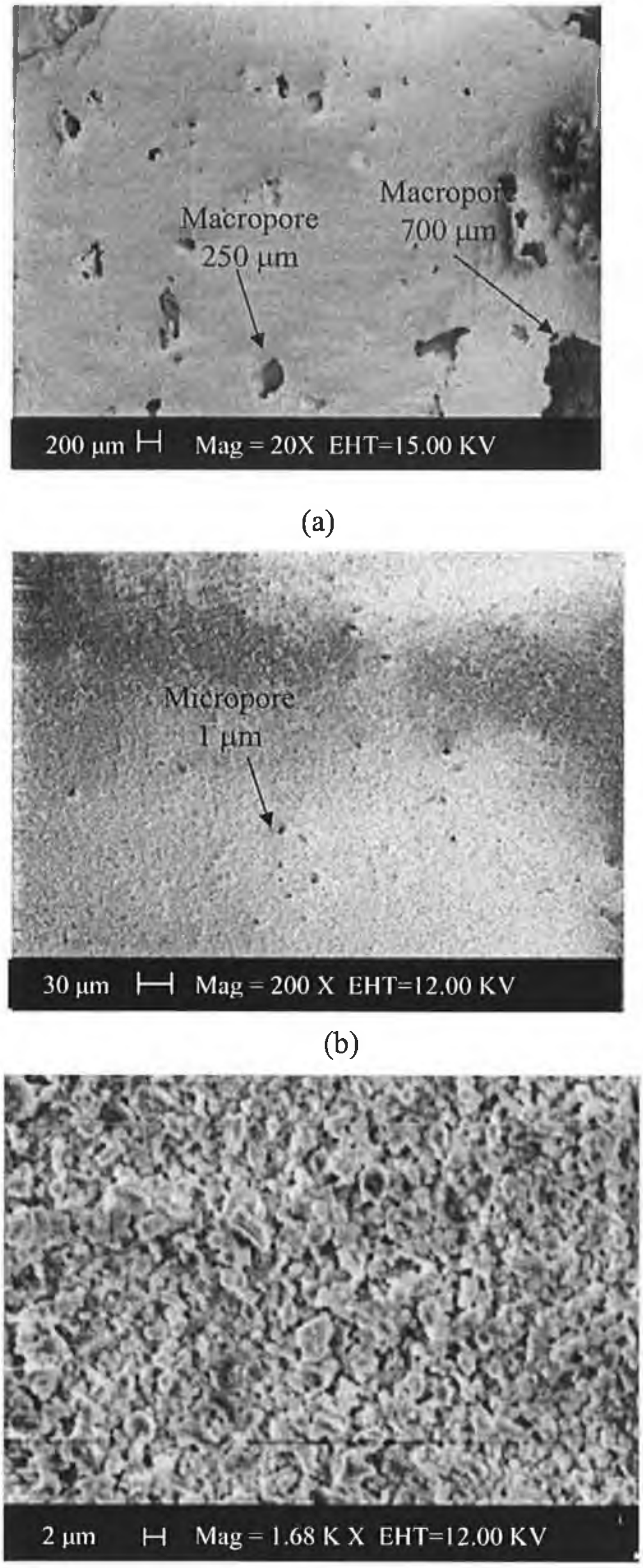

(a)

(b)

(c)

Figure 4.6. Cross sectional scanning electron micrographs of the porous bioceramic 1 in different pore size range (a) macroporosity ; 100 – 900 μm , (b) microporosity ; ~ 1 μm , (c) interparticle porosity.

4.4.2. Load-displacement behaviour of calcium carbonate bioceramic 1

The load-displacement behaviour of the eight produced calcium carbonate based bioceramics were determined (Figure 4.7). It shows the typical load displacement curve for the porous bioceramic under compression testing. In the initial stage the load increased linearly. This corresponds to the linear elastic behaviour for the typical fracture of a brittle ceramic.

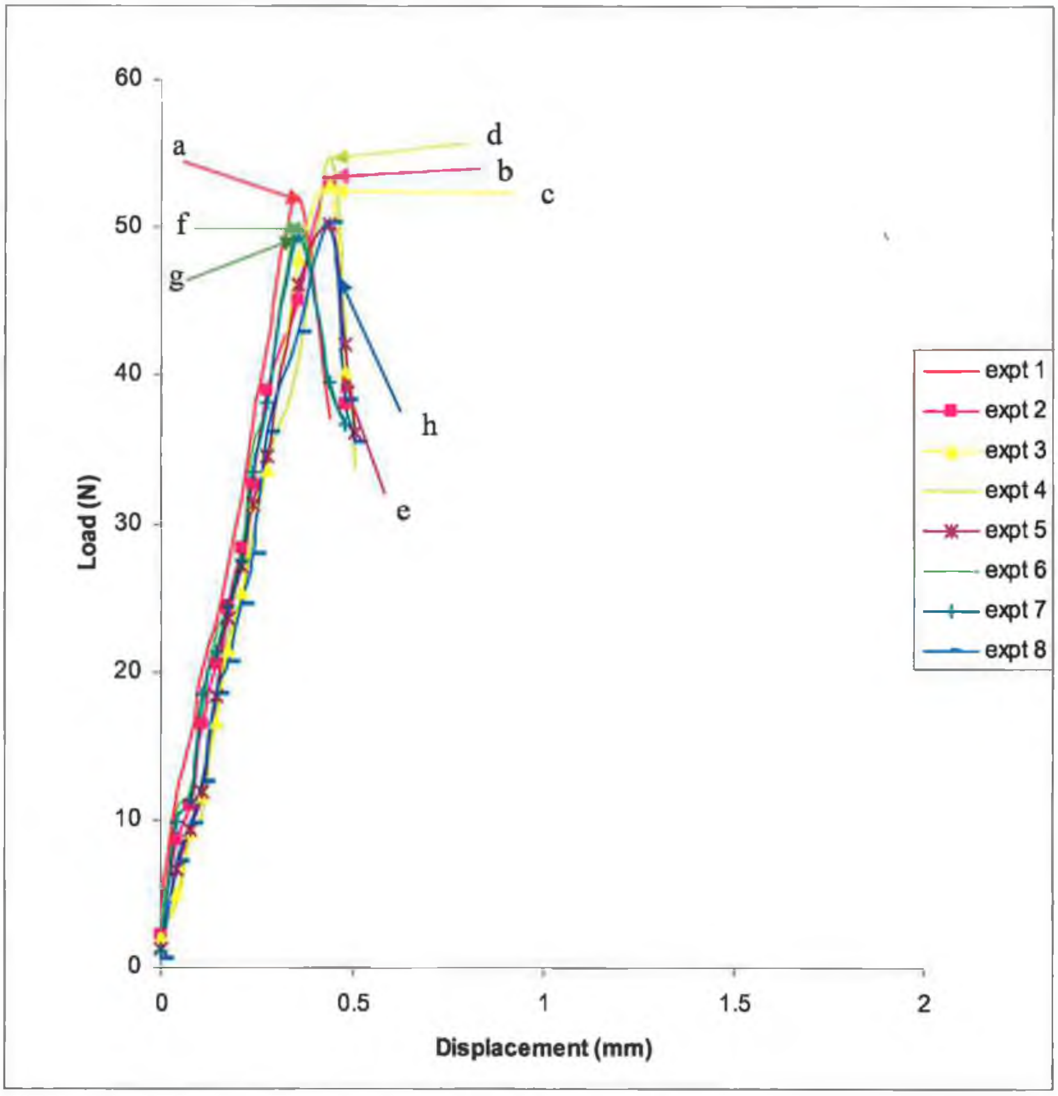

Figure 4.7. Load displacement curve (a-h) of porous bioceramic 1 in different conditions of compaction load, compaction speed and poreformer.

Similar brittle behaviour have been observed for hydroxyapatite or other calcium based cermics [141]. The compressive load was determined from the load displacement curve obtained from the INSTRON machine, where the load reached a maximum. At the crushing point, propagation of macroscopic cracks has resulted in a drop in the load. The sharp peak indicates that failure proceeds cracking, without any plastic deformation region.

4.4.3. Structural Analysis

Figure 4.8(a) shows the XRD pattern of calcium carbonate powder before compaction which indicated that the powder contained the calcite polymorph $CaCO_3$. This diffraction pattern fully fits with the pattern 72-1937. (Joint Committee for Powder Diffraction Studies-JCPDS). After compacting the calcium carbonate and naphthalene powder the compacts were heated at 368 K to sublimate the naphthalene. It has been already reported that naphthalene starts to change into gas at 323 K and burns out completely below 423 K [151]. The diffraction pattern of porous bioceramic was also observed (Figure. 4.8(b)). No structural change or new phase formation was found in the new porous ceramic, which confirms that complete burn out of the naphthalene powder (pore former) occurred without forming any complex compounds post processing. It has been found in literature that naphthalene powder can be removed at high temperature without reacting with calcium base powder [131].

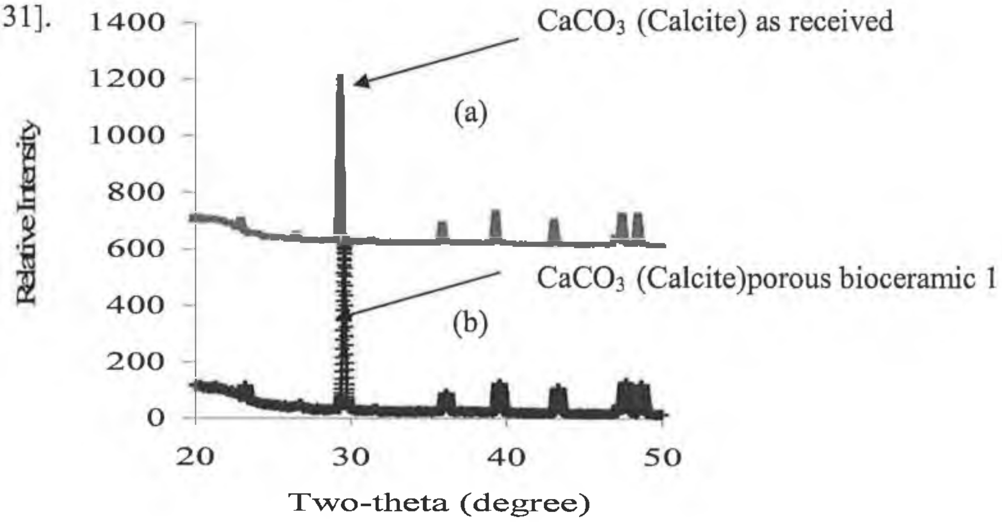

Figure 4.8. X-Ray diffraction patterns of Calcite ($CaCO_3$)powder (as received), (b) Calcium carbonate after compaction and drying (porous bioceramic 1)

4.5. Effect of the particle size of pore former on porosity and compressive load of porous bioceramic 2

As discussed above, the strength of the porous ceramics is mainly determined by the weight fraction of the porosity. Besides, it has also been also shown that the particle size of the pore former has an influence on the ceramics mechanical strength and porosity [131]. However, Lucas et al. [88] states that, particle size of the pore former has an effect on the mechanical strength but not on the total porosity. Due to this contradictory information in literature, the influence of the naphthalene particle size on the porosity and compressive load of the calcium carbonate bioceramic was investigated. Two particle size distributions 250-350 μm and 400-600 μm with different percentage of the naphthalene 5 and 20% were tested.

Table 4.5 Porosity and compressive load (C_s) of bioceramic 2 for the various conditions: different percentage and particle size, of the pore former (naphthalene).

Expt. No.	**Pore fomer (naphthalene) Particle Size (μm)**	**Pore former (naphthalene) (%)**	**Porosity (%)**	**Compressive load (N)**	**(MPa)**
1	250-350	5	31	508.992	2.24
2	250-350	20	48.96	253.422	1.12
3	400-600	5	30.17	499.744	2.20
4	400-600	20	51.22	160.812	0.71

% of change in compressive pressure (MPa) , contains 5% pore former

$$= \frac{2.24 - 2.20}{2.20} x100\% \ = 1.8\% \ldots\ldots \text{Equation(4.6)}$$

% of change in compressive strength (MPa) , contains 20% pore former

$$= \frac{1.12 - 0.71}{0.71} x100\% \ = 58\% \ldots\ldots \text{Equation(4.7)}$$

% of change in porosity, contains 5% pore former$= \frac{31 - 30.17}{30.17} x100\%$

$$= 2.8\% \ldots\ldots \text{Equation (4.8)}$$

% of change in porosity, contains 20% pore former$= \frac{51.22 - 48.96}{48.96} x100\%$

$$= 4.6\% \ldots\ldots \text{Equation (4.9)}$$

Table 4.5 shows that the particle size of the naphthalene has a remarkable influence on the compressive load of the porous ceramic. A decrease in the size of the naphthalene leads to an increase of the compressive load (from 1.8-58 %). However, very low change of porosity has been observed (4.6-2.8 %). The compressive load of the ceramics prepared by using 250-350 µm naphthalene were two times stronger (58% increase) as compared to those using 400-600 µm naphthalene under the 20 % weight fraction of naphthalene. It has been already suggested that compressive load decreases with the increasing macro pore size [142] which supports our results. The difference in compressive load of ceramics prepared by using 250-350 µm and 400-600 µm under 5 % weight fraction of naphthalene, have been found to be very low and the effect of particle size of the pore former was not significant. This can be explained by the predominance of the pore former percentage effect, compared to that of the pore former size, on the compressive load.

As described previously, the pore former size has very little influence on the bioceramic porosity. These results disagree with those reported by Lin et al. [129] who indicated that increasing the particle size of the pore former (polyethylene glycol (PEG)), increases the percentage of porosity. However, this may be due to the different characteristics of the different pore formers used.

In comparison with the first experimental results, the compressive load increased significantly with decreasing and controlled pore former particle size. Moreover, a sharp decrease in compressive load has been observed with increasing porosity. This is in agreement with the MCA (minimum contact area) model that suggests that for constant pore size, the strength of porous ceramic decreases sharply with increasing percentage of porosity [129,139].

Even if the compressive load of the samples prepared using 250-350 µm naphthalene particle size is higher than the samples prepared using those having size of 400-600 µm, the naphthalene large particle size (400-600 µm) with 20 % weight fraction in combination with chitosan and chitin is used in the next section of the study in order to determine the maximum strength with maximum pore size of this new biocomposites and examine its potential. It can be assumed that large pore size will be effective for micro organism's life cycle and attachment.

4.6. Characterisation of porous calcium carbonate bioceramic 2

4.6.1. Microstructural Observation

The microstructures of the porous bioceramic 2 prepared using two different particles size of naphthalene 250-350 μm and 400-600 μm were determined (Figure 4.9 (a),(b)) . These Figures show more uniform macropores in the porous ceramic for both pore former particle size ranges compared to those obtained by using wide range (100-900 μm)of pore former particle size as compared to the first experimental design (Figure 4.6). No significant difference was found between the microstructures as shown in Figures 4.9 (a) and (b), except a difference in pore size (250-350 μm and 400-600 μm) . Thus, these micrographs suggested that the particle size of the pore former has the substantial effect on the mechanical properties of the ceramics as mention in section 4.4.1.

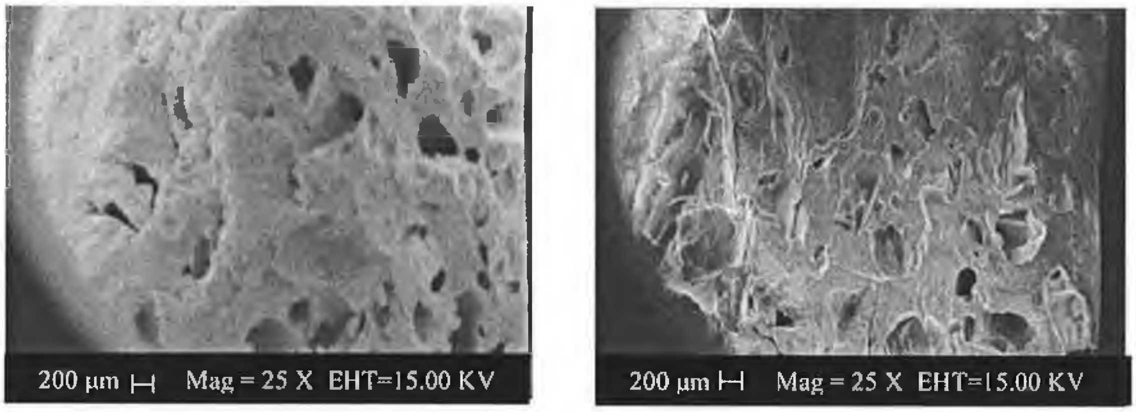

(a) (b)

Figure 4.9. Cross sectional scanning electron micrographs of the porous bioceramic 2 in different particle size ranges of the pore former; (a) 250-350 μm , (b) 400-600 μm.

4.6.2. Load-displacement behaviour of calcium carbonate bioceramic 2

As shown in Figure 4.10, the load-displacement curve behaviour of porous ceramic prepared by adding pore former particle size ranges 250-350 μm and 400-600 μm, with different weight fraction of pore former (5 and 20%) as compared to those observed for porous bioceramic 1. The load dropped when the material failed or at its ultimate compressive load. The elastic region of the ceramic with a porosity of 30-31% was significantly higher than the more porous (48.96-51.22 %) types for both particle size ranges. Indeed, the curve behaved in a similar manner at each percentage of pore former increase from 5 and 20% over both particle size ranges. So it can be concluded that the sharp decrease in load as shown in Figure 4.10 (b,d) compared to those presented in Figure 4.10 (a,c) is mainly due to the percentage of higher pore former used. Therefore, it can be suggested that the pore former particle size has less of an effect on the behaviour of the load displacement curve for the bioceramic 2 than the percentage of pore former.

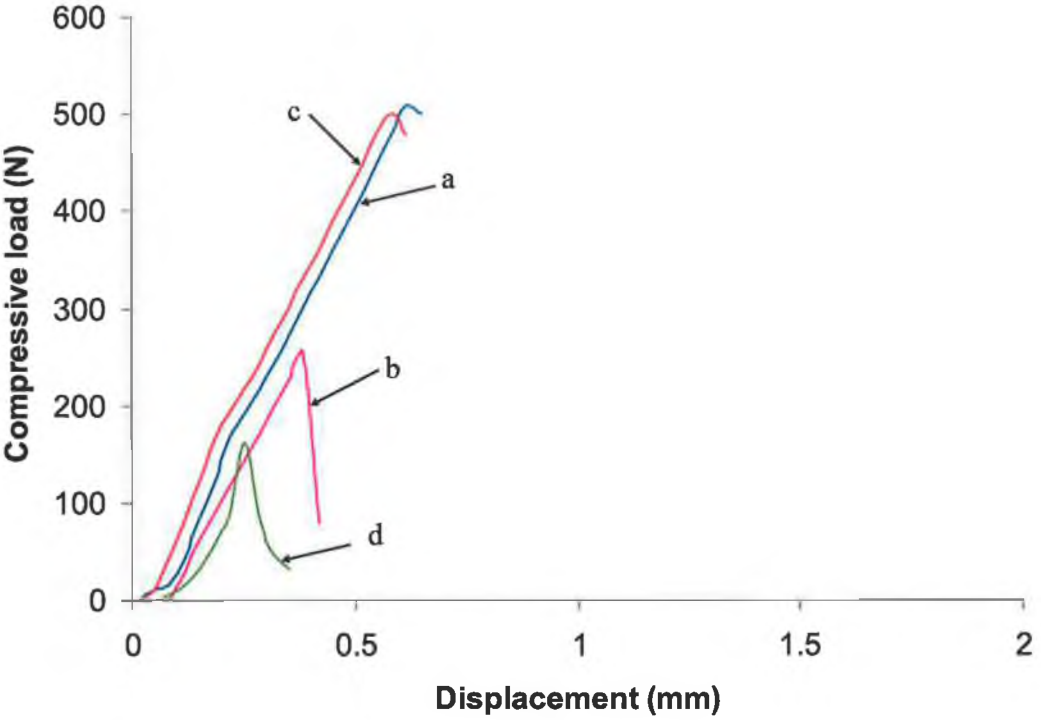

Figure 4.10: A typical load-displacement curve of confined axial compression test of porous ceramics in combination of different particle size and percentage of pore former: (a) 250-350 μm, 5%, (b) 250-350 μm, 20%, (c) 400-600 μm, 5%, (d) 400-600 μm, 20%.

4.7. Effect of the chitin and chitosan on compressive load of calcium carbonate biocomposite.

Sea shells are extraordinarily tough and have unique crack and shatter-resistant properties. An abalone shell, for instance, is chiefly made of calcium carbonate which is organised into multisided tablets that are closely packed in layers. A rubbery polymer, glues the tablets together and serves as a cushion between the layers. The shells do not break when a crack forms as it propagates along complicated paths which diffuse the crack – the polymer also absorbs the damage. To mimic the natural seashell structure using this research a novel fabrication method has been applied to calcium carbonate biocomposites with combination of two biopolymers (chitin and chitosan). Though the particle size 250-350 μm of naphthalene showed better results, 400-600 μm particle size of naphthale were used to produce biocomposites in order to determine the maximum strength with maximum pore size and increase micro organism attachment . All of the optimising parameters (compaction load; 220 MPa, compaction speed; 20 mm/min; percentage of pore former; 20%, particle size; 400-600 μm) were kept constant.

4.7.1. Modified Simplex Centroid mixture experimental design

To optimise the synthesis of such biomimic calcium carbonate biocomposites, a mixture experimental design was used. The effect of the polymer nature and amount on the compressive load was investigated. This mixture design involved (Table 4.6) ten experiments and the properties of the bioceramics were determined by analysing one response, compressive load (C_s, N). For each experiment 3 samples were tested and mean values are presented (Table 4.6)

Table 4.6. Compressive load (C_s) of biocomposite for the various mixture conditions: $CaCO_3$(Ca), Chitosan (Chs) and Chitin (Cht)

Expt	Responses			Variables	
	Ca Wt %	Chs Wt%	Cht Wt%	C_s (N)	(MPa)
1	1	0	0	166	0.732
2	0.7	0.3	0	788	3.473
3	0.7	0	0.3	758	3.341
4	0.85	0.15	0	779	3.434
5	0.85	0	0.15	245	1.080
6	0.7	0.15	0.15	781	3.442
7	0.9	0.05	0.05	253	1.115
8	0.75	0.2	0.05	793	3.495
9	0.75	0.05	0.2	766	3.376
10	0.8	0.1	0.1	773	3.407
11	0.8	0.1	0.1	774	3.412
12	0.8	0.1	0.1	771	3.398

4.7.2. Data Analysis

Statistical analysis of the obtained data was determined using the MODDE 7.0 software. Table 4.7 shows the output analysis of the regression coefficients of the polynomial models describing the relationship between compressive load (C_s) and the three variables (Ca, Chs, Cht). It indicates that the response (Cs) was best described by the polynomial models with the agreed coefficient of determination (R^2).

Table 4.7: R^2 of the polynomial models and P-values of both linear and interaction effects of Ca, Chs, and Cht for compressive load (C_s) of the produced biocomposite.

	C_s
Ca	0.0380789
Chs	0.00354729
Cht	0.300542
Ca*Ca	0.427369
Chs*Chs	0.02036
Cht*Cht	0.241161
Ca*Chs	0.0678905
Ca*Cht	0.540689
Chs*Cht	0.738774
R^2	0.887
Constant	693.278

The statistical analysis of the data showed that $CaCO_3$ (Ca) and Chitosan (Chs) had more of an effect on the compressive load ($P_{-value} < 0.05$). However, the Chitin (Cht) had a lower effect ($P_{-value} > 0.05$) than chitosan. After eliminating the non-significant effects and interactions the reduced model for compressive load (C_s) is expressed as follows:

$$C_s = 693.278 - 445.06\ (Ca) + 2861.61\ (Chs) - 12483.7\ (Chs*Chs) \text{ ....Equation (4.10)}$$

The relationship between the factors ($CaCO_3$, Chitin and Chitosan) and response (Compressive load) can be best understood by examining their mixture contour plots. These representations are generated by plotting contours of the response versus its factors shown in Figure 4.11.

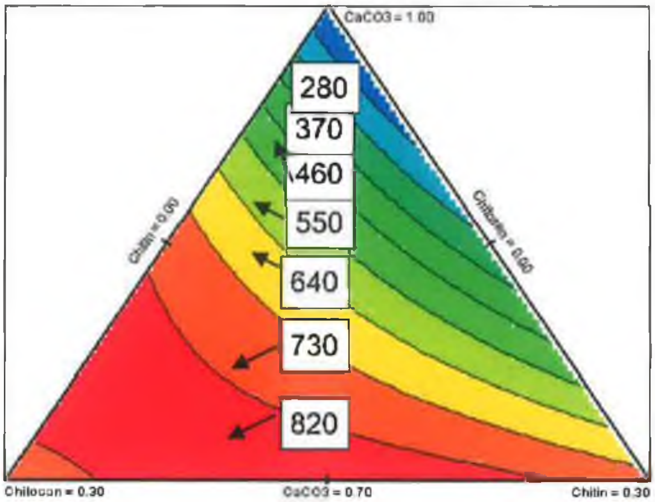

Figure 4.11. Mixture contour plot for compressive load (N)

The compressive load (C_s) model demonstrates that the calcium carbonate has an negative effect which means increasing amount of calcium carbonate (from 70% to 100% wt fraction) decreases the compressive load of calcium carbonate biocomposite (from 820 N-280 N). However, the addition of chitin and chitosan increased the compressive load. These results are in agreement with other researchers who have used biopolymers to improve the mechanical properties of calcium based ceramics [61, 68]. The mechanism for this reinforcement has been postulated to be complication of the functional groups of chitosan or chitin with calcium ions [130]. From a mechanical viewpoint, this strength increase is due to the formation of the mechanical bonding between calcium carbonate and chitin or chitosan during compaction. It can be noted that the microcrystalline cellulose which is structurally analogous to that of chitin or chitosan, is used as a polymeric binder for calcium carbonate powder to improve the mechanical strength followed by uniaxial compression [89].

Even if the polymer's addition enhances the biocomposites strength, the improvement rate depends on the polymer nature. Indeed, the first model pointed out that chitosan has more positive effect on the compressive load, while the influence of the chitin has less effect. To understand this behaviour, Figure 4.12 was developed and presents the individual effect of chitin and chitosan on compressive load (which can also be seen in figure 4.11). It shows that an addition of 30% polymer increased the compressive load from 166 to 788 N and from 166 to 758 N respectively for chitosan and chitin. However, decreasing the addition of chitosan from 30% to 15% caused a slight drop in compressive load from 788 to 779 N. While reducing the chitin from 30% to 15%, caused the load to drop very sharply from 758 to 245 N. According to Sawayanagi [85], increasing the amount of chitin or chitosan can improve the mechanical strength of the ceramics which is basically dependent on the powder combination in nature. In fact, it was reported that in terms of hardness, chitosan produced the highest followed by cellulose and chitin.

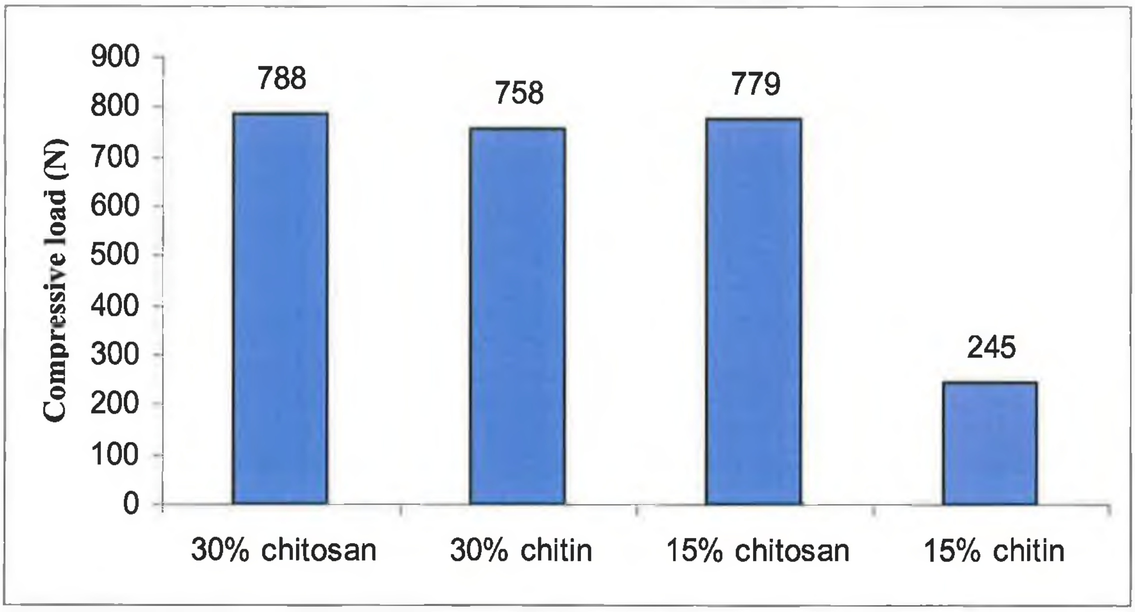

Figure. 4.12. Effect of the different percentage of chitin and chitosan on compressive load of porous biocomposite (a) 30% chitosan,(b) 30% chtin, (c) 15% chitosan, (d) 15% chitin.

To understand further the influence of the combination of chitin and chitosan mixture with calcium carbonate powder on compressive load, a prediction model was developed using MODDE 7.0 as shown in Figure 4.13. Individually, the addition of 5 to 20 % of chitin or chitosan increased the compressive load linearly (Figure 4.13). However, the influence of chitosan on the compressive load is far greater. For example, the presence of 5% of chitin produced a compressive load of 134.334 N, while the addition of the same amount of chitosan gives a much strong ceramic (408.152 N).

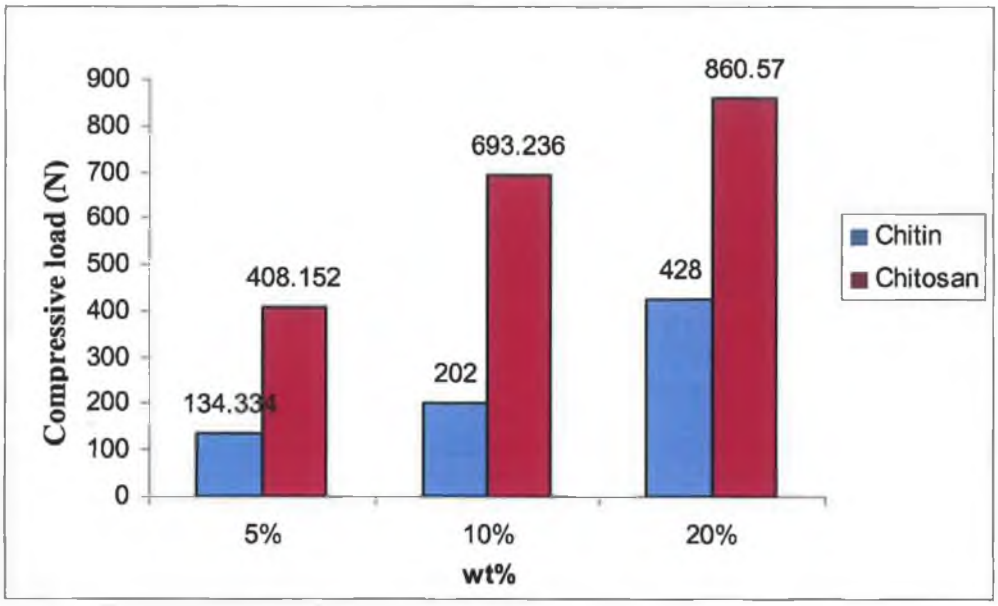

Figure 4.13: Pre model of the effect of chitin and chitosan on compressive load (N) of porous $CaCO_3$ with increasing percentage of 5-20%.

Figure 4.14 represents the effect of different combinations of chitin and chitosan on compressive load obtained from the experimental results (3 samples were tested in each experiments and mean values are presented here in the results). The compressive load (N) obtained using the 20/5 % chitosan/chitin combination is slightly higher than that reached by adding the 5/20% chitosan/chitin combination. This confirms the dominant effect of chitosan compared to that of chitin.

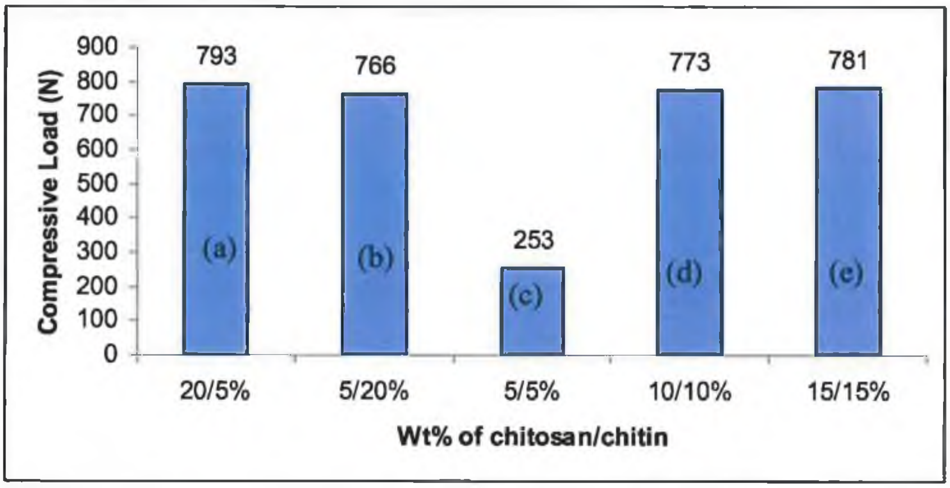

Figure 4.14: The effect of different combinations of chitosan/chitin (a) 20/5%, (b) 5/20%, (c) 5/5%, (d) 10/10%, (e) 15/15% on compressive load of porous $CaCO_3$ biocomposites obtained from experimental results.

Overall it can be concluded that the addition of a high percentage of chitosan has a significant influence on increasing the compressive load of different combinations of the biocomposites

4.7.3. Data optimisation and models validation

To determine the optimal operating conditions to gain high compressive load, the optimiser function of MODDE 7.0 was used. The obtained results (Table 4.8) show that a biocomposite with a compressive load of about 944.349 N when a combination of Calcium carbonate (70%), Chitosan (16.06%) and Chitin (13.94%) is used.

Table 4.8: Optimal powder combination obtained by Modde 7.0 Optimizer

	$CaCO_3$	**Chitosan**	**Chitin**	**Compressive load (N)**
1	0.7	0.1606	0.1394	944.349
2	0.7	0.1608	0.1392	944.352
3	0.7005	0.1609	0.1386	944.352
4	0.7	0.1572	0.1428	943.172
5	0.7	0.1608	0.1392	944.352
6	0.7	0.1609	0.1391	944.352
7	0.7	0.165	0.135	944.232
8	0.7	0.1612	0.1388	944.354
9	0.7	0.1611	0.1389	944.279

The adequacy of the models describing the compressive load (Cs, N) was examined by an additional independent experiment using 70% of calcium carbonate, 15% chitosan and 15% chitin. The comparison of the predicted (Cs= 944 N) and experimental (Cs= 781 N) biocomposite strength indicates some agreement between these data, implying that the empirical model could be used to describe the relationship between the percentage of polymer added and the compressive load of the porous biocomposite using the uniaxial die compaction process.

Both experimental results and the statistical model suggested that the addition of two biopolymers with a certain amount of calcium carbonate powder showed better compressive load than bioceramic 1 and bioceramic 2. On the other hand the addition of only 15-30% chitosan showed similar results. From an economic view-point, one can conclude that the addition of 15% chitosan would provide the best combination, due to its high initial powder cost.

4.8 Characterization of porous calcium carbonate biocomposite

4.8.1. Microstructural Observation

Figure 4.15 (a) and (b) show the cross section of calcium carbonate compact containing chitosan and chitin respectively. SEM micrographs of chitosan composite (Figure 4.15) revealed the presence of flake shape chitosan (Figure 4.15(a)) incorporated in the calcium carbonate powder, exhibiting a similar porous structure as observed in Figure 4.9. The pores were evident for both chitin and chitosan composites, however, compared with the

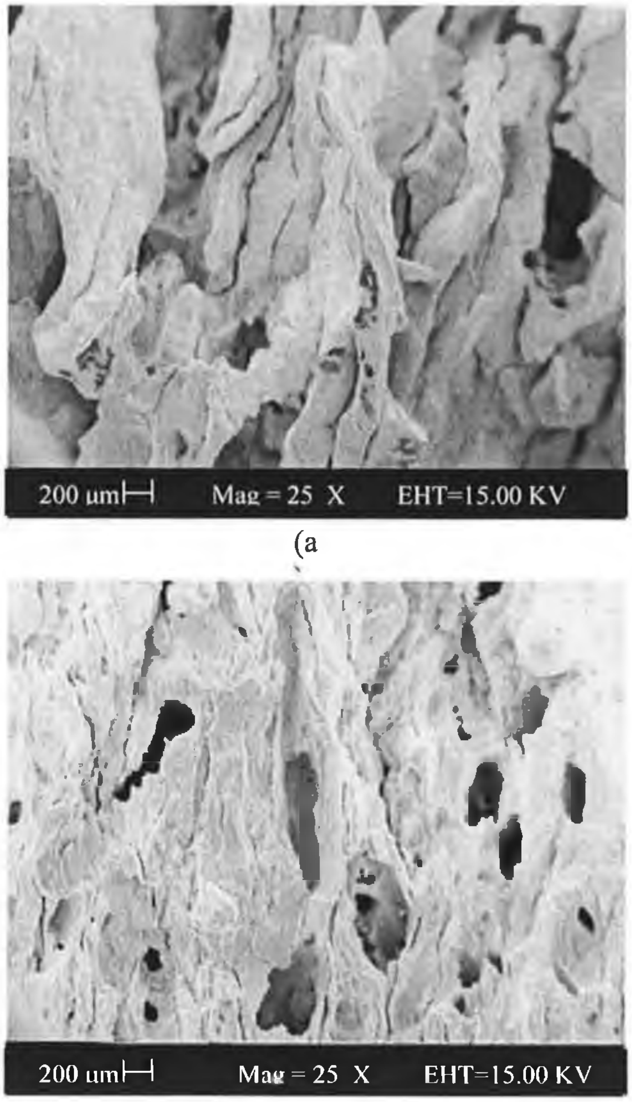

(a

(b)

Figure 4.15. Scanning electron micrographs of the porous biocomposite containing (a) chitosan , (b) chitin.

chitin composite, the chitosan composite showed a significant difference in pore shape and distribution. In addition the macro pores were more visible than micro pores in the chitosan biocomposite. This may be due to the presence of the large elongated flake shapes of chitosan powder. These micrographs suggest that the chitosan composite could influence the compressive load greater than that of the chitin composite

4.8.2. Load-displacement behaviour Calcium carbonate biocomposite

Figure 4.16 shows the series of load-displacement curves of pure calcium carbonate bioceramic and calcium carbonate biocomposite for different percentages of chitin and chitosan. The combination of a 5/5 % chitin/chitosan (Figure 4.16(b)) and 15% chitin (Figure 4.12(c)) calcium carbonate biocomposite showed the similar load drop except the change in elastic region than pure calcium carbonate biocermic (Figure 4.16(a)).

Other combination of the biopolymer with calcium carbonate biocomposite revealed the similar behaviour to each other as shown in Figure 4.16 (d-j) but significantly different from pure calcium carbonate bioceramic (Figure 4.16(a)). These curves (Figure 4.16 (d-j)) showed a linear elastic region to exist. It has been noticed that the elasticity increases with decreasing porosity [156]. However, in this experiment the porosity was approximately constant. Hence, it is difficult to explain the reason of the slope difference for the different composition of the biopolymer as no research suggested the compression behavior of the calcium carbonate biocomposite with chitin and chitosan biopolymer via powder metallurgy manufacturing route. Therefore, it can be concluded that the elastic behaviour of these biocomposites depends on the different composition of the biopolymer. After the linear elastic region the specimens showed a sharp yielding followed by a small plastic region. During this stage the displacement of the curve increases while the load remains constant. Consequently as the porous compact begins to densify, the load increases with displacement. Other researchers have also observed a relatively similar compressive load-displacement pattern for chitosan and β-tricalcium phosphate porous polymer foam biocomposite, produced by the freeze drying method [61].

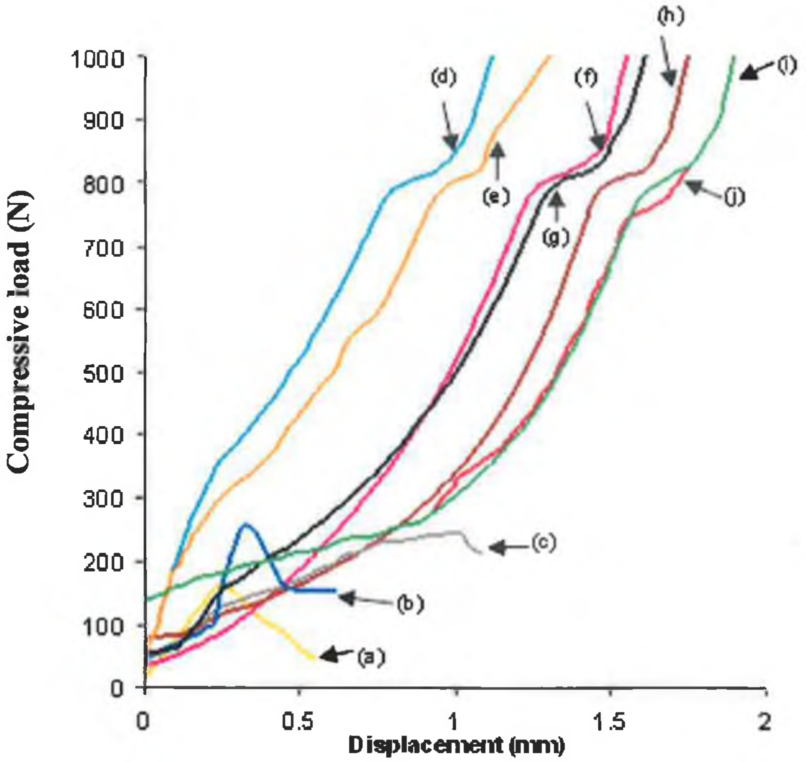

Figure 4.16. Load-Displacement curve of the mixture of chtin and chitosan with calcium carbonate biocomposite, (a) pure calcium carbonate bioceramic, addition of (b) 5/5% chitosan/chitin, (c) 15% chitin, (d) 15/15% chitosan/chitin, (e) 5/20%chitosan/chitin, (f) 30% chitin, (g) 20/5% chitosan/chitin, (h) 15% chitosan, (i) 10/10 chitosan/chitin, (j) 30% chitosan

4.9. Comparison of Porosity and compressive load between natural seashell and calcium carbonate bioceramic 1, bioceramic 2 and biocomposite.

From literature it was found that in wet conditions seashells offer high strength, (sustaining loads of approximately 1200 N [47] and very low porosity of 2-4% [49]. But in dry conditions (heated to around 850 °C) they provide higher porosity (50%) [49] but sacrifice their strength, (to approximately 40 N [18]. Furthermore, high temperature curing of sea shells encourages the formation of CaO phase from $CaCO_3$, which may not be a favorable compound as a filter material for microbes growth because of its high pH (12.5).

For this study, compressive load test of two size of seashell (3 samples were tested for each size) are carried out. Figure 4.17 shows the load displacement curve of large and small natural seashells. As shells have a dome like shape, strength was not easily determined, so compressive load was measured. It was found that the maximum compressive load for large and small seashells were 50 N and 200 N respectively. It can be noted that other research [47] measured the strength of the bihalves (two parts of the seashell together) of the seashell. In this case, the strength of only one part of the shell was measured. The value of the compressive load may vary due to this reason.

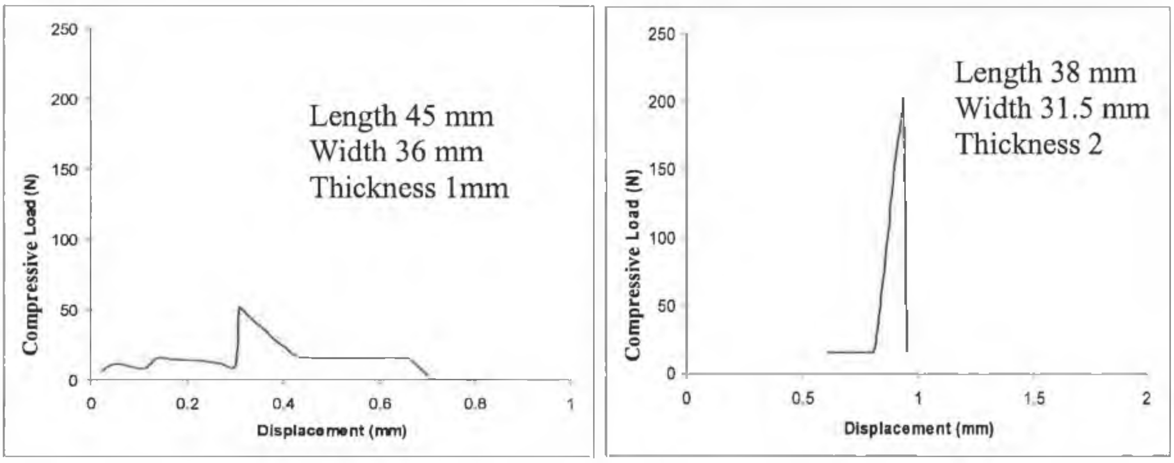

(a) (b)

Figure 4.17. Load displacement curve for natural seashell (a) Large shell, (b) Small shell.

Figure 4.18 shows the comparison in compressive load between natural seashell and synthetic porous calcium carbonate bioceramics and biocomposites. Bioceramic 1 which was prepared with control process parameters showed a similar strength to that of a large seashell but lower than that of a small shell. After controlling the pore size of the calcium carbonate compact (bioceramic 2), the strength observed was found to be higher than the large shell but still lower than that of a small shell. The addition of the biopolymer (30% chitosan) increased the strength of the calcium carbonate biocomposite significant compared with both large and small shells. Needless to say that the porosity of the synthetic calcium carbonate biocomposite was obtained significantly higher porosity (~50%) than natural seashell (2-4%) as found in literature [49]. It should be noted that this research considers only the microporosity of the natural seashell itself not the bulk porosity of the sea shell filter bed and then compared to that of the artificial bioceramic/biocomposites proposed in this project work.

Therefore, this result confirms that this disk shaped calcium carbonate biocomposite provides higher compressive load and porosity compared to that of the dome shaped natural sea shell in dry condition without showing any structural change. Hence it is possible to fabricate synthetic shell media with attributes similar to or even enhanced, compared to their counterparts.

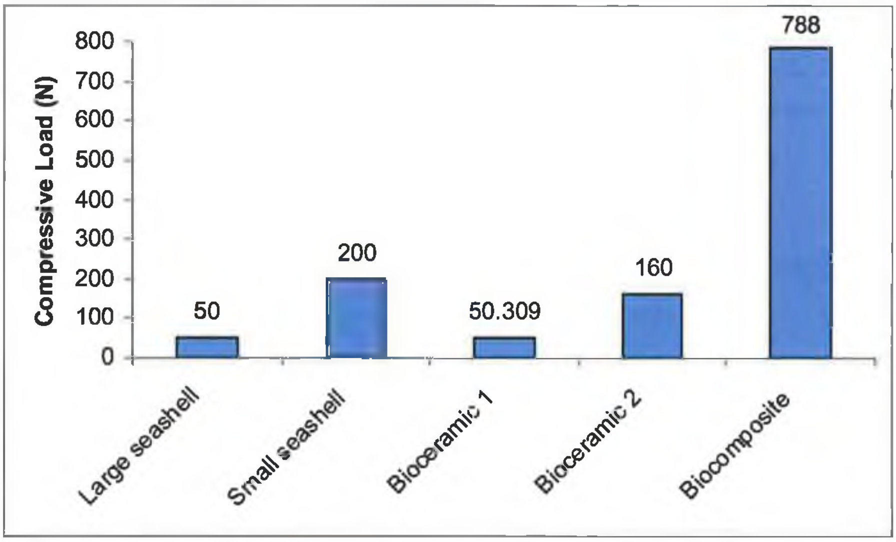

Figure 4.18. Compressive load of natural seashells and calcium carbonate bioceramics and biocomposite.

4.10. Effect of Water and Steam on porous calcium carbonate biocomposites

Shell media are usually emerged in a humid environment in biofiltraion process. To understand the behaviour of the porous calcium carbonate biocomposites in this environment, two tests were carried out in the presence of water and steam. Unfortunately, in presence of water, the compacts begun to loose their interparticle strength and tuned into a powder slurry in a minute. On the other hand in presence of steam the compacts were not completely broken down but started loosing powder and became difficult to handle. These results indicate that though the strength of the calcium carbonate is higher than that of natural seashell, this is still not high enough to withstand the presence of water or steam. If the water instability of this biocomposite could be predicted in the preliminary stage of this research then some other different approach could have been followed.

As we described in literature that in natural seashell, calcium carbonates are chemically bonded with the biopolymers which may lead to its resistance in water. In summary, chemically bonded calcium carbonate structure is more stable than mechanically bonded calcium carbonate particles when subjected to water or steam.

CHAPTER 5 CONCLUSION AND FUTURE WORK

5.1 Conclusions

The aim of this research was to produce a highly porous and high compressive load capacity bioceramic/biocomposite as a filter bed for the application of biofiltration process and the following conclusions were derived:

- Porous and strong disk shape calcium carbonate bioceramic can be produced using the uniaxial die compaction method

- Porosity (P_r) and compressive load (C_s) of the calcium carbonate bioceramics depended on the addition (%) of the pore former naphthalene (P_f) and on the compaction load/pressure (P_c). Compaction speed (V_c) has no effect on the resulting porosity and compressive strength

- A calcium carbonate bioceramic 1 providing a compressive load of 50.309 N and porosity level of 50.33 % can be manufactured by choosing optimal process parameters; 1) a compaction load (pressure) 50 kN (220 MPa) , 2) 20 % of pore former used at a compaction speed of 20 mm/min. This porosity (P_r) of 50.33% found for the bioceramic 1 is much higher than that found in natural seashells (2-4%). The compressive load (Cs) 50.309 N for the porous calcium carbonate bioceramic 1 is similar to that for large thin natural seashells (50 N).

- Particle size of the pore former has no effect on the total percentage (%) of the porosity. The macropore sizes produced in the bioceramic 2 depend on the particle size of pore former. The compressive load of the porous calcium carbonate bioceramic increases with decreasing particle size of pore former or pore size. Controlling the pore size (400- 600 µm) of the bioceramic resulted in improved compressive load (160.812 N) nearly similar to that of small thick natural seashell (200 N).

- The addition of the biopolymers; chitin and chitosan significantly increased the compressive strength of the porous calcium carbonate biocomposite.

- The compressive load improvement of porous calcium carbonate depends on the amount and nature of the biopolymer. Addition of 15 and 30 % chitosan resulted in the compressive load of 779 and 788 N, respectively. For chitin, the addition of 15 and 30 % resulted the compressive load 245 and 758 N respectively. So either 30% chitin or 15% chitosan can be used to get 758-779N load bearing capacity.

- Mixing of two biopolymers (chitin and chitosan) together with calcium carbonate showed better compressive load. The addition of 20/5 % chitosan/ chitin resulted in the highest compressive load (793 N). High compressive load (781 N) resistance was also found for 15/15 % chitosan/chitin biocomposite

- The calcium carbonate biocomposite produced in this present work via die compaction technique has shown better properties (porosity, compressive strength) than natural seashell.

- However, the porous calcium carbonate biocomposite dissolved in the presence of water or steam due to the low bonding strength between its particles. This mechanically bonded un-sintered ceramic is unable to withstand any load in water or steam in its current state.

5.2 Recommendations for future work

Based on the conclusions found from this research the following recommendations are suggested for future work in this area:

- An investigation should be conducted on high compaction load/ pressure to improve the mechanical bonding between the powder particles

- An investigation into the effect of compaction speed on the compressive strength of porous calcium carbonate biocomoposite ($CaCO_3$ + polymer), as this research only looked at calcium carbonate and the naphthalene pore former.

- An investigation of the effect of other polymers (less expensive than chitin and chitosan) on the final compressive load of calcium carbonate biocomposite.

- A die designed to manufacture seashell shaped calcium carbonate bioceramic/ biocomposites.

- A study of the effect of cold isostatic pressing on the particle bonding of porous calcium carbonate compact.

- It is important to investigate other chemical or casting processes that could be used to manufacture artificial seashell to improve strength and withstand the presence of water.

Publications

The following publications have resulted so far from this research

Paper

- T. Akter, J. Stokes, M. Ardhaoui and M.S.J. Hashmi, "An Investigation into the Porosity and Compressive Strength of Calcium Based Materials Produced by the Die Compaction Technique, Proceedings of the Euro Powder Metallurgy PM2005 Congress and Exhibition, Vol. 1 (2005), pp. 523-528.

Poster

- T. Akter, J. Stokes , M.S.J. Hashmi, T. Prescott and A. Rafferty, " Manufacturing of Synthetic Shell Media for Industrial Waste Air Treatment Process Using Powder Metallurgical Methods", 8th Annual Sir Bernard Crossland Symposium and Postgraduate Research Workshop, Proceedings, (2005), pp. 173.

References:

[1] M. Schwartz, "Composite Materials Handbook", Second Edition, McGraw-Hill, Inc., (1992), ISBN 0-07-055819-1

[2] E. P. DeGarmo, J. T. Black and R. Kohsher, "Materials and Processes in Manufacturing", Seventh Edition, Macmillan Publishing Company, (1988), ISBN 0-02-946140-5

[3] G. O'Donnell, "Process Optimisation and Numerical Modelling of Powder Metallurgical Aluminum Matrix Composites", PhD Dissertation, Dublin City University, (1999)

[4] Composites, ASM handbook, Vol 21, ASM International, Materials Park, Ohio, IBSN: 0-87170-703-9

[5] A. Kelly and Y. N. Rabotnov, "Fabrication of Composties", Hand book of composites, Elsevier Science Publishers, Vol. 4, (1983), pp 383-387, ISBN: 0-444-86447-4

[6] R. Warren, "Ceramic-Matrix Composite", Blackie and son Ltd., (1992), ISBN 0-216-92682-3

[7] K. K. Chawal, "Ceramic matrix Composites", Published by Chapman & Hall, (1993), ISBN 0-412-36740-8

[8] B. Pokroy and E. Zolotoyabko, "Microstructure of natural plywood-like ceramics: a study by high-resolution electron microscopy and energy-variable X-ray diffraction", Journal of Materials Chemistry, Vol. (13), (2003), pp.682-688

[9] D. W Bruce and D. O'Hare, "Inorganic Materials", Second Edition. John Wiley & Sons Ltd., England, (1996), ISBN: 0-471-960357

[10] S. A. Wainwright, W. D Biggs, J. D. Currey and J. M. Gosline, “Mechanical Design in Organisms,” Princeton University Press, Princeton, NJ, (1982), ISBN: 0-691-0830-8

[11] R. Murugan and S. Ramakrishna, “Development of nanocomposites for bone grafting “, Composites Science and Technology, in press, (2005)

[12] C. R. Yang, Y. J. Wang, X. F. Chen and N. R. Zhao, “Biomimetic fabrication of BCP/COL/HCA scaffolds for bone tissue engineering”, Materials Letters, in press, (2005)

[13] C. Li and D. L. Kaplan, “Biomimetic composites via molecular scale self-assembly and bio mineralization”, Current Opinion in Solid State and Materials Science, Vol. 7, (2003), pp. 265–271

[14] R. L. Reis, “Current Opinion in Solid State and Materials Science”, Biomimetics, Vol. 7, (2003), pp.263–264

[15] M. Sarikaya, “An introduction to biomimetics: a structural viewpoint”, Microsc Res. Tech., Vol. 27, (1994), pp.360-75

[16] G. Mayer and M. Sarikaya, “Rigid Biological Composite Materials: Structural Examples for Biomimetic Design”, Experimental Mechanics, Vol. 42, (2002), pp. 395-403

[17] S. Weiner and L. Addadi, “Design strategies in mineralized biological materials”, Journal of Materials Chemistry Vol. 7, 1997, pp.689-702

[18] N. M. Neves and J. F. Manot, “Structure/mechanical behavior relationships in crossed-lamellar sea shells”, Materials Science and Engineering C, Vol. 25, (2005), pp.113–118

[19] Z. Tang, N. A. Kotov, S. Magonov and B. Ozturk, “Nonostructured artificial nacre” , Nature materials , Vol. 2, (2003), pp.413-418

[20] G, -L. Yoon, B. –T. Kim, B. –O. Kim and S. –H. Han, “Chemical–mechanical characteristics of crushed oyster-shell”, Waste Management, Vol. 23, (2003), pp.825–834

[21] X. Li and P. Nardi, “Micro/nanomechanical characterization of a natural nanocomposite material- the shell of Pectindae”|, Nanotechnology, Vol. 15, (2004), pp.211-217.

[22] R. Siegel , I. Orlic, D. D. Cohen, S. J. Markich and R. A. Jeffree, “Manganese profiles in freshwater mussel shells”, Nuclear Instruments and Methods in Physics Research B, Vol. 181 (2001), pp.593-597

[23] P. Cubillas, S. Kohler, M. Prieto, C. Chairat and E. H. Oelkers, “Experimental determination of the dissolution rates of calcite, aragonite, and bivalves”, Chemical Geology, Vol. (216), (2005), pp.59-77

[24] Y. Dauphin, “Structures, organo mineral compositions and diagenetic changes in biominerals”, Current Opinion in Colloid & Interface Science, Vol. 7, (2002), pp.133-138

[25] R. Menig, M. H. Meyers, M. A. Meyers and K. S. Vecchio, Quasi-Static and Dynamic Mechanical Response of Haliotis Rufescens (Abalone) Shells, Acta materialia, Vol. 48, (2000), pp.2383-2398

[26] T. Kato, A. Sugawara and N. Hosoda, “Calcium Carbonate- Organic Hybrid Materials”, Adv. Mater., Vol. 14, (2002), pp.869- 877

[27] A. G. Checa and A. Rodriguez-Navarro, “Geometrical and crystallographic constraints determine the self-organization of shell microstructures in Unionidae (Bivalvia: Mollusca)” , Proc. Biol. Sci., Vol. 268, (2001), pp.771-778

[28] J. L. Arias and M. S. Fernandez, “Biomimetic processes through the study of mineralized shells”, Materials Characterization, Vol. 50, (2003), pp.189– 195

[29] A. Lin, M. A. Meyers, “Growth and structure in abalone shell, Materials Science and Engineering A”, Vol. 390, (2005), pp.27–41

[30] V. M. Rusu, C. –H. Ng, M. Wilke, B. Tiersch, P. Fratzl and M. G. Peter, "Size-controlled hydroxyapatite nanoparticles as self-organized organic–inorganic composite materials", Biomaterials, Vol. 26, (2005), pp.5414–5426

[31] Y. Levi-Kalisman, G. Falini, L. Addadi and Steve Weiner , "Structure of the Nacreous Organic Matrix of a Bivalve Mollusk Shell Examined in the Hydrated State Using Cryo-TEM", Journal of Structural Biology, Vol. 135, (2001), pp.8–17

[32] F. Marin, G. Luquet, "Molluscan shell proteins", Comptes Rendus Palevol, Vol. 3, (2004), pp.469–492

[33] F. Marin, P. Corstjens, B. D. Gaulejac, E. D. Vrind-De Jong and P. Westbroek, "Mucins and Mollusan calcification: Molecular Characterization of mucoperlin, a novel mucin-like protein from the nacreous shell layer of the fan mussel pinna nobilis (Bivalvia, Pteriomorphia) ", J. Biol. Chem., Vol. 275, (2000), pp.20667-75

[34] D. Tsukamoto, I. Sarashina, and K. Endo, "Structure and expression of an unusually acidic matrix protein of pearl oyster shells", Biochemical and Biophysical Research Communications, Vol. 320, (2004), pp.1175–1180

[35] C. E. Bowen and H. Tang, "Conchiolin-Protein in Aragonite Shells of Mollusks", Comp. Biochem. Physiol., Vol. 115A, (1996), pp. 269-275

[36] I. M. Weiss, S. Kaufmann, K. Mann and M. Fritz, "Purification and Characterization of Perlucin and Perlustrin, Two New Proteins from the Shell of the Mollusc Haliotis laevigata", Biochemical and Biophysical Research Communications, Vol. 267, (2000), pp.17–21

[37] P. K. Ajikumara, B. J. M. Lowb, S. Valiyaveettil , "Role of soluble polymers on the preparation of functional thin films of calcium carbonate" , Surface & Coatings Technology, Vol. 198, (2005), pp.227– 230

[38] X. Shen, A. M. Belche, P. K. Hansma, G. D. Stucky, and D. E. Morse, "Molecular Cloning and Characterization of Lustrin A, a Matrix Protein from Shell and Pearl Nacre of Haliotis rufescens", The Journal of Biological Chemistry , Vol. 272, (1997), pp.32472–3248

[39] A. G. Checa, A. B. R. guez-Navarro and F. J. Esteban-Delgado, "The nature and formation of calcitic columnar prismatic shell layers in pteriomorphian bivalves", Biomaterials, Vol. 26, (2005), pp.6404–6414

[40] S. Kamat, X. Su, R. Ballarini and A. H. Heuer , "Structural basis for the fracture toughness of the shell of the conch Strombus gigas", Nature, Vol. 405, (2000), pp.1036-1040

[41] B. L. Smith, T. E. Schaffer, M. Viani, J. B. Thompson, N. A. Frederick, J. Kindt, A. Belcher, G. D. Stucky, D. E. Mors and P. K. Hansma, "Molecular mechanistic origin of the toughness of natural adhesives, fibres and composites", Nature, Vol. 399, (1999), pp.761 - 763

[42] H. Gao , B. Ji, I. L. Jäger , E. Arzt, and P. Fratzl , "Materials become insensitive to flaws at nanoscale: Lessons from nature", Proceedings of the national academy of sciences of United states of America , Vol. 100 , (2003), pp.5597-5600

[43] K. Okumura and P. -G. de Gennes, "Why is nacre strong? Elastic theory and fracture mechanics for biocomposites with stratified structures", The European Physical Journal E, Vol. 4, (2001), pp.121–127

[44] R. Menig, M. H. Meyers, M. A. Meyers and K. S. Vecchio, "Quasi-static and dynamic mechanical response of Strombus gigas (conch) shells", Materials Science and Engineering A, Vol. 297, (2001), pp.203–211

[45] S. J. Eichhorn, D. J. Scurr, P. M. Mummery, M. Golshan, S. P. Thompson and R. J. Cernik, "The role of residual stress in the fracture properties of a natural ceramic", J. Mater. Chem., Vol. 15, (2005), pp.947–952

[46] J. A. Blundon and V.S. Kennedy, “Mechanical and behavioural aspects of blue crab, callinectes sapidus (Rathbun), predation on Chesapeake Bay Bivalves”, Journal of Experimental Marine Biology and Ecology, Vol. 65, (1982), pp.47-65

[47] G. M. Garden, “Instrumentation for mussel (perna canaliculus) shell strength measurements”, Computers and Electronics in Agriculture, Vol. (19), (1998), pp.311-315

[48] N. Almqvist, N. H. Thomson , B. L. Smith, G. D. Stucky, D. E. Morse and P. K. Hansma, “Methods for fabricating and characterizing a new generation of biomimetic materials”, Materials Science and Engineering C, Vol. 7 (1999), pp.37–43

[49] L. Cheng, B. Chen, N. Liu, Z. Luo and K. Cen, “Effect of characteristic of sorbents on their sulfur capture capability at a fluidized bed condition”, Fuel, Vol. 83, (2004), pp.925–932

[50] I. Naruse, K. Saito and T. Murakami,“Application of wasted sea-shell to desulfurizer in fluidized bed coal combustion”, Proceedings of the 15th International Conference on Fluidized bed Coal Combustion, Paper No. FBC99-0088, (1999)

[51] N. Hosoda and T. Kato, “Thin Film Formation of Calcium Carbonate Crystals: Effects of Functional Groups of Matrix Polymer”, Chem. Mater., Vol. 13, (2001), pp.688-693

[52] Y. M. Lee, S. H. Kim and S. J. Kim, “Preparation and characteristics of b-chitin and poly (vinyl alcohol) blend”, Polymer, Vol. 37, (1996), pp. 5897-5905

[53] Y. Zhang, C. Xue, Y. Xue, R. Gaoa and X. Zhangc, “Determination of the degree of deacetylation of chitin and chitosan by X-ray powder diffraction”, Carbohydrate Research, Vol. 340, (2005), pp.1914–1917

[54] N.V. Majeti and R. Kumar, “A review of chitin and chitosan applications”, Reactive & Functional Polymers ,Vol. 46, (2000), pp.1–27

[55] E. Khora and L. Y. Lim, “Implantable applications of chitin and chitosan”, Biomaterials, Vol. 24, (2003), pp.2339–2349

[56] R. A. A. Mozzarelli (Ed.), ‘‘Natural Chelating Polymers Pergamon”, New York Press, (1973), ISBN: 0-08-017235-0

[57] P. Stolarek and S. Ledakowicz, “Pyrolysis kinetics of chitin by non-isothermal thermogravimetry” , Thermochimica Acta, Vol. 433 ,(2005) ,pp.200–208

[58] F. S. Kittur, K. V. H. Prashanth, K. U. Sankar and R. N. Tharanthan, “Characterization of chitin , chtiosan and their carboxymethyl derivatives by differential scanning calorimetry”, Carbohydrate Polymer ,Vol. 49, (2002) , pp.185-193

[59]. T. Wanjuna , W. Cunxinb and C. Donghua, “Kinetic studies on the pyrolysis of chitin and chitosan”, Polymer Degradation and Stability, Vol. 87, (2005), pp.389-394

[60] J. Nunthanid, S. Puttipipatkhachorn, K. Yamamoto, G. F. Peck, “Physical properties and molecular behaviour of chitosan films”, Drug Dev Ind Pharm., Vol. 27, (2001), pp.143-57

[61] Y. Zhang and M. Zhang, “Microstructures and mechanical characterization of chitosan scaffolds reinforced by calcium phosphates”, Journal of Non-Crystalline Solids, Vol. 282, (2001), pp.159-164

[62] I. Yamaguchi, S. Itohd, M. Suzukie, A. Osakae and J. Tanaka, “The chitosan prepared from crab tendon I: the characterization and the mechanical properties”, Biomaterials, Vol. 24, (2003), pp.2031–2036

[63] D. K. Singh, A. R. Ray, “Characterization of grafted chitosan films”, Carbohydrate Polymers, Vol. 36, (1998), pp.251-255

[64] Z. Ge, S. Baguenardb, L. Y. Lima, A. Weec and E. Khor, “Hydroxyapatite–chitin materials as potential tissue engineered bone substitutes”, Biomaterials, Vol. 25 , (2004), pp.1049–1058

[65] S. Higashi, T. Yamamuro, T. Nakamura, Y. Ikada, S. -H. Hyon and K. Jamshidi ,”Polymer hydroxyapatite composites for biodegradable bone fillers”, Biomaterials, Vol. 7, (1986), pp.183-187

[66] T. Kawakami, M. Antoh, H. Hasegawa, T Yamagishi, M. Ito and S. Eda, “Experimental study on osteoconductive properties of a chitosan-bonded hydroxyapatite self-hardening paste”, Biomaterials, Vol. 13, (1992), pp.759-763

[67]. A. C. A. Wan, E. Khor, G. W. Hastings, “Preparation of a chitin–apatite composite by in situ precipitation onto porous chitin scaffolds”, Journal of Biomedical Materials Research, Vol. 41, pp. 541-548

[68]. A. C. A. Wan, E. Khor, G. W. Hastings, “Hydroxyapatite Modified Chitin as Potential Hard Tissue Substitute Material”, Journal of Biomedical Materials Research Part B: Applied Biomaterials, Vol. 38, pp. 235-241

[69] H. Uda, Y. Sugawara and M. Nakasu, “Experimental studies on hydroxyapatite powder carboxymethyl chitin composite: injectable material for bone augmentation”, Journal of Plastic, Reconstructive & Aesthetic Surgery, Vol. 59, Issue 2, (2006), pp. 188-196

[70] A. D. Martino, M. Sittingerc and M. V. Risbud, “Chitosan: A versatile biopolymer for orthopaedic tissue-engineering”, Biomaterials, Vol. 26, (2005), pp.5983–5990

[71] S. V. Madihally and H. W. T. Matthew, “Porous chitosan scaffolds for tissue engineering”, Biomaterials, Vol. 20, (1999), pp.1133-1142

[72] L. Kong , Y. Gao, W. CaO, Y. Gong, N. Zhao and X. Zhang, “Preparation and characterization of nano-hydroxyapatite/chitosan composite scaffolds”, Journal of biomedical Materials Research Part A, Vol. 75A, (2005), pp. 275-282

[73] X. Pang and I. Zhitomirsky, “Electrodeposition of composite hydroxyapatite–chitosan films’, Materials Chemistry and Physics, Vol. 94, (2005), pp. 245-251

[74] X. Wang, Q. L. Feng, F. Z. Cui and J. Ma, “The Effect of S- Chitosan on the physical properties of Calcium Phosphate Cements”, Journal of Bioactive and compatible Polymers, Vol. 18, (2003), pp.45-57

[75] H. H. K. Xu and C. G. Simon Jr, “Fast setting calcium phosphate–chitosan scaffold: mechanical properties and biocompatibility”, Biomaterials, Vol. 26, (2005), pp.1337–1348

[76] A. Matsuda, T. Ikoma, H. Kobayashi and J. Tanaka, “Preparation and mechanical property of core-shell type chitosan/calcium phosphate composite fiber’, Materials Science and Engineering C, Vol. 24, (2004), pp.723–728

[77] Z. Lia, H. R. Ramaya, K. D. Hauchb, D. Xiaoc and M. Zhang , “Chitosan–alginate hybrid scaffolds for bone tissue engineering” , Biomaterials, Vol. 26, (2005), pp.3919–3928

[78] G. Saraswathy, S. Pal, C. Rose and T. P. Sastry, “A novel bio-inorganic bone implant containing deglued bone, chitosan and gelatine” , Bull. Mater. Sci., Vol. 24, (2001), pp. 415–420

[79] Y. X. Xua, K. M. Kimb, M. A. Hannaa, and D. Nag, “Chitosan–starch composite film: preparation and characterization”, Industrial Crops and Products, Vol. 21, (2005), pp.185–192

[80] S. F. Wang , L. Shen , Y. J. Tong, L. Chen , I. Y. Phang , P. Q. Lim and T. X. Liu, “Biopolymer chitosan/montmorillonite nanocomposites: Preparation and characterization”, Polymer Degradation and Stability, Vol. 90, (2005) , pp.123-131

[81] G. Cardenas and S. P. Mirnda, “FTIR AND TGA studies of chitosan composite films”, Chil. Chem. Soc., Vol. 49, (2004), pp.291-295

[82] A. Sarasam and S. V. Madihally, “Characterization of chitosan–polycaprolactone blends for tissue engineering applications”, Biomaterials, Vol. 26 (2005), pp.5500–5508

[83] L. Illum, “Chitosan and its use as a pharmaceutical excipient”, Pharm Res. sep , Vol. 15, (1998), pp.1326-31

[84] P. R. Rege, D. J. Shukla and L. H. Block, “Chitinosans as tableting excipients for modified release delivery systems”, International Journal of Pharmaceutics, Vol. 181, (1999) , pp.49–60

[85] Y. Sawayanagi, N. Nambu and T. Nagai, “Compressed tablets containing chitin and chitosan in addition to tactose tor potato starch”, Chem. Pharm. Bull., Vol. 30, (1982), pp.2995

[86] A. Lucas , J. F. Michel, J.Gaudle, C.Carel , Macroporous composite for carrying one or more medicinal substances and for use as a bone reconstruction material, and method for making same .Patent WO 97/26024, 1997

[87] A. Lucas, J. Gaude, C. Carel, J.-F. Michel and G. Cathelineau, “A synthetic aragonite-based ceramic as a bone graft substitute and substrate for antibiotics”, International Journal of Inorganic Materials, Vol. 3, (2001), pp.87–94

[88] A. Lucas-Girot, Sangleboeuf, A. Ouammou, T. Rouxelc and J. Gaude, “A synthetic aragonite-based bioceramic: influence of process parameters on porosity and compressive strength”, Biomaterials, Vol. 23, (2002), pp.503–510

[89] S. Mattsson and C. Nystrom , “Evaluation of strength-enhancing factors of a ductile binder in direct compression of sodium bicarbonate and calcium carbonate powders” , European Journal of Pharmaceutical Sciences , Vol. 10, (2000) , pp.53–66

[90] M. D. L. G. Serra and L. VillafuerteRobles , “Compactibility of agglomerated mixtures of calciumcarbonate and microcrystalline cellulose”, International Journal of Pharmaceutics , Vol. 258, (2003) , pp.153–163

[91] Using Bioreactors to control air pollution, EPA-456/R-03-003, (2003), U.S. Environmental Protection Agency

[92] D. A. Carlson and C. P. Leiser, “Soil beds for the control of sewage odors,” J.Wat. Poll.Contr., Vol. 829, (1966) , pp.9-15

[93] K. F. Cocky and C. R. Neff, “Innovative biological degradation system for petroleum hydrocarbons treatment,” Presented at the NWWA/API conference on petroleum Hydrocarbons and Organic chemicals in Ground Water, Houston, TX, (1988), pp.9-23

[94] G. Leson and A. M. Winer, “Biofiltration: An Innovative Air Pollution Control technology for VOC Emissions”, Air & Waste management Association, Vol. 41, pp. 1045-1054

[95] Y. Cohen, “Biofiltraion- the treatment of fluids by microorganisms immobilized into the biofilter bedding material: a review”, Bioresource Technology Vol. 77, (2001), pp.257-274

[96] M. Zilli, C. Guarino, D. Daffonchio, S. Borin and A. Converti , “Laboratory-scale experiments with a powdered compost biofilter treating benzene-polluted air”, Process Biochemistry , Vol. 40, (2005) , pp. 2035–2043

[97] Wan Namkoong, Joon-Seok Park, Jean S. VanderGheynst , Biofiltration of gasoline vapor by compost media , Environmental Pollution 121 (2003) , pp.181–187

[98] M. –C. Delhom, L. Bibeau, M. Heitz, “A study of the impact of particle size and adsorption phenomena in a compost-based biological Filter”, Chemical Engineering Science, Vol. 57, (2002), pp. 4999 – 5010

[99] C. Lu , M. –R. Lin , J. Lin and K. Chang, “Removal of ethylacetate vapor from waste gases by a trickle-bed air biofilter”, Journal of Biotechnology, Vol. 87, (2001), pp.123–130

[100] B. A. Sheridan, T. P. Curran and V. A. Dodd, “Assessment of the influence of media particle size on the biofiltration of odorous exhaust ventilation air from a piggery facility”, Bioresource Technology, Vol. 84, (2002), pp.129–143

[101] C. Guay, et al., “Design of peat bed biofilter for treating aqueous and gaseous effluents containing petroleum hydrocarbons”, Vecteur Environment, Vol. 36, (2003), pp. 63-64

[102] E. R. Iyrez-Lopez, J. Corona-Hernandez, L. Dendooven, P. Rangel and F. Thalasso, “Characterization of five agricultural by-products as potential biofilter carriers”, Bioresource Technology, Vol. 88, (2003), pp.259–263

[103] Y. Yang and E. R. Allen , “Biofiltration control of Hydrogen Sulfide 1. Design and Operational Parameters”, Air & Waste Manage. Assoc., Vol. 44, pp. 863-868

[104] M. Hirai, M. Kamamoto, M. Yani and M. Shoda, “Comparison of the Biological H_2S Removal Characteristics among Four Inorganic Packing Materials”, Journal of Bioscience and Bioengineering , Vol. 91, (2001), pp.396-402

[105] J-S. Lim, S-J. Park, J-K. Koo and H. Park, “Evaluation of Porous ceramic as Microbial Carrier of Biofilter to Remove Toluene Vapor”, Environmental Technology, Vol. 22, pp.47-56

[106] J. T. M. Emily, I. A. P. Leenen, D. Santos, C. F. K. Grolle, J. Tramper and R. H. Wijffels, “Characteristics of and selection criteria for support materials for cell immobilization in waste water treatment, Water. Reseach, Vol. 30, (1996), pp. 2985-2996

[107] J. P. Phillips and K. J. Mullins, “An effluent Treatment system”, Patent number: WO9635502, (1996)

[108] F. I. Khan and A. K. Ghoshal , “Removal of Volatile Organic Compounds from polluted air, Journal of Loss Prevention in the Process Industries , Vol. 13, (2000) , pp.527–545

[109] L. G. Garner and T. A. Barton, “Biofiltration for Abatement of VOC and HAP Emission”, Metal Finishing, Vol. 100, (2002), pp.12-18

[110] F. Thummler and R. Oberacker, “Introduction to powder metallurgy”, The institute of materials, London, (1993), ISBN: 0-901716-26-X

[111] C-Y. Huang and G. S. Daehn, “Effect of cyclic pressure on the low temperature consolidation of several composite powder systems “, Acta Materialia, Vol. 45, (1997), pp.4283- 4296

[112] B. Kundu, M. K. Sinha and D. Basu , “Development of Bio-active integrated ocular Implant for Anophthalmic Human Patients”, Trends, Biomater. Artif. Organs, Vol. 16, (2002), pp. 1-4

[113] R. M. German, “Powder Metallurgy Science”, Metal Powder Industries Federation, New Jersey, (1984), ISBN: 0-918404-60-6

[114] J. -H. Choi, I. -S. Ahn, Y. -C. Bak, S. -Y. Bae, S. -J. Ha and H. -J. Jang , “Preparation of high porous metal filter element for the fail-safety function”, Powder Technology , Vol. 140, (2004) , pp.98– 105

[115] Powder Metallurgy, ASM Metals Handbook, Ninth edition, Vol. 7, (1984), ISBN: 0-87170-013-1

[116] D. W. Richerson, “Modern Ceramic Engineering; properties, processing and use in design”, Marcel Dekker INC, New York, (1982), ISBN: 0-8247-1843-7

[117] A. Simchi, “Effects of lubrication procedure on the consolidation, sintering and microstructural features of powder compacts’, Materials and Design, Vol. 24, (2003), pp.585–594

[118] B. J. Briscoe and S. L. Rough,”The effects of wall friction on the ejection of pressed ceramic parts”, Powder Technology, Vol. 99, (1998), pp.228-233

[119] J. Hongjun, M. Yonggang, W. Shizhu and J. Hong , “Effects of external electric fields on frictional behaviors of three kinds of ceramic/metal rubbing couples”, Tribology International , Vol. 32, (1999) , pp.161–166

[120] M. T. Hillery and V. J. McCabe, “Wire drawing at elevated temperatures using different die materials and lubricants”, Journal of Materials Processing Technology, Vol. 55, (1995), pp.53-57

[121] K. Hanada, K. Hatsukano, K. Matsuzaki, K. Umeda, M. Ishiwata and M. Tsukita , “Graphite coating of tool steel by pressure spraying” , Journal of Materials Processing Technology , Vol. 164–165, (2005) , pp.856–861

[122] D. Tadic, M. Epple, “Mechanically stable implants of synthetic bone mineral by cold isostatic pressing”, Biomaterials, Vol. 24, (2003), pp.4565–4571

[123] E. Peon, G. Fuentes, J. A. Delgado, L .Morejon , A. Almirall and R. Garcia , “Preparation and characterizarton of porous bolck of synthetic hydroxyapatite”, Latin American Applied Research, Vol. 34, (2004), pp.225-228

[124] M. H. P.Silva , A. F. Lemons, J. M. F. Ferreira, J. D. Santos , Mechanical characterisation of porous glass reinforecd hydroxyapatie ceramics- Bonelike, Materials Research . Vol.6, (2003)., pp. 321-325.

[125] C. Sun and D. J. W. Grant, “Effects of initial particle size on the tableting properties of L-lysine monohydrochloride dihydrate powder”, International Journal of Pharmaceutics, Vol. 215, (2001), pp.221–228

[126] P. Narayan, B. C. Hancock, "The influence of particle size on the surface roughness of pharmaceutical excipient compacts, Materials Science and Engineering A", Vol. 407, (2005), pp.226–233

[127] C. Nicolazo, H. Gautier, M. -J. Brandao, G. Daculsic and C. Merle, "Compactibility study of calcium phosphate biomaterials", Biomaterials, Vol. 24, (2003), pp.255–262

[128] S. Galen and A. Zavaliangos, "Strength anisotropy in cold compacted ductile and brittle powders", Acta Materialia, Vol. 53, (2005), pp.4801–4815

[129] K. Lin, J. Chang, Y. Zeng, W. Qian, "Preparation of macroporous calcium silicate ceramics", Materials Letters, Vol. 58, (2004), pp. 2109-2113

[130] G. A. Soares, et al., "Influence of processing parameters on structural characteristics of porous calcium phosphate samples: A study using an experimental design method", Materials. Research, Vol. 8, (2005), pp 71-76

[131] J. C. L. Huec, T. Schaeverbeke, D. Clement, J. Faber and A. Le Rebeller, "Influence of porosity on the mechanical resistance of hydroxyapatie ceramics under compressive stress", Biomaterials, Vol. 16, (1995), pp. 113-118

[132] J. E. Barralet, T. Gaunt, A. J. Wright, R. Gibson and J. C. Knowles, "Effect of porosity reduction by compaction on compressive strength and microstructure of calcium phosphate cement", Journal of biomedical Material Research , Vol. 63, (2002), pp. 1-9

[133] J. C. Le Huec, T. Schaeverbeke, D. Clement, J. Faber, and A. Le Rebeller, "Influence of Porosity on the Mechanical Resistance of Hydroxyapatite Ceramics Under Compressive Stress", Biomaterials, Vol. 16, (1995), pp. 113–118

[134] A. Bignon, J. Chouteau, J. Chevalier, G. Fantozzi, J. P. Carret, P. Chavassieux, G. Boivin, M. Melin, and D. Hartmann, "Effect of Micro- and Macroporosity of Bone

Substitutes on their Mechanical Properties and Cellular Response, Journal of Materials Science Materials in Medicine, Vol. 14, (2003), pp. 1089–1097

[135] W. L. Suchanek and M. Yoshimura, “Processing and Properties of Hydroxyapatite-Based Biomaterials for use as Hard Tissue Replacement Implants”, Journal of the American Ceramic Society, Vol. 13, (1998), pp. 94-117
[136] R. J. Roberts and R. C. Rowe, “Brittle/ductile behaviour in pharmaceutical materials used in tabletting”, Int. J. Pharm., Vol. 36, (1987), pp. 205-209

[137] J. E. Rees and P. J. Rue, “Time-dependent deformation of some direct compression excipients”, Journal of Pharmacy and Pharmacology, Vol. 30 (1978), pp. 601-607

[138] N. A. Armstrong and L. P. Palfrey, “The effect of machine speed on the consolidation of four directly compressible tablet diluents”, Journal of Pharmacy and Pharmacology, Vol. 41, (1989), pp.149-151

[139] F. W. Nyongesa and B. O. Aduada, “Fracture strength of porous ceramics: stress concentration vs minimum solid area models”, African Journal of Science and technology, Science and Engineering Series, Vol. 5, (2004), pp. 19-27.

[140] R. W. Rice, “Porosity of Ceramics”, Marcel Dekker, New York, (1998), ISBN: 0824701518

[141] K. Takahashi, Y. Fujishiro, S. Yin and T. Sato, “Preparation and compressive strength of a-tricalcium phosphate based cement dispersed with ceramic particles”, Ceramics International, Vol. 30, (2004), pp.199–203

[142] D. –M. Liu, “Influence of Porosity and pore size on the compressive strength of Porosut Hydroxyapatite Ceramic”, Ceramics International, Vol. 23, (1997), pp. 135-139

[143] M. Trecant, J. Guicheux, G. Grimandi, M. Leroy and G. Daculsi, "Dynamic Compaction: a new process to compact therapeutic agent-loaded calcium phosphates" , Biomaterials, Vol. 18, (1997) , pp.141-145

[144] H. Abe, K. Sato, M. Naito, K. Nogi, T. Hotta, J. –I. Tatami and K. Komeya , "Effects of granule compaction procedures on defect structure, fracture strength and thermal conductivity of AlN ceramics" , Powder Technology , Vol. 159, (2005), pp.155 – 160

[145] S. Zhu, S. Ding, H. Xi, Q. Li and R. Wang, "Preparation and characterization of SiC/cordierite composite porous ceramics", Ceramics International, in press, (2005)

[146] L. M. R. guez-Lorenzo, M. Vallet-RegmH and J. M. F. Ferreira, "Fabrication of hydroxyapatite bodies by uniaxial pressing from a precipitated powder", Biomaterials, Vol. 22, (2001), pp.583-588

[147] C. Wu, J. Chang, J. Wang, S. Nia and W. Zhai, "Preparation and characteristics of a calcium magnesium silicate (bredigite) bioactive ceramic", Biomaterials, Vol. 26, (2005), pp.2925–2931

[148] X. Wang, H. Fan, Y. Xiao and X. Zhang, "Fabrication and characterization of porous hydroxyapatite/β-tricalcium phosphate ceramics by microwave sintering", Materials Letters, Vol. 60, (2006), pp. 455-458

[149] Z. Gou, J. Chang and W. Zhai, "Preparation and characterization of novel bioactive dicalcium silicate ceramics", Journal of the European Ceramic Society, Vol. 25, (2005), pp. 1507-1514

[150] K. Lin, J. Chang, Y. Zeng and W. Qian, "Preparation of macroporous calcium silicate ceramics", Materials Letters, Vol. 58, (2004), pp.2109–2113

[151] Hu Chen, Yingjun Wang, Jian Wang and Kaihui Nan, "Preparation of Porous β-TCP Ceramics", Key Engineering Materials, Vol. 280-283, (2005), pp. 1515-1518

[152] T. Rajeswara Rao , "Kinetics of calcium carbonate decomposition", Chemical Engineering & Technology, Vol.19, (2004), pp. 373 – 377

[153] G. A. Lewis, D. Mathieu and R. Phan-Tan-Luu, Pharmaceutical Experimental Design, Marcel Dekker, New York (1999)

[154] J. A. Cornell, "Experiments and mixtures", Designs Models and the Analysis of Mixture Data (2nd ed.), J. Wiley and Sons, New York (1990).

[155] X. Wang, Q. L. Feng, F. Z. Cui, and J. Ma, "The effects of S-chitosan on the physical properties of calcium phosphate cements", Journal of bioactive and Compatible Polymers, Vol. 18, (2003), pp. 45-57

[156] S. B. Lee, Y. H. Kim, M. S. Chong and Y. M. Lee, "Preparation and characteristics of hybrid scaffolds composed of b-chitin and collagen", Biomaterials, Vol. 25, (2004), pp.2309–2317